supervising scientist report 134

Effect of vegetation and surface amelioration on simulated landform evolution of the post-mining landscape at ERA Ranger Mine, Northern Territory

Kenneth G Evans,
Garry R Willgoose,
Michael J Saynor
& Tony House

Environment Australia
Department of the Environment

supervising scientist

Kenneth G Evans – Environmental Research Institute of the Supervising Scientist, Locked Bag 2, Jabiru NT 0886 Australia. (Also Department of Civil, Surveying and Environmental Engineering, The University of Newcastle, Callaghan, NSW 2308, Australia.)

Garry Willgoose – Department of Civil, Surveying and Environmental Engineering, The University of Newcastle, Callaghan, NSW 2308, Australia.

Michael J Saynor – Environmental Research Institute of the Supervising Scientist, Locked Bag 2, Jabiru NT 0886 Australia.

Tony House – Environmental Research Institute of the Supervising Scientist, Locked Bag 2, Jabiru NT 0886 Australia. Present address: Menzies School of Health Research, PO Box 41096, Casuarina, NT 0811, Australia.

This report should be cited as follows:

Evans, Kenneth G, Willgoose, Garry R, Saynor, Michael J & House, Tony, 1998. *Effect of vegetation and surface amelioration on simulated landform evolution of the post-mining landscape at ERA Ranger Mine, Northern Territory*. Supervising Scientist Report 134, Supervising Scientist, Canberra.

The Supervising Scientist is part of Environment Australia, the environmental program of the Commonwealth Department of the Environment and Heritage.

Supervising Scientist
Environment Australia
GPO Box 787, Canberra ACT 2601 Australia

ISSN 1325-1554

ISBN 0 642 24337 9

Printed in Darwin by NTUniprint.

Contents

Tables

Figures

Executive summary

The effect of vegetation and surface ripping on evolution of the ERA Ranger Mine (ERARM) post-mining landform was assessed using the SIBERIA landform evolution model.

Data were collected from four sites on the waste rock dump at ERARM—(1) the cap site which was unvegetated and unripped with a surface slope of 0.028 m/m; (2) the batter site, surface slope 0.207 m/m, also unvegetated and unripped but with a covering of coarse rock material; (3) the soil site, surface slope 0.012 m/m, which had ≈90% vegetation cover of low shrubs and grasses and had been topsoiled and surface ripped; and (4) the fire site, surface slope 0.023 m/m, which was topsoiled and ripped and is presently vegetated with well established trees, grasses and shrubs.

Natural rainfall events were monitored on the four sites to collect rainfall, runoff and soil loss data to parameterise the SIBERIA sediment discharge equation. The SIBERIA sediment discharge equation was calibrated using output from a sediment transport model of the form $T = \beta_2 S^{n_1} \int Q^{m_1} dt$, and the DISTFW rainfall-runoff model. Low frequency high intensity events resulted in the greatest soil loss. Therefore, it is important that sediment loss during high intensity events is predicted accurately. Storms with a range of intensities were selected to derive the sediment transport model. DISTFW hydrology model parameters were derived by fitting four monitored events simultaneously.

SIBERIA simulations of post-mining rehabilitated landform evolution showed that for the unvegetated and unripped surface, the landform at 1000 y would be dissected by localised erosion valleys (maximum depth = 7.6 m) with deposited fans (maximum depth = 14.8 m) at the outlet of the valleys. Simulated valley form has been recognised in nature which indicates that SIBERIA models natural processes efficiently. For the vegetated and ripped condition reduced valley development (maximum 1000 y depth = 2.4 m) and deposition (maximum 1000 y depth = 4.8 m) occurred in similar locations as for the unvegetated and unripped case (ie on steep batter slopes and in the central depression areas of the landform).

For the vegetated and ripped condition simulated maximum valley depth in the capping over the tailings containment structure was about 2.2 m. By modelling valley incision, decisions can be made on the minimum depth of tailings cover required to prevent tailings from being exposed to the environment within a certain time frame. A reduction in thickness of 1 m of capping material over tailings equates to about 1 000 000 Mm^3/km^2 tailings dam area. This represents a saving of about \$1 500 000/km^2 in earthworks. Incorporation of SIBERIA simulations in the design process may result in cost reduction while improving confidence in environmental protection mechanisms.

Acknowledgments

Thank you to Dr A Johnston, Director of the Environmental Research Institute of the Supervising Scientist (***eriss***), for his support and encouragement.

Mr BL Smith and Mr R Hall, Technical Officers, ***eriss*** assisted with field work and laboratory analysis; and Mr DR Moliere, Professional Officer, ***eriss*** assisted with data reduction and preparation of appendixes.

ERA Ranger Mine provided the study sites and provided support in many ways during this project. Thank you to Ms C Unger (ERA Environmental Services) who was involved in the initial planning of the project and co-ordinated the study with ERA. The following ERA Ranger Mine and ERA Environmental Services staff are acknowledged: Mr P Savory, Dr P Reid (deceased), Mr G Stewart, Ms H Nisbet, Mr M Rajagopalan and Mr R MacAllister.

Thank you to Mr A Mount and Dr S Tims, ***eriss***, for assistance with computer support and programming. Thank you to Mrs J Mount, ***eriss***, for her assistance in the library and the ***eriss*** Corporate Services staff, in particular, Mr D Lehmann, Mrs J Smith, Mrs H Waterson, Mrs G Barrowcliff and Mr A Ralph for their assistance.

Dr R Loch, Landloch Pty Ltd, Dr W Erskine, The University of New South Wales, Dr D Freebairn, Queensland Department of Natural Resources and Professor J Kalma, Hunter Water Corporation Chair in Environmental Engineering, The University of Newcastle, are thanked for there review of this report and for helpful comment and discussion.

The installation of the erosion plots on the cap and batter sites was initiated by Dr S Riley and he advised on plot construction and the methods of collection and reduction of hydrology data from those sites.

1 Introduction

1.1 Study objectives

The objectives of this project were:

- Document the process of data collection, parameter derivation and landform modelling which can be incorporated in mine planning and design to reach rehabilitation objectives.
- Assess the effects of vegetation and surface amelioration on landform evolution modelling, using SIBERIA, of the waste rock dump at the ERA Ranger Mine (ERARM) to exploit the flexibility of SIBERIA to better model the effect of vegetation on runoff and erosion.

1.2 Planning stable post-mining landforms

The basic aim of mine planning is the design of mine layouts and schedules that achieve optimisation of operations, minimum costs and maximum resource recovery (Jeffreys et al 1986). Increasing public awareness and stricter enforcement of regulatory requirements for rehabilitation of sites after mining make environmental planning an essential part of mine planning. Such planning should address the following: definition of post-mining land uses; selective handling of waste rock or spoil; landform design that satisfies drainage and erosion requirements; and the establishment and maintenance of vegetation (Hannan & Bell 1993).

An important part of environmental planning for surface mines is the design of stable final landforms for waste rock dumps or spoil piles as it controls most aspects of rehabilitation planning. The design of post-mining landforms needs to be considered at all stages and incorporated in the total mine plan. The following issues need to be considered with respect to landform design: location ie in-pit or out-of-pit; shape; slope form; drainage and earthworks cost. The final landform design will impact on mine layout, equipment types and economics of the operation. To successfully incorporate landform designs in planning, it is necessary to predict the stability of the final landform. Through the application of erosion modelling, techniques are being developed that can be used to predict the surface stability of landforms.

1.3 Erosion modelling

Models to predict surface stability can be placed in two broad categories: soil loss prediction or soil erosion models where erosion is the main concern, and topographic evolution models (Evans et al 1991). The majority of soil erosion models have been developed for agricultural purposes, but some models are being assessed for their application to mining and a selection is discussed below. The following descriptions of models are taken, in part, from Evans (1992).

1.3.1 Soil loss prediction models

These models can be used to predict the amount of material lost from an area either over a long period or as a result of a single rainfall/runoff event.

1.3.1.1 The Revised Universal Soil Loss Equation (RUSLE)

The RUSLE (Renard et al 1994), an empirical soil erosion model, is based on statistical analysis of erosion data collected from field plots.

Application of the RUSLE is site-specific and aims to allow for variables peculiar to an individual site. The RUSLE predicts long-term average soil losses from field areas under specific cropping and management. It cannot model deposition.

1.3.1.2 Chemical, Runoff and Erosion from Agricultural Management Systems (CREAMS)

The CREAMS model, developed by the United States Department of Agriculture (Knisel 1980), has a process-based approach to the prediction of erosion and sediment yield in field-sized areas. Model components are available that address the hydrology and chemistry of a catchment (Foster 1982, Silburn & Loch 1989). The model is based on a continuity equation that models sediment load that varies with distance downslope and is equal to the sum of lateral sediment inflow and the detachment or deposition of sediment by flow. CREAMS incorporates rainfall and runoff properties, soil properties and management factors. Erosion on bare soils is calculated and then empirical factors from the RUSLE are applied so soil conservation practices may be considered (Loch et al 1989). Soil properties that need to be determined are grain roughness and erodibility. Deposition can be modelled.

1.3.1.3 Water Erosion Prediction Project (WEPP)

This is a processed-based prediction model (Miller & Lee 1989) which computes sediment transport and deposition on a landscape. WEPP divides hillslope erosion into interrill and rill erosion processes. Interrill erosion is the combination of raindrop impact detachment and lateral transport of sediment into rill flow areas. Rill erosion is the combination of detachment and transport of sediment by concentrated flows in rills (Lopes et al 1989).

1.3.2 Topographic evolution models

These models give an indication of the long-term geomorphological development of a formed surface subjected to erosion and deposition processes (Evans et al 1991). In contrast to models in the previous section they allow the landform to change in response to erosion and deposition. They can also be used to predict the development of drainage problem areas and gullies.

Kirkby (1971) considered a topographic evolution model (process-response models) as based on a continuity equation simply modelled where aggradation occurred when more material entered an area than was removed and where net erosion occurred when less material entered an area than was removed. Advances in computing technology now allow this concept to be applied to nodes on a digital terrain map (DTM). This concept allows 3-D graphic representation of simulations by recently developed models.

1.3.2.1 SIBERIA

This is a sophisticated 3-D topographic evolution model modelling both runoff and erosion. It predicts the long-term evolution of channels and hillslopes in a catchment. The location and speed with which gullies develop are controlled by a channelisation initiation function that is related to runoff and soil erodibility (Willgoose et al 1989). The model solves for two variables: elevation, from which slope geometries are determined and an indicator function that determines where channels exist. The evolving drainage system of a catchment can be modelled. Three sediment transport processes are considered in the determination of elevation. These are tectonic uplift, fluvial processes and mass movement. Channel growth is governed by an activation threshold. A surface may commence with no gullies, but when the activation threshold (which depends on discharge and slope gradient) is exceeded, a channel develops. The model has continued to be enhanced by Willgoose and co-workers (eg Moglen & Bras 1994). While SIBERIA can model both transport- and detachment-limited sediment transport, its primary mode of use is for transport-limited environments.

1.3.2.2 Other models

A model developed by Howard (1994, 1997) combines the effects of mass-wasting, rainsplash and fluvial erosion processes. Fluvial erosion is modelled as a combination of detachment-limited erosion in steep channels and transport-limited erosion in lower gradient alluvial channels. This allows modelling incorporating the spatial distribution of surface properties such as exposed bedrock in the upper reaches of a channel and less competent material in the lower reaches.

Tucker (1996) developed a model, GOLEM, that is capable of modelling both detachment-limited and transport-limited sediment transports and predicts on what parts of the landscape each of these processes acts.

1.4 The application of erosion models to design

Post-mining landform design is controlled by the standard of surface stability. The standards that affect design may be general or specific. Examples of general standards are the objectives of Queensland environmental policy (DRI 1991), namely: achievement of an acceptable post-mining land use; achievement of a stable post-disturbance landform; and preservation of downstream water quality.

Examples of more specific standards are those proposed by Waggitt and Riley (1992) as stabilisation objectives for the rehabilitation of the ERA Ranger Mine (ERARM) in the Northern Territory, Australia. These proposals clearly quantify stability standards for post-mining landforms in terms of erosion rates, annual sediment export rates, rill and gully incision and wash load concentrations.

Stages of mine planning up to project commitment are preliminary mine design, final mine design and feasibility studies (fig 1.1). The chemical and physical properties of waste rock or overburden should be thoroughly characterised before the final design is completed. The post-mining landform design, based on waste rock characterisation and modelling, should form part of the final mine design so that it can be included in feasibility studies (fig 1.1).

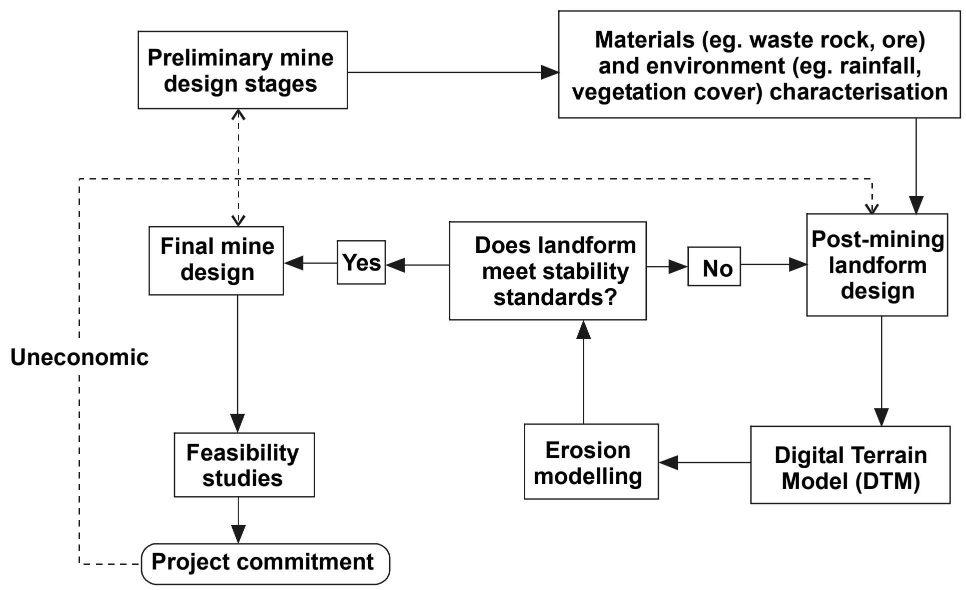

Figure 1.1 Mine planning stages incorporating post-mining landform design based on erosion modelling

A digital terrain map (DTM) of a 3-D earthworks design of the post-mining landform can be produced using engineering software (eg Phillips 1991, O'Reagan et al 1991). The landform should then be modelled and predicted erosion losses or stability compared with required standards. Willgoose and Riley (1993) used SIBERIA to model the stability of the proposed 'above-grade' rehabilitated landform at ERARM over simulated periods of 1000 years. The modelling predicted severe valley formation in the centre of the structure and 0.5m to 1 m denudation of slopes between gullies. To improve stability it may be necessary to change the design where erosion is most severe.

If modelling predicts that the required standards will be met then the design can be included in the final mine design. If the prediction indicates standards may not be met then the landform should be redesigned and remodelled until the required standards are met (fig 1.1).

However, a good design is one that not only meets stability requirements but can also be constructed economically. The final mine design will form the basis for a decision to commit to the project (White et al 1993). The final landform design has considerable influence on costs and may influence decisions on mining methods. If there is insufficient confidence to commit to the project after feasibility studies, then the final plan including rehabilitation planning should be reconsidered.

Once mining has commenced and waste rock dumps are being constructed, further characterisation of the waste rock should be undertaken, the landform remodelled and the design adjusted if necessary.

1.5 Model parameters

Erosion and runoff modelling requires determination of model parameter values. These values are site-specific and need to be determined by different methods. The parameters to be determined depend on the model used and the choice of model is controlled by a combination of factors such as:

- likely environmental impact
- cost of data collection for model parameter derivation
- process regime
- rehabilitation standards.

Many model parameter values can be measured directly, however, some parameter values need to be determined indirectly from data collected through spoil or waste rock characterisation, monitoring or rainfall simulation.

If the standard stipulates a maximum allowable annual sediment loss from rehabilitated areas then the Revised Universal Soil Loss Equation (RUSLE) (Renard et al 1994) may have application in the initial stages of assessment and design. The RUSLE gives an indication of soil loss rates. All parameters in this empirical model can be measured directly except for erodibility which can be determined from particle size analysis using a nomograph (Wischmeier & Smith 1978) or particle size analysis and soil properties (Loch & Rosewell 1992). Information for these methods can be obtained from cores or bulk samples. Other methods are long-term monitoring or rainfall simulation techniques. Rainfall simulation was used by Stein (1983) to determine erodibilities of reclaimed mine soils in the USA. Once mining commences long-term monitoring should be conducted to strengthen confidence in parameter values and soil loss predictions.

Where long-term stability needs to be predicted, or if the standard specifies maximum allowable denudation rates, rill or gully incision rates or wash load concentrations (Waggitt & Riley 1992), then a topographic evolution model should be used. For SIBERIA, the main input parameters are related to mean annual sediment yield and gully development (Willgoose & Riley 1993). The mean annual sediment yield is assessed through a combination of modelling sediment loss from a catchment using an overland flow erosion model and modelling discharge-area relationships and runoff series. The gully development parameter is determined through a combination of rainfall-runoff modelling and sediment transport/erosion modelling (Riley & Williams 1991). Relationships with soil/spoil physical properties have not been attempted at this stage.

1.6 Effect of vegetation and surface amelioration on erosion and hydrology

It is proposed as part of the rehabilitation of ERARM that the waste rock dump will cover more than 4 square kilometres in area and reach to 17 metres above the local ground surface (Unger et al 1989). It is important that (1) the rehabilitated landform provide for long-term containment of radio-active tailings and (2) that erosion does not limit revegetation and ecosystem restoration on the rehabilitated areas of the mine site nor diminish the aesthetics of the area. In addition to vegetation, it is likely that surface amelioration such as surface ripping and rock mulching may be carried out on the rehabilitated landform to increase infiltration, reduce erosion and enhance plant growth. Therefore it is likely that any influence on SIBERIA input parameters will result from a combination of vegetation and surface amelioration.

Soil loss by erosion is influenced by a number of interactive processes between soil and vegetation (Stocking 1994) which include physical binding of soil by roots and stems, retention of runoff by stalks and litter, increased infiltration around roots, improved structural and water-retaining qualities resulting from incorporation of organic matter and faunal activity and electrochemical and nutrient bonding between roots and soil. Vegetation reduces the erosivity of rain by causing the dissipation of kinetic energy on contact with foliage and reducing flow velocity of runoff. This reduces soil loss, which is dependent on height and continuity of foliage, root density and the thickness of ground cover (Morgan 1986). However, Stocking (1994) considered that vegetative cover was not a soil loss cure-all. Stocking cites very low erosion rates ($\approx$500 kg ha^{-1} yr^{-1}) under natural forests but cautions that accelerated erosion can occur under planted trees which may result from large droplets forming on leaves and falling with increased kinetic energy; or trees out-competing ground cover resulting in exposed areas of soil. Rainfall simulation studies in semi-arid mulga woodlands of Australia (Greene et al 1994) have shown that runoff rate has decreased with increasing plant cover, which is probably due to plants funnelling water down their stems and increasing infiltration around the roots through developed macropores. In the same study no significant effect of plant cover on sediment concentration was observed. The implication of this is, that for these plant cover conditions (<100% cover and sparse tussocky basal cover), erosion reduces as plant cover increases and this effect is controlled by the volume of runoff since sediment concentration in the runoff is not significantly affected. Rainfall simulator studies were conducted on two mine sites on the Queensland coalfields (Loch & Bourke 1994, 1995) to assess the effect of vegetation cover on erosion of topsoil over spoil. The results indicated that topsoil erosion reduces greatly with increasing vegetation cover and that, at one site, interrill sediment concentration in runoff reduced with surface cover. In addition, for the flow rates studied it appeared that difference in type of ground vegetation cover was not important with respect to soil loss ratio, however, this may not apply to higher flow rates. In a study to refine the Water Erosion Prediction Project

(WEPP) (Foster 1987) input parameters, Simanton et al (1991) compared natural vegetated plots and plots with the canopy cover clipped to 20 mm height and the clippings removed. Their analysis showed that there were no significant differences between sites for runoff coefficients, final infiltration rates or initial rainfall abstractions. However, erosion rate on the clipped plots was slightly less than that on the natural plots. Disruption of overland flow by vegetation can result in concentration, deflection and dispersion of surface flow. Deflection reduces flow velocity resulting in reduced erosivity of flow and concentration increases flow velocity and depth resulting in faster and deeper erosion in areas of sparse vegetation (Rogers & Schumm 1991). A desk-top study of the WRD at ERARM (Willgoose 1995), using published erosion-vegetation correlations, predicted that erosion rates from areas with fully developed vegetation were about 6% of the erosion from unvegetated areas and that erosion rates from areas where the undergrowth were not fully developed could vary from 6% to 75% of the rate from unvegetated areas. Willgoose (1995) considered that undergrowth was the major contributor in erosion rate reduction.

Surface amelioration such as ripping or deep tillage is undertaken at mine sites to increase vegetation growth (eg Ward et al 1983) through improvement of infiltration. Finnegan (1993) used results of rainfall simulation studies on various ripping patterns on the WRD at ERARM to derive parameters for the Field-Williams hydrology model. The results indicated that all patterns increased infiltration compared with previous studies on unripped surfaces (Willgoose & Riley 1993). However, this comparison was made between data from rainfall simulation and natural rainfall. There is little information on the effect of ripping on erosion/infiltration from mine sites. Comparisons can be made with agricultural studies, however, the main difference is that generally mine surfaces are ripped once to facilitate infiltration and vegetation establishment and agricultural fields are tilled on a regular basis. Packer et al (1992) cite several studies which suggest that continuous cultivation or tillage reduces soil structure and stability. Results from their long-term study on agricultural soils showed that runoff from traditionally tilled soils increased over 7 years and runoff from areas of direct drilling decreased with time. A watershed in the arid area of south eastern Arizona USA was ripped and runoff observed for 12 years (Simanton et al 1978). Results indicated that initially a tenfold decrease in runoff was observed; the ripping was effective for 5 years; there was little change in the existing vegetative cover and the rip lines were gradually smoothed by the rainfall. Observation of the ripped sites on ERARM indicate that material is removed from the crests of the rip lines and deposited in the depressions. It appears that the ripped surfaces are gradually smoothing.

WRD surfaces can also have a covering of coarse competent rock fragments either as a result of the nature of the material placed there during dumping, through management practices by placement of a rock mulch or through preferential removal of fines. All situations may result in a reduction in erosion. Laboratory rainfall simulation studies (Agassi & Levy 1991) have shown that as stone cover increases, infiltration increases and erosion decreases. Agassi and Levy (1991) considered that with respect to infiltration runoff water was absorbed by soil underneath the stones because this soil had maintained its initial infiltration properties and that stone cover reduced both splash and runoff-initiated erosion.

1.7 Study outline

SIBERIA is new technology. The authors believes that the first research into the application of landform evolution modelling to post-mining rehabilitated landform design was conducted by Willgoose and Riley (1993). Willgoose and Riley (1993) used SIBERIA to model the ERARM ‘above-grade’ landform using parameters derived from data collected from areas of the waste rock dump (WRD) with no vegetation or surface amelioration, such as ripping or rock mulching. Data were collected from erosion and runoff plots on the cap area of the waste rock dump using techniques of rainfall simulation and monitoring of natural storm events. The plot sizes ranged from approximately 1 m^2 to 120 m^2.

Engineering earthworks design as used in the construction of landforms is based on analysis using a DTM. SIBERIA is also based on a DTM and can quantify erosion both temporally and spatially, which is most useful in design of erosion control structures. Software has been developed which interfaces SIBERIA with earthworks design packages (Willgoose pers comm). Considering these features and the positive results of Willgoose and Riley (1993) this study focuses on the further refinement of SIBERIA.

Evans and Willgoose (1994) hypothesised that vegetation and surface amelioration may affect the input parameters for SIBERIA. Willgoose (1995) conducted a sensitivity study of the effects of vegetation on evolution of the ERARM post-mining landform using data from Willgoose and Riley (1993) and cover factors based on the Universal Soil Loss Equation (USLE) (Wischmeier & Smith 1978). SIBERIA, like the USLE, RUSLE and CREAMS (Knisel 1980), can incorporate a cover factor which accounts for the vegetation and rock mulch effect and a conservation practices factor which accounts for the effects of surface treatments such as ripping. The cover factor in the RUSLE and CREAMS can be used in SIBERIA just as in the RUSLE and CREAMS (eg Willgoose 1995). However, because of the flexibility of SIBERIA formulations, a better result is achieved by calibrating the hydrology and erosion inputs to SIBERIA incorporating the effects of cover and surface treatment. If SIBERIA input parameter values are affected by vegetation and surface amelioration then the long-term erosional stability of the post-mining landform can be reassessed and the design adjusted accordingly. This study advances the knowledge gained from the Willgoose and Riley (1993) study and uses measured mine site data to assess the effects of surface treatments on SIBERIA input parameter values.

The collection of data which can be used to derive SIBERIA input parameters and subsequent derivation of parameters and landform modelling, as shown in figure 1.1, can be a complex and difficult process. Chapters two and three document the complete process of data collection, parameter derivation and landform modelling which can be incorporated in mine planning.

In this study data for vegetated and ripped areas of the WRD at ERARM were collected from ≈600 m^2 erosion and runoff plots through natural rainfall monitoring. Similar data for unvegetated and unripped sites had been collected previously.

In chapter four monitoring data are used to derive erosion model parameters through multiple regression and hydrology model parameters using the recently developed non-linear regression software, DISTFW-NLFIT (Willgoose et al 1995). This study is the first to apply the capabilities of the software to fit a single set of model parameter values to multiple storms of varying intensities and durations. These parameter values are used to derive input parameters for SIBERIA.

Finally, in chapter five the proposed above grade landform for ERARM is modelled using SIBERIA with parameters derived for a site without vegetation or surface ripping and with parameters derived for a site with vegetation and surface ripping. The results are compared to assess the affect of the treatments on the landform modelling process. The results for the unvegetated, unripped site are compared with the results of Willgoose and Riley (1993). Discussion is also presented comparing SIBERIA simulated landforms with landforms observed in nature, and how SIBERIA can be used to assess the adequacy of tailings containment structures and optimise landform design.

2 Field study methods and data reduction

ERARM is an open cut mine in the Alligator Rivers Region (ARR) of the Northern Territory Australia. At the conclusion of mining ore will have been removed from two pits (no 1 and no 3) (fig 2.1). Options for rehabilitation of tailings are (1) stored above-ground in the tailings dam and in pit 1 or (2) stored in pit 1 and tailings from the dam to be stored in pit 3. Whichever option is chosen, rehabilitation design must provide for the long-term containment of radioactive tailings (ie over a period of thousands of years) and ensure that weathering and erosion of the containment structure, in an area which experiences high rainfall intensities, do not result in the release of contaminants that would degrade the environment or aesthetics of the surrounding Kakadu National Park.

The ERARM is adjacent to the World Heritage Listed Area of Kakadu National Park and exploits a stratabound uranium deposit hosted by the lower member of the Early Proterozoic Cahill Formation. The WRD at ERARM consists of rocks from the lower member that comprises carbonates, carbonaceous schists and mica and quartz feldspar schist (Needham 1988). The waste rock is highly weatherable (Milnes 1988) and large competent chloritic schist fragments break down into medium and fine gravel and clay-rich detritus within a two to three year period (Riley & Gardiner 1991). The section of the WRD where this study was conducted rises to approximately 12 m above the surrounding land surface. The area receives high-intensity storms and rain depressions between October and April (Wet season) with little rain falling during the remainder of the year (Dry season). The average annual rainfall is 1480 mm.

2.1 Study sites

Four areas of the WRD (fig 2.1) were studied. The first, the cap site has an average slope of 0.028 m/m, in the area studied. The surface is covered with fine material overlying a hard pan-like surface which develops cracks during the prolonged Dry season.

Excavations of approximately 1 m on the cap site indicate an impervious layer of fine material which Riley (1992) suggests can be over 1 m deep and results from vertically downward transportation of the fine material. As a result there is limited infiltration and increased runoff. The second area is on a batter slope and has an average slope of 0.207 m/m in the area studied. The batter site is covered with coarser material than the cap site.

The surface condition of the cap and batter sites at the time of the study was not representative of the proposed final rehabilitated condition which may include surface treatment such as rock mulching or ripping and revegetation. There was negligible vegetation on the cap and batter sites.

The third study area was on an area of the cap referred to as the soil site. This site was a top-soiled, surface ripped and revegetated area of the upper surface of the northern part of the WRD. The soil site had an average slope of 0.012 m/m and was vegetated with low shrubs and grasses providing approximately 90% coverage.

The fourth study area was on the fire trial site on a lower level, above and to the south of retention pond 4 (RP4). The fire site had an average slope of 0.023 m/m and was originally top-soiled and surface ripped and is now vegetated with well established trees (eucalyptus and wattle species) that are approximately 10 years old.

The spear grass on the sites grows vigorously during the Wet season to ≈3 m tall and then dies off during the Dry season leaving a cover of dry straw mulch.

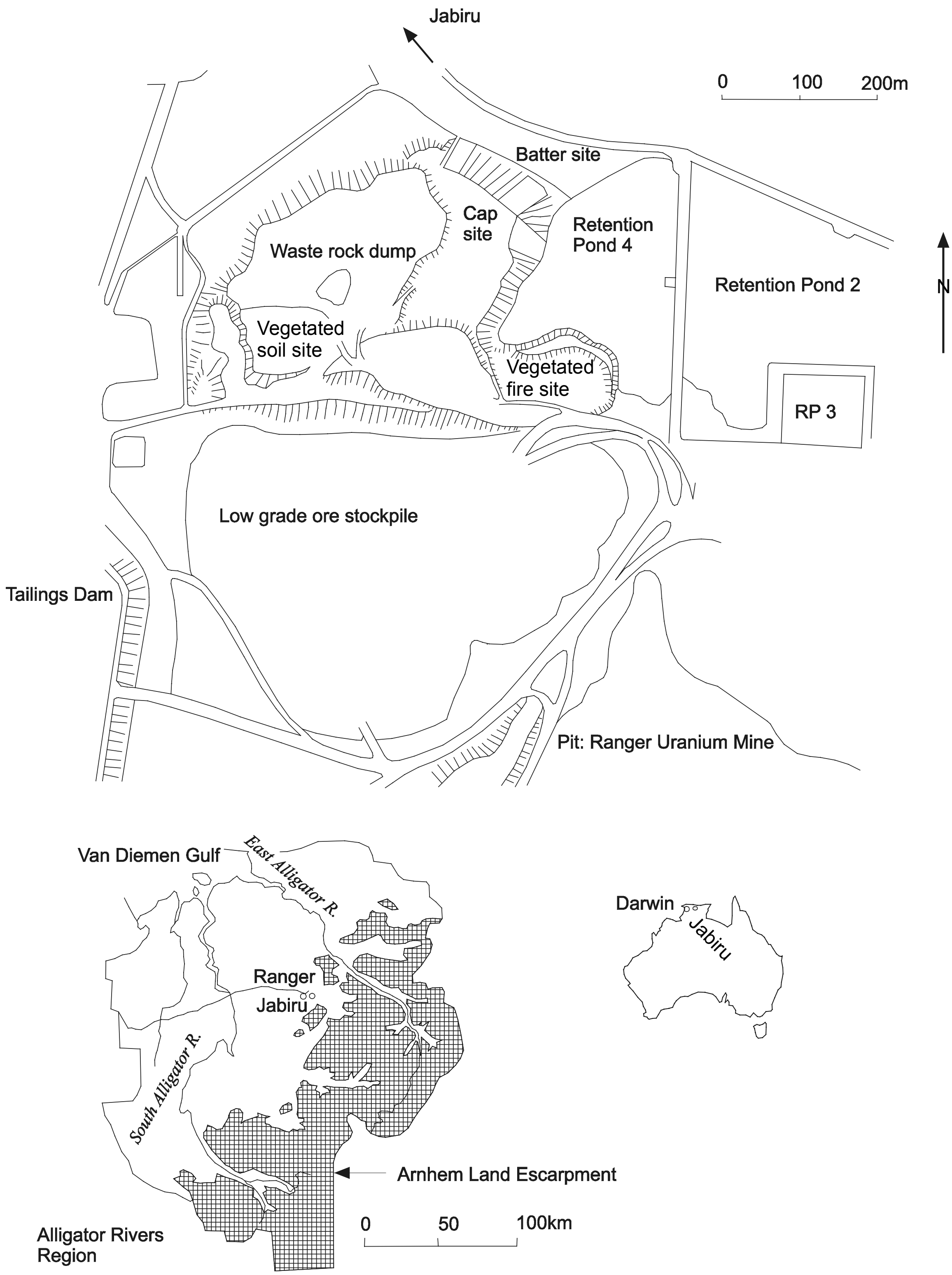

Figure 2.1 Location of the study sites on the ERA Ranger Mine

2.2 Runoff and erosion plots

Large scale runoff and erosion plots were constructed on each of the four sites. The cap site plot was 29.4 m long by 20.1 m wide (591 m^2), the batter site 37.7 m long by 15.9 m wide (600 m^2), the soil site 30 m long by 20 m wide (600 m^2) and the fire site 30 m long by 20 m wide (600 m^2) (fig 2.2). An initial topographic survey of the heavily vegetated study sites was conducted to determine slope gradient and direction to assist with plot location and orientation.

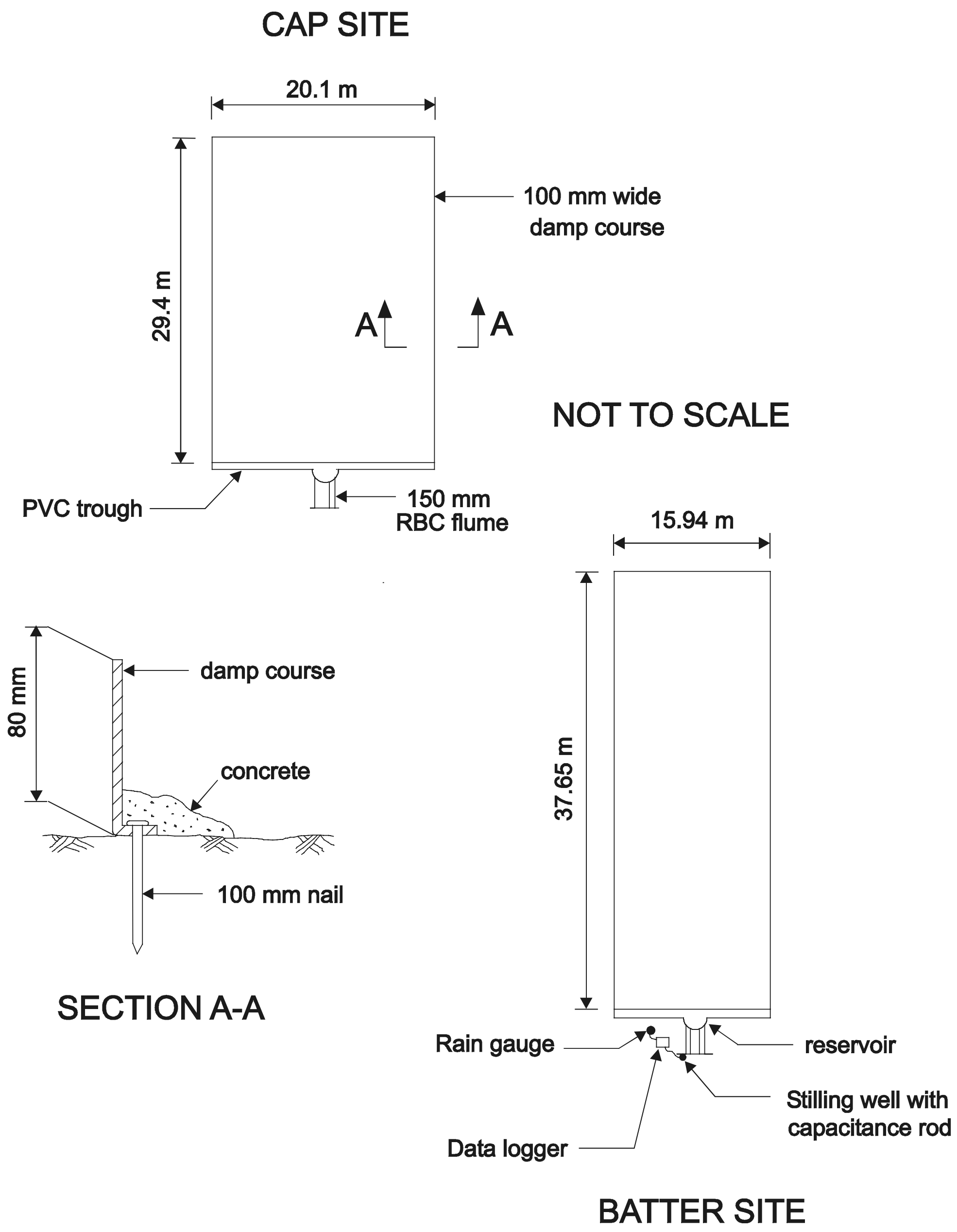

Figure 2.2 Layout of runoff and erosion plots. Details of damp course placement are shown in section A-A. The soil site and fire site had layouts similar to the cap site and with the dimensions given in the text. Because of drainage difficulties, the reservoir and flume on the fire site was placed at the left end of the trough and not in the centre as shown here.

2.2.1 Plot layout

Plot borders were constructed using 100 mm wide damp course. The damp course was bent across its width in the shape of an ‘L’, with one leg approximately 20 mm long and the other leg approximately 80 mm long. Damp course was laid continuously along the up-slope end and the two sides of the plots which had been previously measured and marked out using star posts and string. The damp course was held in place by pushing a 100 mm nail through the 20 mm long leg in to the WRD surface. This gave an upright wall of approximately 80 mm height. Concrete, of a mixture of 3:1, sand to cement, was then laid along the outer edge of the damp course covering the 20 mm long leg and the nails. This held the damp course in place and prevented runoff from escaping under the damp course (fig 2.2).

Half section 250 mm diameter PVC stormwater pipe troughs were placed at the down slope ends of the plots to catch runoff and channel it through rectangular broad-crested (RBC) flumes (Bos et al 1984) where discharge could be measured. Trenches were carefully dug (to avoid disturbance of the plot surface) along the down-slope edge of the plot across the full width. The trench was sloped (>0.02 m/m) toward the centre of the plot so that runoff could be directed through a centrally located RBC flume on the cap, batter and soil sites. On the fire site the flume was placed at one end of the trough. These trenches, the full width of plots, were up to 500 mm deep and in many places required jack-hammering through large competent rock fragments that had to be left in situ because their removal would cause damage to the plot surface. The half pipes were placed in the troughs and concrete placed between the pipe and the plot surface and smoothed to form an apron. The pipe joins were then sealed using a silicon sealant.

A reservoir was constructed at the centre of the plots (at one end on the fire site) where the troughs met so that bedload sediment in the runoff would drop out. The reservoirs were approximately 500 mm deep, 500 mm wide and 1000 mm long with the long axis normal to the down-slope end of the plot. A 150 mm RBC flume with a trapezoidal broad-crested control section was placed at the downstream end of the reservoir so that discharge could be measured. The surface of the reservoir was concreted and smoothed and blended into the trough outlets and flume inlet and rocks were placed along the top of the reservoir between the troughs and the flume and covered with concrete to prevent runoff entering the reservoir from the sides. The flumes, with a single stilling well, were concreted in place.

The low slopes of the cap, soil and fire sites and the depth to which the troughs had been placed on those plots, required a drainage channel so that runoff could be cleared away from the flume and not back-up in to the flume during an event.

2.2.2 Survey

The plot surfaces were surveyed using a TOPCON Geodetic Total Station (GTS-3C) on a 1 m^2 grid. Topographic contour maps (figs 2.3 to 2.6) were produced using SURFER software. Three-dimensional views of the sites are shown in figure 2.7. One line perpendicular to flow of elevations at 100 mm spacings across all plots was also surveyed.

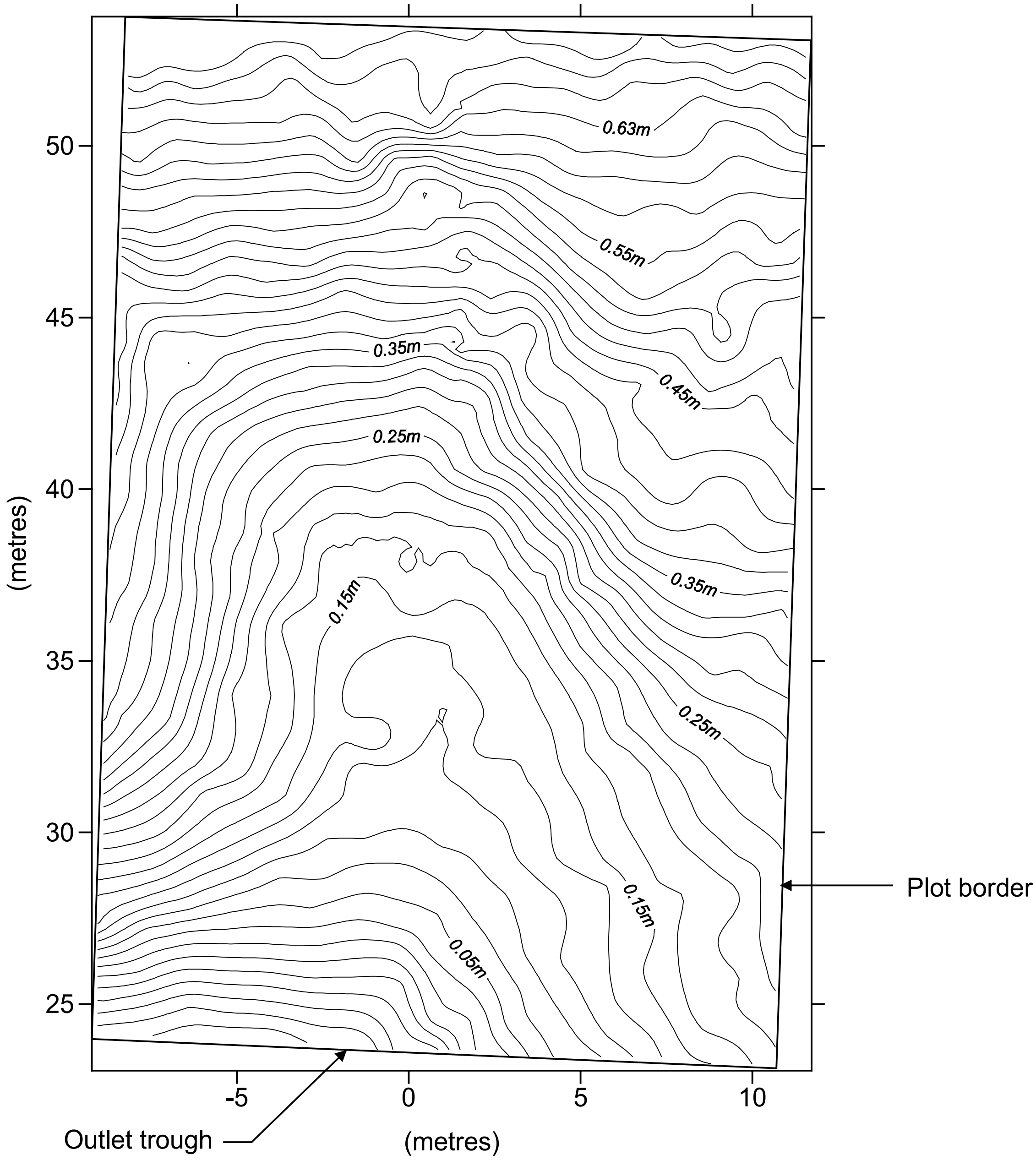

Figure 2.3 Contour map of the cap site

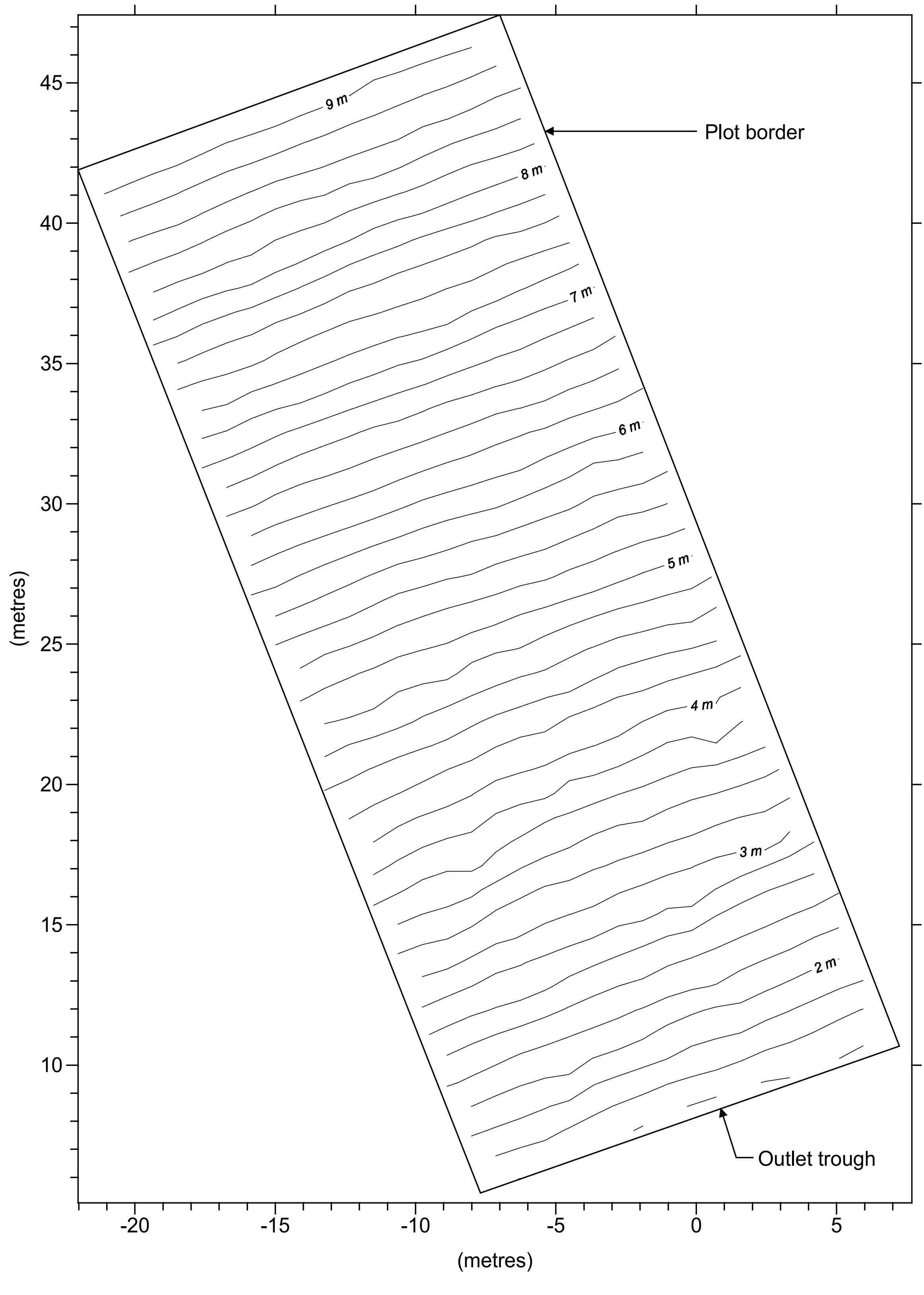

Figure 2.4 Contour map of the batter site

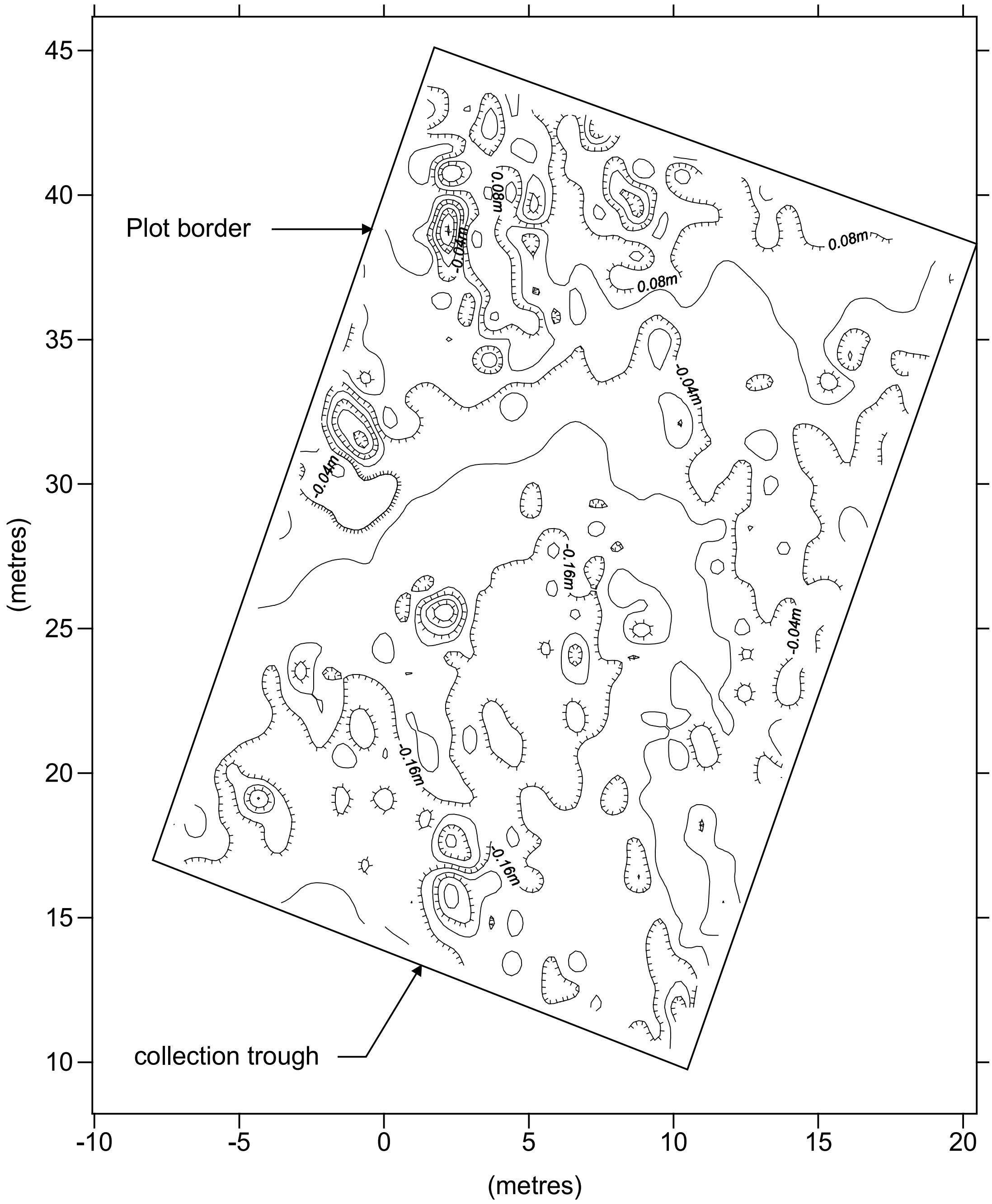

Figure 2.5 Contour map of the soil site

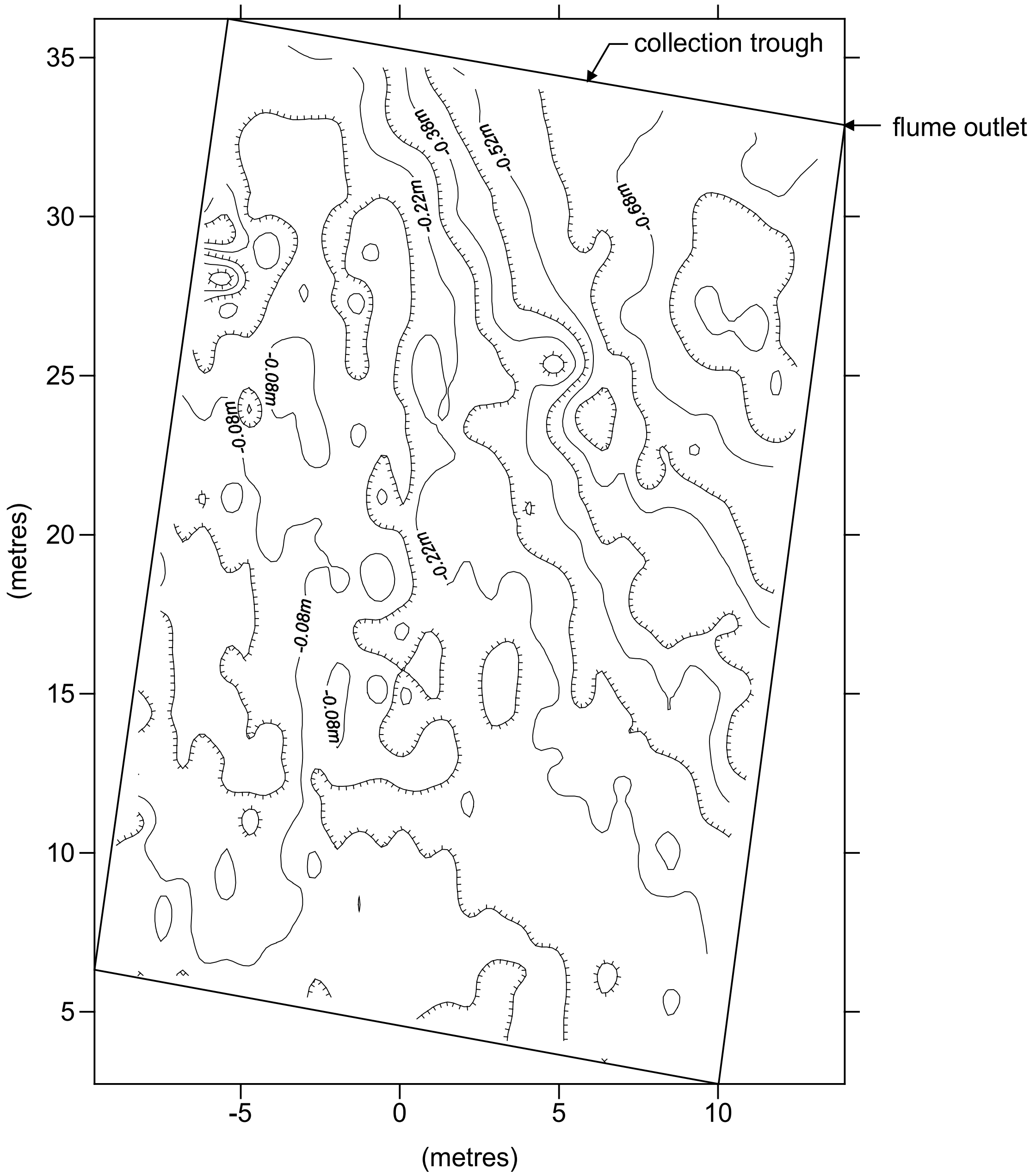

Figure 2.6 Contour map of the fire site

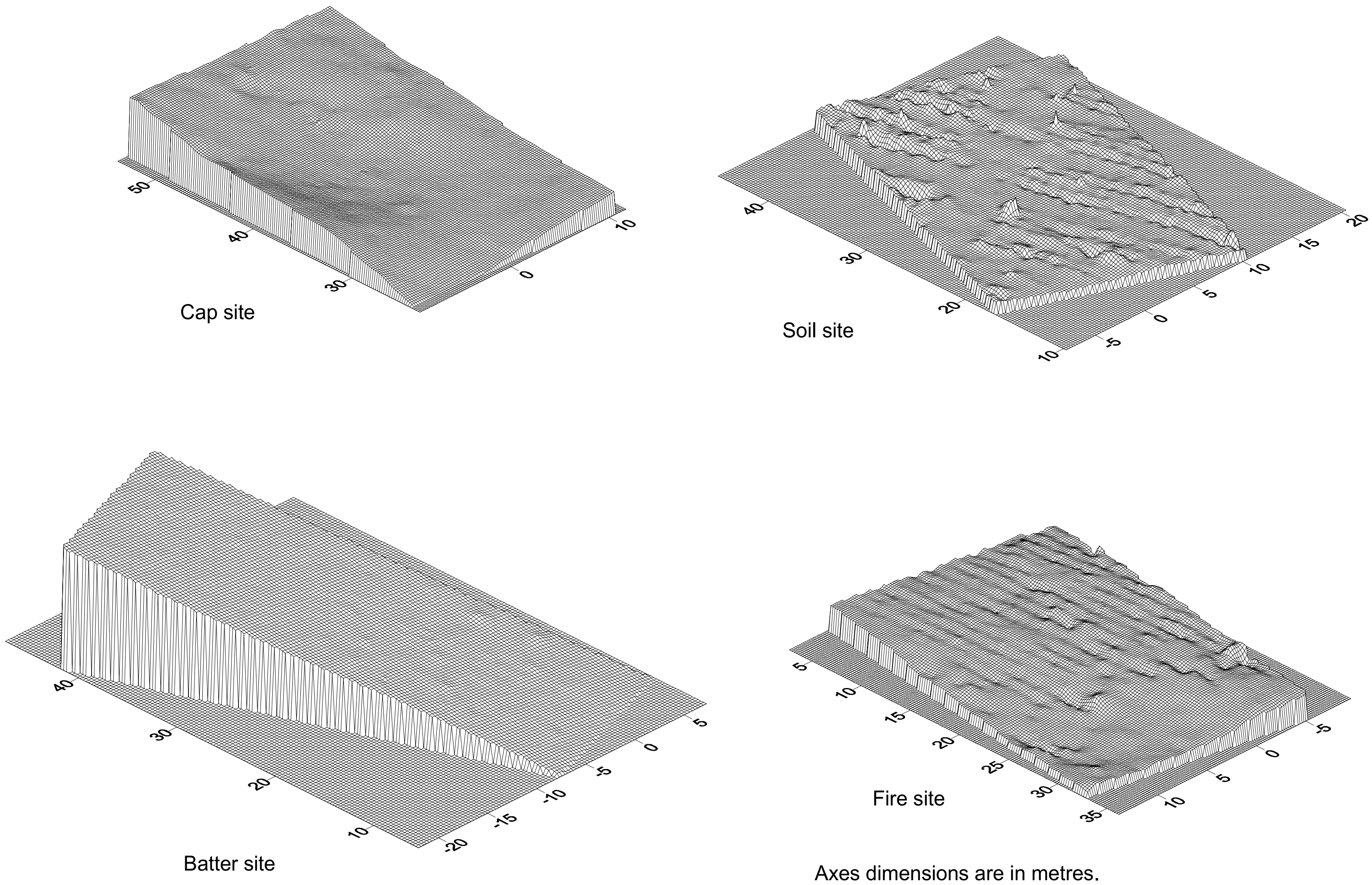

Figure 2.7 Three-dimensional view of the plot surfaces. Dimensions are in metres.

2.3 Monitoring of natural rainfall events

During the latter half of the 1992/93 Wet season (Evans & Riley 1993a,b) and the 1993/94 Wet season, plots on the cap and batter sites were monitored during natural rainfall events to collect hydrology and sediment loss data. During the 1994/95 Wet season, plots on the fire site and soil site were monitored during natural rainfall events to collect hydrology and sediment loss data (Saynor et al 1995).

2.3.1 Hydrology data

Rainfall was measured using a tipping bucket rain gauge placed near the reservoir at the cap and batter sites and in the centre of the soil site and fire site.

Stage in the RBC flume was measured automatically (logged) and manually (observed). Automatic measurements were taken using a capacitance rod (water level sensor) placed in the stilling well and manual measurements were taken off the stilling well by an observer. The capacitance rod output is frequency (Hz).

The rain gauge and capacitance rod were connected to a computer controlled DATATAKER datalogger. The data from the datalogger were downloaded to a portable computer after each event. The water height in the stilling well and time were noted at the start of flow over the weir in the flume and when flow ceased over the weir in the flume. This measurement was considered to be zero head and therefore zero discharge.

Down loaded event data were stored in text files and reduced to the final data files through the following steps.

1. Data files were imported into a QUATTRO PRO spreadsheet and parsed. Parsing required creating a format and then editing the format. It was necessary to convert time data to 24 hour time and then decimal days.
2. A frequency for zero head was selected. The time for the manually recorded zero flow was compared with automatically logged times. The frequency at the time of zero flow was assumed to be the frequency for zero head. Head (h) in millimetres was determined by subtracting the selected frequency for zero head from the logged frequency values and dividing the result by two for the cap and batter site. The division by two was necessary since each unit of frequency (Hz) was equal to 0.5 mm of head for the cap and batter site water level sensors. For the soil site and fire site the water level sensors where calibrated in the laboratory by measuring frequency for various water levels. The following conversion equations were derived where v = frequency and h = head (mm).

Fire site:

$$h = a + b/v + cv^3 \tag{2.1}$$

where

$a = -755.377$

$b = 859037.71$

$c = 2.7395 \times 10^{-8}$

Soil site:

where capacitance $v \geq 714$ Hz

$$h = a + bv + cv^2 + dv^3 + ev^4 \tag{2.2}$$

where

$a = 43193.675$

$b = -195.248$

$c = 0.336$

$d = -2.595 \times 10^{-4}$

$e = 7.525 \times 10^{-8}$

where capacitance v <714 Hz

$$h = a + bv + cv^3 \quad (2.3)$$

where

$a = 3509.08$

$b = -5.775$

$c = 2.692 \times 10^{-6}$

3. Head was then converted to discharge (Q) (L s^{-1}) using the following formula (Evans & Riley 1993c):

$$Q = 18.4h \times 940h^2 \quad (2.4)$$

Note: Head value must be converted to metres when using this equation.

4. Line graphs showing the hydrographs were plotted to assess the validity of the zero head value.

2.3.2 Sediment

Runoff water samples were collected during monitored events and analysed for suspended sediment concentrations. Bedload samples were collected at the conclusion of each event.

Suspended sediment samples were collected in 600 ml Bunzl flasks at the downstream end of the weir in the flume. Records were kept of sediment sample times. Sediment concentration (g L^{-1}) was determined using gravimetric methods. Total suspended sediment loss was determined through integration of the sedigraph produced by comparison of sediment concentration with the hydrograph similar to the method of Simanton et al (1991).

Collected bedload was placed in pre-weighed aluminium containers, dried at 105°C and reweighed to obtain the mass of sediment and containers. The container mass was then subtracted from the oven dried mass to give a total bedload mass.

3 SIBERIA model parameter derivation

The SIBERIA landform evolution model has been described in numerous articles eg Willgoose et al (1989, 1991abc, 1992) and Willgoose and Riley (1993). Its use is documented in Willgoose (1992). At a late stage in this work version 8 of SIBERIA which includes the capability to model soil development and improved sediment transport modelling was released. All results in this project are done with version 7.05 of SIBERIA. The description below is based on these papers.

Willgoose et al (1991a) considered that catchment form determines flood and erosion response of a catchment and flood and erosion response over geologic time influences catchment form. Difficulties in understanding interactions between processes, form and temporal change result from long timescales of catchment evolution, observing changes and attributing differences between catchments to differences in age or process because of spatial and temporal heterogeneity. Computer models, such as SIBERIA, can examine temporal trends and sensitivity to physical inputs (erodibility, tectonic uplift and runoff).

SIBERIA is a process-response model of erosion development of catchments and their channel networks. Long-term changes in elevation with time resulting from large-scale mass transport processes (tectonic uplift, fluvial erosion, creep, rainsplash and landsliding) are modelled as average affects of processes ie individual landslides are not modelled but the cumulative effect of many landslide events is modelled. The model describes how a catchment will look, on average, at a given time and differentiates channel and hillslope. Different transport processes are modelled in each regime. Channels are dominated by fluvial erosion and hillslope by a mixture of fluvial and diffusive processes. A channel forms when a channel initiation function (CIF) exceeds a threshold (channel initiation threshold (CIT)). The CIF is nonlinearly dependant on hillslope and discharge and a channel is considered to have formed when the CIF exceeds a CIT; for instance, when shear stress exceeds a shear stress threshold. Channel dimension (depth and width) are determined by regime equations (Leopold et al 1964).

The changes in elevation are described by the following mass transport continuity equation (Willgoose et al 1991ab, 1992):

$$\frac{\partial z}{\partial t} = c_0(x,t) + \frac{1}{\rho_s(1-n)}\left(\frac{\partial q_{sx}}{\partial x} + \frac{\partial q_{sy}}{\partial y}\right) + D\left(\frac{\partial^2 z}{\partial x^2} + \frac{\partial^2 z}{\partial y^2}\right) \tag{3.1}$$

where

z = elevation (m)

t = time (s)

$c_0(x,y)$ = rate of tectonic uplift (m s^{-1})

x,y = the horizontal directions (m)

q_{sx}, q_{sy} = rate of fluvial sediment transport per unit width in the x, y directions (g s^{-1} m^{-1})

D = elevation diffusivity (m^2 s^{-1})

ρ_s = density of sediment (g m^{-3})

n = porosity of sediment

The differential equation for the channel initiation function is (Willgoose et al 1991a,b, 1992):

$$\frac{\partial Y}{\partial t} = f\left(d_t, Y, \frac{a}{a_t}\right) \tag{3.2}$$

where

$Y = 1$ (the point in the catchment is a channel), or

$Y = 0$ (the point in the catchment is a hillslope)

d_t = rate of channel growth at a point

a = channel initiation function

a_t = channel initiation function threshold

Willgoose et al (1991b) noted that the exact form of equation 3.2 was not as critical as the functional form of the CIF.

SIBERIA predicts the long-term average change in elevation of a point by predicting the volume of sediment lost from a node. Fluvial sediment transport rate through a point (q_s) is determined in SIBERIA by the following equation:

$$q_s = \beta_1 q^{m_1} S^{n_1} \tag{3.3}$$

where:

S = slope (m/m)

q = discharge (m^3 y^{-1})

β_1= sediment transport rate coefficient

SIBERIA does not directly model runoff (Willgoose 1992) but uses sub-grid effective parameterisation which conceptually relates discharge to area (A) draining through a point as follows (Leopold et al 1964):

$$q = \beta_3 A^{m_3} S^{n_3} \tag{3.4}$$

To run the SIBERIA model for a field site it is necessary to derive parameter values for β_1, m_1, n_1, and m_3. For ease of derivation of β_1, it is normally assumed that β_3 = 1.

To obtain the parameter values for equations 3.3 and 3.4 it is necessary to:

1. Fit parameters to a soil transport equation using data collected from field sites;
2. To calibrate a hydrology model using rainfall-runoff data from field sites; and
3. Derive long-term average SIBERIA model parameters for the landform being modelled.

The following sections describe this three-step parameter derivation process. Figure 3.1 shows a flow chart of this process.

3.1 Sediment transport equation

The total sediment loss model used in this study is derived from the equation described in Willgoose and Riley (1993) of the form:

$$q_{sw} = \beta_2 q_w^{m_1} S^{n_1} \tag{3.5}$$

where:

q_{sw} = sediment discharge/unit width (g s^{-1} m^{-1})

q_w = discharge/unit width (L s^{-1} m^{-1})

S = local slope (m/m)

β_2, m_1 and n_1 are parameters fixed by flow geometry and erosion physics. Equation 3.5 incorporates a shear stress component as described by Willgoose and Riley (1993). Willgoose and Riley (1993) used this equation form to fit parameter values for a relationship between instantaneous discharge and sediment discharge. Smith and Bretherton (1972) considered that the equation applies to all elements of a surface ie, channel or nonchannel elements and applies to bedload transport. However, they also considered that an equation of this form may apply to total sediment transport.

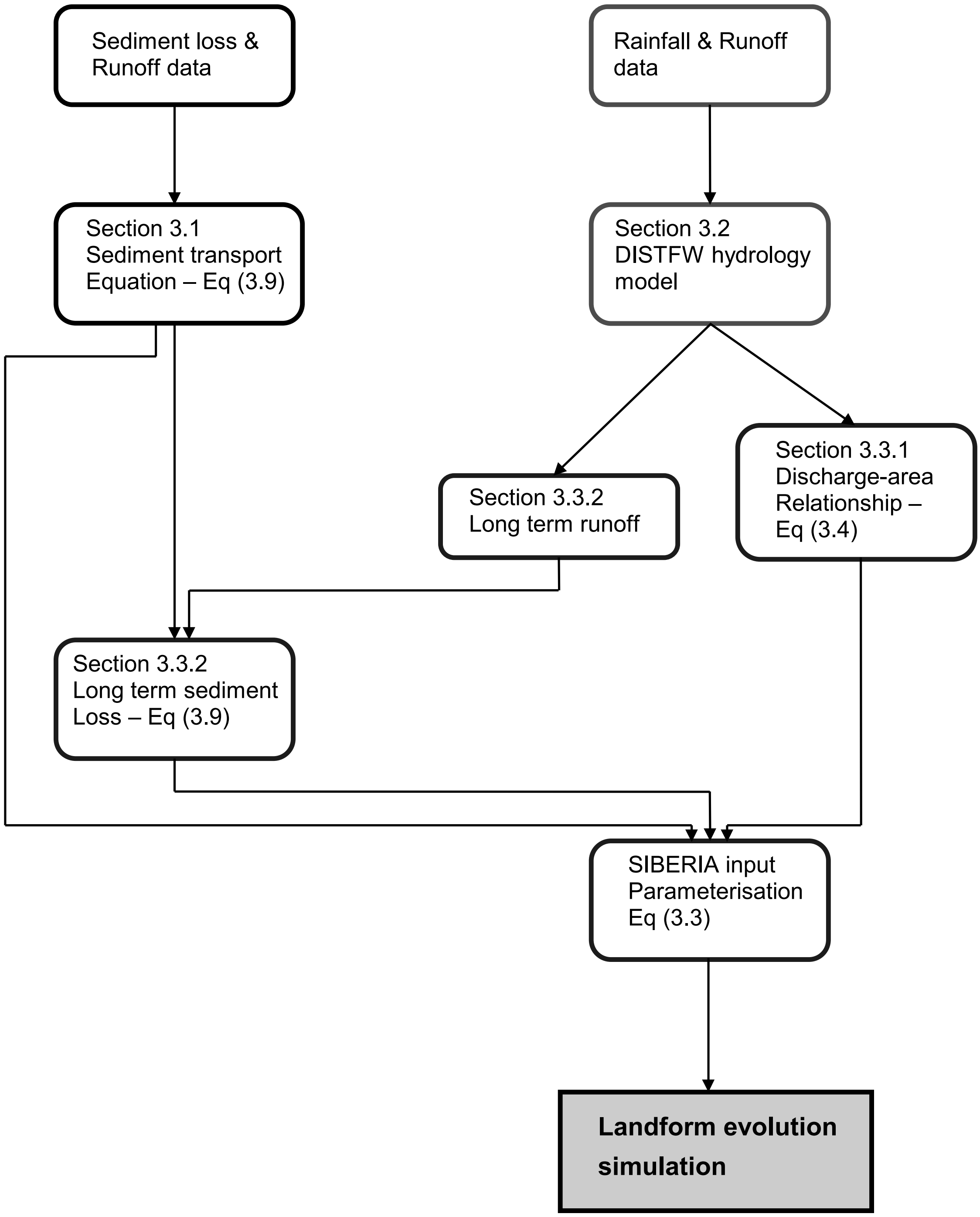

Figure 3.1 Flow chart showing the SIBERIA parameter value derivation process

From equation 3.5, total sediment discharge (Q_s) (g s^{-1}) can be determined by

$$Q_s = \beta_2 w q_w^{m_1} S^{n_1} \qquad (3.6)$$

where

w = width (m)

total instantaneous discharge (Q) is

$$Q = w\, q_W \text{ (L s}^{-1}\text{)} \qquad (3.7)$$

Therefore Q_s can be expressed as

$$Q_s = \beta_2 w^{(1-m_1)} Q^{m_1} S^{n_1} \qquad (3.8)$$

Total sediment loss (T) (g) during a rainfall event can be determined from the following equation

$$T = \beta_2 S^{n_1} w^{(1-m_1)} \int Q^{m_1} dt \qquad (3.9)$$

where

$\int Q^{m_1} dt$ = cumulative function of runoff over the duration of the event

3.1.1 Sediment transport equation: Parameter fitting

The parameters n_1, m_1 and β_2 in equation 3.9 were fitted using log-log linear regression.

Equation 3.9 above can be expressed as

$$log\ T = log\ \beta_2 + n_1\ log\ S + x\ log\ Y \qquad (3.10)$$

where

$$Y = w^{(1-m_1)} \int Q^{m_1} dt \qquad (3.11)$$

To fit m_1, an arbitrary value of m_1 was selected and used to determine a value for $\int Q^{m_1} dt$ (cumulative Q^{m_1}) for each event. This value was then used for Y in equation 3.10 for regression analysis. This process was continued until the value of the coefficient, x, was equal to 1. The m_1 value for the condition, $x = 1$, was selected as the fitted value. Log β_2 was fitted as a constant.

3.2 Calibration of DISTFW rainfall-runoff model parameters

The DISTFW model is a digital terrain rainfall-runoff model based on the sub-catchment based Field-Williams Generalised Kinematic Wave Model (Field & Williams 1983, 1987). The model and its application to mine spoils and waste rock have been described in detail by Willgoose and Riley (1993), Finnegan (1993), Arkinstal et al (1994) and Willgoose and Kuczera (1995). DISTFW divides a catchment into a number of sub-catchments connected together with a channel network draining to a single catchment outlet.

The model includes (Finnegan 1993):

1. Nonlinear storage of water on the hillslope surface
2. Philip infiltration (Philip 1969) from the surface storage to the channel

3. Discharge from the surface storage to the channel
4. Discharge from ground water storage to the channel
5. Routing of the runoff in channels by use of the kinematic wave (Field 1982)

Hortonian runoff is modelled.

The DISTFW uses digital terrain map (DTM) data on a square grid and each grid is considered to be a sub-catchment. Drainage from node to node and through nodes occurs by a kinematic wave on the overland flow. The kinematic assumption that friction slope equals the bed slope is used and discharge is determined from the Mannings equation. For this study, it was assumed that infiltration drained to a very deep aquifer and did not discharge to the surface within a study site so the groundwater component of the model was disabled.

Antecedent soil moisture (initial wetness) is difficult to measure prior to a rainfall event. Therefore it was assumed that antecedent soil moisture was low so initial wetness was set low in the model. Initial wetness can be adjusted for individual events to improve fitted hydrograph volume.

The parameters fitted in this study were:

- sorptivity (initial infiltration) Sphi
- long-term infiltration phi
- kinematic wave speed c_r and exponent e_m
- timing, the amount the predicted hydrograph leads the data, when necessary to allow for errors in timing in data collection

Parameters were fitted using a non-linear regression package, NLFIT version 1.10g (Kuczera 1989, 1994) as provided by the University of Newcastle. Basically, an observed rainfall event and the resulting discharge hydrograph are used to derive the best fit model parameter values that produce a predicted hydrograph similar to the observed hydrograph.

3.2.1 NLFIT Regression program suite

NLFIT is a suite of FORTRAN programs that can be used for regression using complex non-linear models of the form (Kuczera 1994):

$$q_t = f(x_t, \beta) + \varepsilon_t \qquad t = 1,.........,n \tag{3.12}$$

where

q_t = an observed response

x_t = an input vector

$f(x_t, \beta)$ = a predicted response vector

ε_t = a random error

The programs of the suite are, NLFIT, RESPONSE, EDPMF, PREDICT and COMPAT. The programs NLFIT, PREDICT and COMPAT were available and used in this study.

The following summary of the three programs used is taken from Kuczera (1994):

- NLFIT uses observed data and prior information on model parameters to fit parameter values to a predictive model, in this case the DISTFW model.

- PREDICT computes predicted responses with approximate prediction or confidence limits for a future input time series. If a rainfall-runoff event is measured the fitted parameter values using NLFIT can be tested. The measured data are used in PREDICT with calibrated parameter values and a predicted hydrograph and prediction limits are produced. The observed points are also plotted and the graphics show whether or not an acceptable number of observations fall within the limits and if the observed hydrograph follows the predicted hydrograph with the required degree of certainty.
- COMPAT can be used to assess the statistical compatibility of parameters calibrated to the model. This is necessary when for the same site different parameter values are derived for different rainfall and runoff data sets. The program uses .PMF files of different data sets and produces graphic ellipses which indicate the approximate region that the fitted parameters have a 95% chance of falling within. That is they have a 5% chance of falling outside these areas. When the ellipses intersect the parameter values can be considered not to be statistically different.

3.2.2 DISTFW-NLFIT input files

The version of the DISTFW model used has been interfaced with NLFIT (Willgoose et al 1995). This interface allows the user to fit (1) parameters to a single rainfall event or rainfall simulation event for a single site, (2) a number of events at a single site or (3) to fit parameters across a number of sites (this mode has not been used in this study).

To fit parameters to the DISTFW model using NLFIT an input data file (.FW) is required (Willgoose et al 1995). For DISTFW-NLFIT the input file can have one of three formats: (1) a constant width plot, (2) a standard sub-catchment or (3) a DTM grid based catchment. In this study a constant width plot (type 1) .FW file was used for the batter site and standard sub-catchment (type 2) .FW files were used for the cap, soil and fire site. Examples of these files are shown in appendix A.1 (batter site). Details of the requirements of these input files are given in Willgoose et al (1995).

Site topographic survey information is used to determine input for three parts of the file: INCIDENCES, PARAMETERS and CONVEYANCES.

Using the contour maps produced from site surveys, sub-catchments are mapped for study sites. Flow paths through the sub-catchments are used to determine what sub-catchments drain into other sub-catchments which are identified by a unique number. The flow paths are then used to set up a matrix describing the sub-catchment INCIDENCES. For constant width plots (appendix A.1) there is only one row describing the INCIDENCES as each sub-catchment only receives flow from the sub-catchment immediately upstream. For the standard sub-catchment type plot there may be several rows each one reflecting the number of different sub-catchments draining into a catchment.

The physical properties for each sub-catchment for the study plots are given in tables 3.1, 3.2, 3.3 and 3.4. These properties, area, length and upstream and downstream elevation (slope) and model parameters with default values of 1.0 are tabulated in the PARAMETER part of the .FW file. The sub-catchment or plot area is measured from the contour plan using a planimeter, the length is measured along the flow path and width is the average width normal to the flow path. Therefore, because of the tortuosity of the flow paths, multiplying the length by the width does not necessarily give the area shown in the tables 3.1 to 3.4. Elevations are taken from the contour plan.

Table 3.1 Physical properties of the sub-catchments on the cap site

Sub-catchment No.	Area (m^2)	Length (m)	Width (m)	Slope (m/m)	1/width$^{2/3}$
1	73.7	18.0	5.0	0.021	0.341
2	105.1	17.1	7.2	0.021	0.268
3	31.6	12.5	3.0	0.034	0.484
4	37.3	12.0	3.8	0.034	0.412
5	5.2	5.3	0.5	0.025	1.587
6	39.3	16.1	2.7	0.036	0.513
7	62.0	17.4	4.1	0.033	0.388
8	30.3	7.5	4.2	0.036	0.386
9	55.8	3.8	1.7	0.009	0.716
10	44.5	14.0	3.6	0.028	0.428
11	61.3	9.8	6.9	0.020	0.276
12	42.6	10.1	4.7	0.046	0.357
13	2.5	1.5	3.5	0.047	0.481

Table 3.2 Physical properties of the constant width plot batter site

Sub-catchment No.	Area (m^2)	Length (m)	Width (m)	Slope (m/m)	1/width$^{2/3}$
1 to 10	60.0	3.77	15.9	0.207	0.158

Table 3.3 Physical properties of the sub-catchments on the soil site

Sub-catchment No.	Area (m^2)	Length (m)	Width (m)	Slope (m/m)	1/width$^{2/3}$
1	85.7	16.42	4.05	0.022	0.394
2	75.0	20.10	3.88	0.021	0.405
3	71.2	18.76	4.24	0.014	0.382
4	28.8	10.05	2.99	0.021	0.482
5	7.1	4.86	1.76	0.033	0.686
6	23.8	7.37	4.43	0.033	0.371
7	17.7	6.7	2.32	0.042	0.571
8	18.8	8.71	2.23	0.032	0.586
9	13.7	6.03	2.36	0.003	0.564
10	41.4	15.24	2.79	0.012	0.505
11	30.1	10.72	2.88	0.014	0.494
12	4.1	1.59	2.53	0.019	0.539
13	37.3	10.05	3.5	0.006	0.434
14	15.3	6.00	2.55	0.020	0.536
15	11.3	3.02	4.3	0.079	0.378
16	34.4	10.39	3.78	0.020	0.412
17	11.6	3.85	3.13	0.039	0.467
18	8.8	4.19	2.16	0.017	0.598
19	1.9	1.09	0.8	0.028	1.160
20	30.9	13.07	2.26	0.011	0.581
21	30.7	12.06	2.59	0.014	0.530
22	0.01	0.20	0.0028	1.250	50.3

Table 3.4 Physical properties of the sub-catchments on the fire site

Sub-catchment No.	Area (m^2)	Length (m)	Width (m)	Slope (m/m)	$1/width^{2/3}$
1	47.6	12.0	3.6	0.028	0.425
2	31.5	15.7	2.1	0.022	0.602
3	10.1	2.7	3.3	0.019	0.449
4	5.6	1.7	2.8	0.035	0.503
5	34.9	8.5	3.8	0.023	0.409
6	25.9	6.3	4.6	0.010	0.363
7	42.6	16.5	2.2	0.021	0.597
8	24.8	8.0	3.0	0.026	0.483
9	21.5	8.8	2.7	0.017	0.521
10	22.8	11.3	1.9	0.013	0.659
11	15.8	4.7	2.9	0.041	0.489
12	22.9	9.1	2.5	0.033	0.546
13	28.6	9.7	2.3	0.046	0.576
14	24.2	10.9	2.5	0.029	0.544
15	34.2	8.5	4.4	0.039	0.374
16	7.4	3.7	1.7	0.059	0.713
17	17.7	6.8	2.5	0.078	0.543
18	13.0	6.5	2.7	0.031	0.512
19	22.7	10.9	2.6	0.046	0.529
20	14.9	4.7	2.4	0.028	0.561
21	2.2	1.2	1.1	0.042	0.922
22	2.3	1.9	1.6	0.016	0.725
23	31.9	9.3	3.3	0.050	0.456
24	25.9	9.6	2.5	0.050	0.539
25	60.2	18.4	3.2	0.035	0.464
26	14.7	4.0	3.6	0.080	0.424
27	0.01	0.2	0.0028	1.600	50.3

CONVEYANCES are then input for each catchment. For the constant width plot there is only one set of parameters because they are the same for each sub-catchment. For catchment and DTM mode there is a set of parameters for each sub-catchment. The first line gives the catchment number and the number of conveyance parameters. The parameters are kinematic wave parameters, c_r and e_m, and the maximum discharge for these values. All values except c_r are set to default values. A nominal value for c_r is determined using the following equation:

$$c_r = 1/w^{2/3} \tag{3.13}$$

where w is the width of the catchment.

For the soil and fire sites the collection trough at the down-slope end of the plot is considered to be the ultimate downstream catchment collecting all runoff from the plot. This is because more than one catchment drains to the trough. The trough catchment was given a small area, length and width and a very steep slope and this resulted in a high nominal value for c_r which models fast runoff through the trough.

RAINFALL is input using a two column text file (.RF file) (appendix A.2). The first column gives time and the second gives cumulative rainfall (mm) (described as CUMPLUVIO in the

.FW file). This file must have the same event starting time as the .FW file and if multiple rainfall event files are input each must have the same starting and finishing time. The model has the capability to apply a rainfall weighting to each sub-catchment. However, it is very difficult to obtain rainfall amounts for each sub-catchment when monitoring natural events therefore each sub-catchment is given a rainfall weighting of 1.0 when monitoring data are used.

RUNOFF is input using a two column text file (.RO file) (appendix A.3). The first column gives time and the second gives instantaneous discharge ($m^3\ s^{-1}$). This file must have the same event starting time as the .FW and .RF files and if multiple events are input each must have the same starting and finishing time.

3.2.3 Calibration procedure

The parameter calibration procedure using DISTFW-NLFIT is that described in Arkinstal et al (1994) and Willgoose et al (1995). It is a multi-stage process that ensures that a global optimum for the parameters is achieved. The stages are aimed at gradually refining parameter estimates as the observed hydrograph is better fit by the model simulations, and with only those parameters explicitly mentioned being calibrated at any given stage.

1. **Start:** Nominal parameters were chosen. The initial wetness (V) and timing error were set as very small (0.0001 mm and 0.0001 s respectively). The groundwater store supply was set as large (Cg = 1000 mm hr^{-1}) to ensure that no water came from the groundwater, and the surface water supply co-efficient and dimensionless exponent were set low (Cs = 0.003 $m^{(1-2\gamma)}\ s^{\gamma}$) and $\gamma = 0.375$ respectively) so that water flowed out of the surface storage into the kinematic wave without significant routing.
2. **Initialisation:** The long-term infiltration rate (phi – mm h^{-1}) and kinematic rate (c_r - $m^{(3-2m)}\ s^{-1}$) were calibrated to the complete hydrograph to obtain an approximately correct mass balance and timing of the hydrograph rise.
3. **Infiltration:** The sorptivity (Sphi – mm $h^{-0.5}$) and phi were calibrated to the complete hydrograph to accurately distribute losses between initial and continuing losses.
4. **Kinematic wave:** c_r was calibrated to the falling limb of the hydrograph and at the same time e_m, to accurately fit the timing of the hydrographic rise and fall.
5. **Timing:** If there were obvious problems in fitting the timing of the hydrograph, timing was then fitted. Timing is normally only fitted when multiple events are simultaneously used for calibration.
6. **Initial wetness:** Where problems with hydrograph volume were obvious, initial wetness was fitted to individual events.
7. **Polishing:** All parameters calibrated in stages 2 to 6 were simultaneously fitted on the whole hydrograph.

Parameters were fitted, using the above procedure, to the hydrographs for observed storms.

At the conclusion of parameter fitting, NLFIT output files (.PRT, .PMF) (see example, appendixes A.4 and A.5) were generated. The .PRT files are used to produce graphic output and .PMF files are used in COMPAT and PREDICT.

3.3 SIBERIA parameter derivation

Once parameters have been fitted to the sediment transport equation 3.9 and the DISTFW rainfall-runoff model for a site, the results are used to derive SIBERIA input parameters for the landform to be modelled. In this study the landform used was the ‘above-grade’ option for

ERARM initially proposed in 1987 (Unger & Milnes 1992). Determination of parameters for SIBERIA has previously been described by Willgoose and Riley (1993).

The parameters of SIBERIA represent temporal average properties of landscapes and the process over the long term. The parameter values derived for the soil loss and the DISTFW model represent instantaneous values (Willgoose & Riley 1993).

The SIBERIA parameter derivation process involves several steps as described below and is based on the description given by Willgoose and Riley (1993).

3.3.1 Scale analysis: Discharge area relationship

The parameters fitted here define how discharge used in the calculation of sediment transport rate varies with catchment area.

The area discharge relationship is described by the following equation (Willgoose & Riley 1993):

$$q_p = \beta_p A^{m_3} S^{n_3} \tag{3.14}$$

where, q_p = peak discharge, β_P = runoff rate constant, A = area and m_3 and n_3 are fitted parameters.

The equation was fitted using the peak discharges and areas for the largest single catchment on the 30 m digital terrain map of the ERARM 'above-grade' option (fig 3.2).

This catchment was defined by Willgoose and Riley (1993) who considered that hydrological responses of the catchment would be typical of other catchments on the proposed landform. This catchment was approximately 1.6 km^2 and contained 1773 nodes each 900 m^2. The DTM based version of the DISTFW model was used to predict peak discharges of areas in the catchment for mean annual rainfall events. Willgoose and Riley (1993) chose storms of various duration for a 1 in 2 year average return interval (ARI). The mean ARI is 2.33 years which Willgoose et al (1989) showed is the storm that relates the instantaneous erosion physics with long term physics. Since the ARI is used solely to determine the exponents on area and slope in equation 3.14 use of the 1 in 2 year rather than 2.33 year is considered satisfactory, and consistent with the index flood approach to flood frequency analysis (Pilgrim 1987). Accordingly, in the SIBERIA calibration procedure β_3 is normally set to 1, with runoff rate being implicitly calculated and allowed for in the long-term sediment transport analysis of section 3.3.2.

The steps were:

1. Parameters for the DISTFW hydrology model were derived for the study sites using the method described above in section 3.2 – Calibration of DISTFW rainfall-runoff model parameters.
2. From temporal patterns from the Australian Rainfall and Runoff (Pilgrim 1987) rainfall rates for 2 year ARI storms of various duration were determined. The storm durations were 10 min, 15 min, 20 min, 25 min, 30 min, 45 min and 60 min.
3. This step used .FW input files for the stand-alone version of the DISTFW model. Each file used rainfall input files for 2 years ARI storms developed in step 2 above and DTM data for the selected 1.6 km^2 catchment. The parameter multipliers in the .FW files were changed to those derived for step 1 above. That is c_r, e_m, Sphi and phi were changed, the remaining parameters stayed at default values.

4. The DISTFW stand-alone version was run using the .FW input file for each storm duration with the amended multipliers and a peak discharge file for each event was output (.PKDS). The .PKDS file has two columns: (1) the node number and (2) the peak discharge from that node (a node may also drain upstream nodes).
5. The .PKDS files were parsed into a spreadsheet and the maximum peak discharge for each node determined. The peak discharge values were then fitted (log-log linear regression) against the corresponding area discharging through the corresponding node giving values for β_p and m_3 in equation 3.14. This gives the value for m_3 in equation 3.4.
6. Since there were no major changes in the slope (S) in the selected catchment, Willgoose and Riley (1993) ignored the dependence of slope giving $n_3 = 0$.

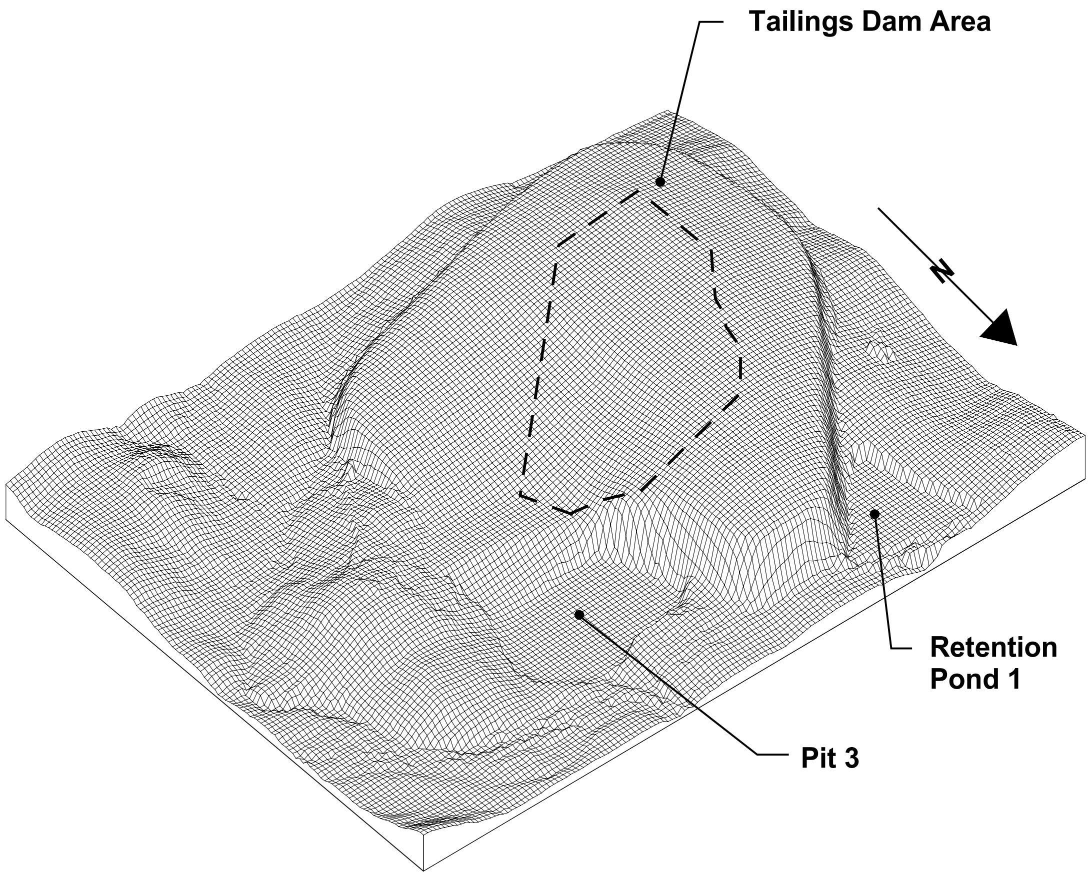

Figure 3.2 The ERARM above-grade option showing the 1.6 km² catchment (from Willgoose & Riley 1993)

3.3.2 Runoff series and long-term sediment loss rate

The runoff series for the Jabiru historical rainfall record was then created. This series was used to determine long-term erosion rate (q_s) in equation 3.3.

The 1.6 km² catchment was again used in an input .FW file (abovehyd.FW) containing DTM data for the catchment.

The steps were:

1. The parameters fitted to the DISTFW in step 1 section 3.3.1 were put in to the .FW file. The input .RO file was runoff from a measured rainfall event. Using this .FW file in the DTM version of the DISTFW model, a discharge file (.PRD1) was produced for the catchment.
2. The .PRD1 file was then converted to a .RO file (runoff).
3. The c_r parameter was then fitted to the catchment using the DISTFW model sub-catchment mode using the input file calib-1.33.FW which describes the 1773 DTM nodes of the catchment in terms of 10 sub-catchments. The .RO file produced in step 2 above and the measured rainfall event were input to calib-1.33.FW and the .FW file was used in NLFIT. All parameters were held constant and c_r was refitted.
4. These parameters were then used to generate long-term runoff for several years of the Jabiru rainfall record. The sub-catchment model of the stand-alone version of the DISTFW model was used because of the large amount of computer processing time required to generate a runoff series using DTM data. The new parameters with the exception of Sphi, fixed at 0.0001 mm hr^{-05} which indicates a saturated catchment and is conservative, were used in an .FW file with an annual rainfall pattern taken from pluviograph records for Jabiru. This produced an annual runoff file (.PRD1) for the 1.6 km^2 catchment.
5. The annual runoff determined in step 4 above was then used in the soil loss equation (3.9) (w = 1 for nodes) to determine an annual sediment loss (Mg y^{-1}) which was converted to a volume (m^3 y^{-1}) by dividing by the bulk density of the waste rock material. Using the annual sediment losses a long term average sediment loss rate was then determined (q_s) for equation 3.3.
6. The value for q_s was then used to determine β_1 (equation 3.3). The value of m_1 and n_1 were those fitted for equation 3.9.

3.3.3 Slope correction

The q_s value (equation 3.3) is derived for a value S = 1 m/m therefore β_1 (equation 3.3) needs to be corrected for use in SIBERIA. In SIBERIA, A is considered to be in nodes ie each node is considered to be 1 unit area, and S reflects the number of metres drop between nodes which are 30 m apart for the DTM. But S for the soil loss equation is in m/m. To correct this in SIBERIA β_1 must be reduced to reflect the slope calculated by SIBERIA and the correction factor is as follows

$$\frac{1}{(DTM\ spacing)^{n_1}} = \frac{1}{30^{n_1}} \tag{3.15}$$

The value β_1 parameter used in SIBERIA must be multiplied by the correction factor derived in equation 3.15.

4 Derivation of sediment transport and DISTFW rainfall-runoff model parameters using monitoring data

SIBERIA modelling requires input from the sediment transport model and the DISTFW rainfall-runoff model. Data from rainfall-runoff events are required to parameterise these models which are then used with natural rainfall data to derive annual runoff series and soil loss. Meyer (1994) considered that 'To obtain realistic estimates of annual erosion rates, results from long-term studies under natural rainfall are required…'. A natural rainfall monitoring program was undertaken to collect the necessary data.

In the study area the seasonal rainfall of the wet/dry tropics provided a good opportunity to obtain natural rainfall data. However, collection of these data was difficult and labour intensive. To parameterise the models complete data sets of sediment loss, rainfall and runoff are required. This requires an observer to be present on site during rainfall events. Not all sites could be monitored simultaneously. This chapter reports the results of natural rainfall monitoring and the derivation of model parameters for use in SIBERIA.

4.1 Results of monitoring of natural rainfall events

The four study sites were monitored during natural rainfall events as described in section 2.3 – Monitoring of natural rainfall events. Because of plot size and location, labour costs and the difficulty of monitoring the sites (essentially impossible to automate field sampling), it was not possible to replicate the treatments. 48 events were monitored on the cap site, 32 events were monitored on the batter site, 43 events were monitored on the soil site and 35 events were monitored on the fire site. Of these events, 5 complete data sets were obtained on the cap site, 4 complete data sets were obtained on the batter site, 10 complete data sets were obtained on the soil site and 9 complete data sets were obtained on the fire site. With respect to sediment loss, only the events where complete data sets were obtained are reported.

4.1.1 Rainfall and hydrology

Total rainfall, maximum 10 minute rainfall intensity (I_{10}), total discharge and runoff coefficient for the monitored rainfalls are given in table 4.1. Cumulative rainfall and runoff hydrographs are given in appendix B.

4.1.2 Sediment loss

Event sediment losses are given in table 4.1 and suspended sediment discharges are given in appendix B.

4.1.3 Discussion

Total rainfall ranged from 6 mm to 50 mm and I_{10} range from 24 mm h^{-1} to 132 mm h^{-1}. The mean runoff coefficients (and standard deviations) for the sites were; batter – 0.41 (0.13), cap – 0.77 (0.18), soil – 0.10 (0.03) and fire – 0.04 (0.02). The batter site event on 16 November 1993 had a low runoff coefficient (0.19) compared with the other events on that site and the cap site event on 21 February 1994 had a high runoff coefficient (1.06) compared with the other events on that site. The runoff coefficient >1 on the cap site on 21 February 1994 could be due to observer error. A coefficient >1 may be possible if runoff was still occurring from a previous event when the monitored event started.

Generally, bedload sediment was the greatest portion of total sediment loss (table 4.1). For all sites there is variation between events in the amount of sediment loss per unit runoff. Discharge and sediment loss per unit runoff were much greater on the cap and batter site than on the soil and fire site for events with similar total rainfall and I_{10}. This indicates the effect vegetation and surface ripping has on discharge and soil loss.

Table 4.1 Monitored rainfall data

Site	Date	Total rainfall (mm)	I_{10}[a] (mm h^{-1})	Total discharge (L)	Runoff coefficient	Suspended sediment loss (g) [Loss per unit runoff (g L^{-1})]	Bedload loss (g) [Loss per unit runoff (g L^{-1})]	Total sediment loss (g) [Loss per unit runoff (g L^{-1})]
Batter	22 Feb 93[b]	7	24	2194	0.52	97 [0.04]	388 [0.18]	485 [0.22]
	18 Mar 93[b]	16	84	4375	0.46	3041 [0.70]	12000 [2.74]	15041 [3.44]
	16 Nov 93[b]	20	44	2021	0.19	263 [0.13]	1079 [0.53]	1341 [0.66]
	09 Dec 93[b]	50	119	14328	0.48	8881 [0.62]	36017 [2.51]	44898 [3.13]
Cap	16 Nov 93[b]	18	54	6509	0.61	4440 [0.68]	6074 [0.93]	10514 [1.62]
	09 Dec 93[b]	49	132	21638	0.75	18930 [0.87]	25007 [1.16]	43937 [2.03]
	10 Dec 93[b]	11	30	4450	0.68	721 [0.16]	814 [0.18]	1535 [0.34]
	20 Dec 93[b]	9	48	3013	0.57	611 [0.20]	2767 [0.92]	3377 [1.12]
	21 Feb 94	16	54	9988	1.06	1683 [0.17]	2914 [0.29]	4597 [0.46]

a Maximum 10 minute rainfall intensity.

b These event data were used in model parameter derivation (section 4.2)

Table 4.1 continued

Site	Date	Total rainfall (mm)	I_{10}[a] (mm h^{-1})	Total discharge (L)	Runoff coefficient	Suspended sediment loss (g) [Loss per unit runoff (g L^{-1})]	Bedload loss (g) [Loss per unit runoff (g L^{-1})]	Total sediment loss (g) [Loss per unit runoff (g L^{-1})]
Soil	17 Jan 95	7	34	288	0.07	30 [0.10]	118 [0.41]	148 [0.51]
	19 Jan 95[b]	18	68	1397	0.13	112 [0.08]	325 [0.23]	437 [0.31]
	20 Jan 95	10	56	596	0.10	59 [0.10]	556 [0.93]	615 [1.03]
	25 Jan 95	39	118	2303	0.10	251 [0.11]	890 [0.39]	1141 [0.50]
	27 Jan 95	7	37	269	0.06	19 [0.07]	86 [0.32]	105 [0.39]
	10 Feb 95[b]	20	55	1142	0.10	89 [0.08]	278 [0.24]	367 [0.32]
	18 Feb 95[b]	48	121	4020	0.14	676 [0.17]	1358 [0.34]	2034 [0.51]
	28 Feb 95	28	73	1805	0.11	299 [0.17]	327 [0.18]	626 [0.35]
	08 Mar 95	12	74	956	0.13	108 [0.11]	235 [0.25]	343 [0.36]
	27 Mar 95[b]	8	42	242	0.05	27 [0.11]	58 [0.24]	85 [0.35]
Fire	17 Jan 95	6	31	122	0.03	10 [0.08]	92 [0.75]	102 [0.84]
	19 Jan 95	13	50	356	0.05	40 [0.11]	99 [0.28]	139 [0.39]
	20 Jan 95	7	41	66	0.02	9 [0.14]	43 [0.65]	52 [0.79]
	25 Jan 95	44	128	1254	0.05	120 [0.10]	248 [0.20]	368 [0.29]
	10 Jan 95	20	59	443	0.04	35 [0.08]	39 [0.09]	74 [0.17]
	18 Feb 95	38	90	1384	0.06	70 [0.05]	438 [0.32]	508 [0.37]
	28 Feb 95	33	86	853	0.04	95 [0.11]	268 [0.32]	363 [0.43]
	01 Mar 95	14	44	130	0.02	16 [0.12]	107 [0.82]	123 [0.94]
	27 Mar 95	8	37	63	0.01	12 [0.19]	14 [0.22]	26 [0.41]

a Maximum 10 minute rainfall intensity.
b These event data were used in model parameter derivation (section 4.2)

Monitoring provided data on storms with a range of total rainfall and rainfall intensity. For the high intensity storms the results (table 4.1) did not agree with the analysis by Evans and Loch (1996) which discussed the unexpected observed higher sediment losses under rainfall simulation (Evans et al 1996) for the lower-sloped cap site than the steeper-sloped batter site and the effect of surface material properties of the sites. For the events on 09 December 1993, similar sediment losses occurred from the cap and batter site even though there was much less runoff from the batter site. For similar medium intensity storms (16 November 1993) there was much greater total discharge and sediment loss from the cap site than the batter site, which agrees with the RUSLE predictions for the cap and batter sites (Evans & Loch 1996). For similar low intensity events (cap 10 December 1993; batter 22 February 1993) there was greater sediment loss and discharge from the cap site. The RUSLE predictions appear to have been valid for small and medium sized events only.

The data from the fire site were not used in model parameter derivation. The vegetation understorey on the fire site was extremely dense and was burnt before the plot was surveyed but after the data were collected. After burning and surveying it was realised that catchments 21 and 22 on the plot formed a deep depression with a crack at the lowest point. Much of the runoff from the plot ran into this depression and did not discharge from the plot into the outlet trough, resulting in very small runoff coefficients (table 4.1). It was considered that this depression was not representative of the vegetated area where the plot was constructed.

4.2 Model parameterisation

The monitoring data were used to parameterise (1) the sediment transport model (section 3.1) and (2) the DISTFW rainfall-runoff model (section 3.2). The results of this parameterisation are used to derive long-term average parameters for the SIBERIA model (section 3.3) reported in chapter 5.

4.2.1 Sediment transport model

Using all data (table 4.1) (except fire site), parameters were fitted to the sediment transport model with a 'lumped' coefficient. The effect of width term (w) has been shown to be insignificant for these sites (Evans 1997) and was excluded. This resulted in the following total sediment loss–discharge relationship for the study sites:

$$T = 0.55 \int Q^{1.38}\, dt \quad (r^2 = 0.89;\ p < 0.001) \tag{4.1}$$

A test was conducted for outliers in the data using standardised residuals (Hair et al 1995). This analysis (fig 4.1) indicated that observation 14 (batter 09 December 1993) was outside the upper threshold (2 standard deviations) and observation 19 (cap 21 February 1994) was outside the lower threshold (-2 standard deviations). These data points were removed and regression analysis was conducted using the remaining data points resulting in the following relationship:

$$T = 0.57 \int Q^{1.38}\, dt \quad (r^2 = 0.90;\ p < 0.001) \tag{4.2}$$

The removal of the outliers had little effect on the significance of the relationship.

Using the data with outliers omitted, the sediment loss model (equation 3.9) was fitted giving the following:

$$T = 0.66\, S^{0.04} \int Q^{1.37}\, dt \quad (r^2 = 0.90;\ p < 0.001) \tag{4.3}$$

The slope (S) exponent (n_1 in equation 3.9) of 0.04 is small and effectively results in a slope term of unity for most slopes. This indicates that the data may not be sufficiently sensitive to fit a realistic n_1 parameter value.

Willgoose and Riley (1993) derived an n_1 value of 0.69 for the ERARM waste rock dump using combined rainfall simulation and monitoring data from cap and batter site plots. Evans et al (1997), using a laboratory rainfall simulator and mine spoil samples from Central Queensland, found that for one mine site the CREAMS erodibility parameter (K) was inversely proportional to $S^{0.624}$ (ie $K \propto \frac{1}{S^{0.624}}$). Other researchers (Foster 1982, Watson & Laflen 1986, Guy et al 1987) derived slope exponents ranging from 0.26 to 0.8. It appears that the value of 0.69 derived by Willgoose and Riley (1993) may be a more realistic value than the one derived here. Based on this, n_1 was fixed at 0.69 and equation (6.2) was refitted to give the following equations for the three sites:

$$T_{cap} = 6.66\, S^{0.69} \int Q^{1.38}\, dt \quad (r^2 = 0.90;\ p < 0.001) \tag{4.4}$$

$$T_{batter} = 1.67\, S^{0.69} \int Q^{1.38}\, dt \quad (r^2 = 0.90;\ p < 0.001) \tag{4.5}$$

$$T_{soil} = 11.9\, S^{0.69} \int Q^{1.38}\, dt \quad (r^2 = 0.90;\ p < 0.001) \tag{4.6}$$

The fitted relationships (equations 4.3 to 4.6) are all significant but under-predict high sediment loss events (fig 4.2). Soil losses predicted using equation 4.3 are similar to those predicted using the three site-specific equations (equations 4.4, 4.5 and 4.6) (fig 4.2).

It was of concern that the high sediment loss events were under-predicted by up to a factor of two by equations 4.3, 4.4 and 4.5. This may result from the different number of data points for each site. There were twice the number of data points on the soil site, all representing low sediment loss events. This may have biased the relationships toward the soil site. The high intensity event on the cap site on 09 December 1993 removed 69% of the total sediment removed by the five reported events (table 4.1). Similarly the same event on the batter site removed 73% of the total sediment removed by the four reported events. A similar trend was observed on the soil site where high intensity events on 25 January 1995 and 18 February 1995 removed 54% of the total sediment removed by the ten reported events.

Similar dominance of large events has been reported in other studies. Over a 14-year period, Wockner and Freebairn (1991) found that out of 81 rainfall events that produced runoff at study sites on the eastern Darling Downs of Queensland, six storms caused 70% of the total soil erosion. Similarly, Edwards (1987) found that 10% of runoff events produced 90% of the total soil loss at long-term sites throughout the cropping regions of New South Wales. A 28 year study of hilly farmland in Ohio, USA, showed that the five largest erosion events on the studied watersheds were responsible for 66% of the total erosion (Edwards & Owens 1991). The form of the sediment transport model supports this. Henderson (1966) considered that $Q_s \propto Q^2$ (equation 3.8). Therefore flow which is ten times larger than average can carry 100 times the average sediment load because the power on Q is >1.

It is important that high sediment loss storms are accurately predicted, as one or two high intensity storms in a Wet season will remove much more sediment from the cap and batter site then a number of low sediment loss events on the soil site. Based on practical knowledge of the local natural system, representative storm events were selected from each site for regression analysis. Four storms, with similar total rainfall and I_{10} from each site were selected from the batter site, cap site and soil site (table 4.1) (fire site data were not included in the analysis). The number of storms selected were controlled by the batter site data set which had only four storms, including the outlier.

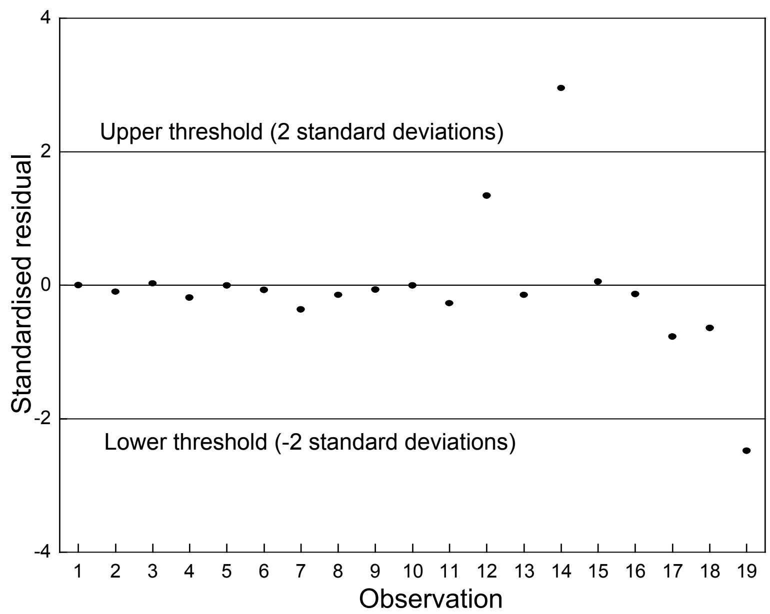

Figure 4.1 Plot of standardised residuals for equation (4.1).
Observations 14 and 19 appear to be outliers.

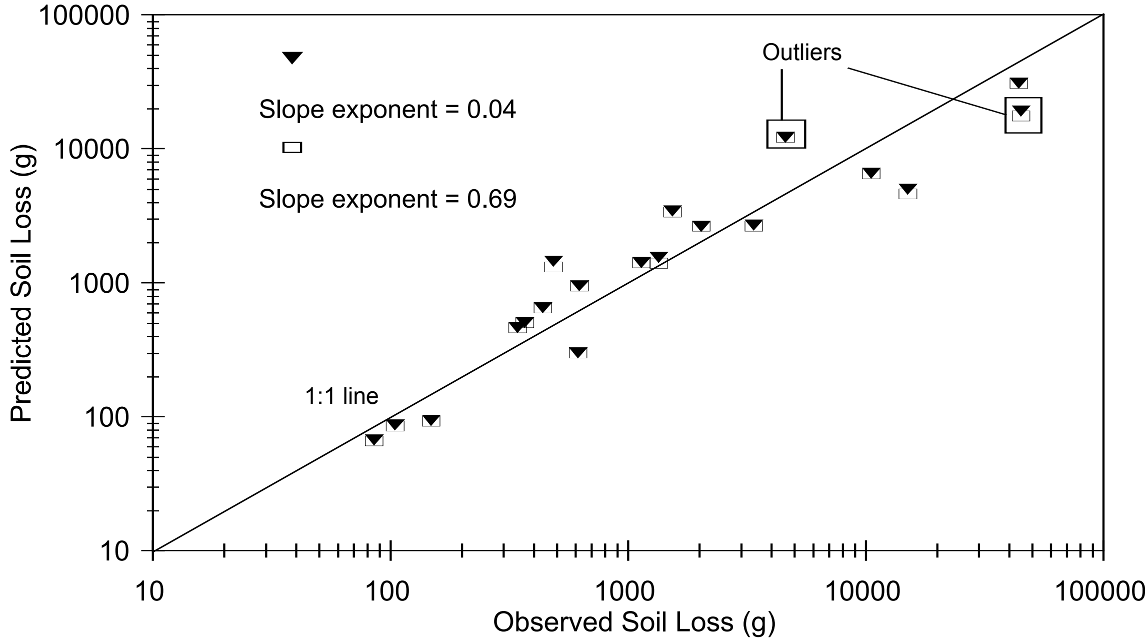

Figure 4.2 Relationship between predicted and observed sediment loss using equations 4.3 (n_1 = 0.04), 6.4, 6.5 and 6.6 (n_1 = 0.69)

The fitted sediment transport model using the selected representative storms was:

$$T = 0.61\, S^{0.06} \int Q^{1.57}\, dt \quad (r^2 = 0.92;\ p < 0.001) \tag{4.7}$$

Again the slope (S) exponent (n_1 in equation 3.9) of 0.06 is small and effectively results in a slope term of unity for most slopes. Therefore, n_1 was fixed at 0.69 and the model refitted giving:

$$T_{\text{cap}} = 5.79\, S^{0.69} \int Q^{1.59}\, dt \quad (r^2 = 0.92;\ p < 0.001) \tag{4.8}$$

$$T_{\text{batter}} = 1.46\, S^{0.69} \int Q^{1.59}\, dt \quad (r^2 = 0.92;\ p < 0.001) \tag{4.9}$$

$$T_{\text{soil}} = 10.4\, S^{0.69} \int Q^{1.59}\, dt \quad (r^2 = 0.92;\ p < 0.001) \tag{4.10}$$

Equations 4.7 to 4.10 are significant and are good predictors of observed sediment loss as predictions are well distributed around the 1:1 line (fig 4.3). Soil losses predicted using equation 4.7 are similar to those predicted using the three site specific equations (equations 4.8, 4.9 and 4.10) (fig 4.3). The sediment transport model constant (β_2) reflects differences between sites such as surface cover, surface treatment and erodibility. For these site specific equations the hydrograph volume ($\int Q^{m_1} dt$) explains 92% of the variation in sediment loss.

The discharge (Q) exponent (m_1) (equations 4.8, 4.9 and 4.10) of 1.59 derived here compares reasonably with the m_1 value of 1.68 derived for small cap and batter site plots by Willgoose and Riley (1993). These equations will be used to predict input into SIBERIA. It appears that for these data, n_1 has little effect on the soil loss model.

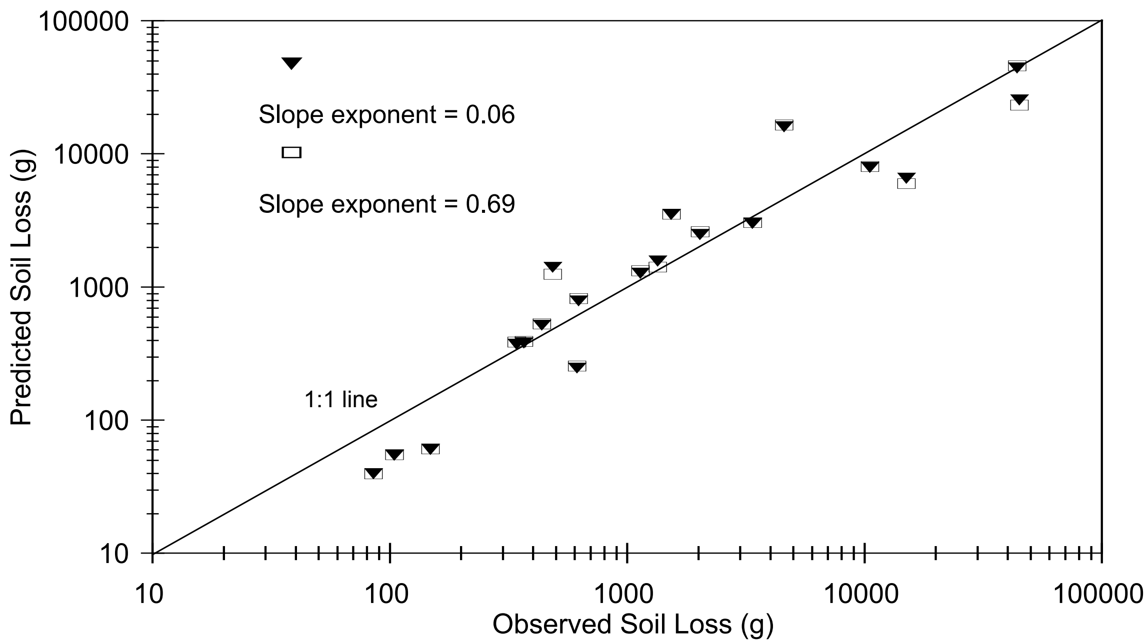

Figure 4.3 Relationship between predicted and observed sediment loss using equations 4.7 (n_1 = 0.06), 6.8, 6.9 and 6.10 (n_1 = 0.69)

It is an interesting observation that for the high sediment loss event on 09 December 1993, equation 4.8 closely predicted the observed sediment loss from the cap site (43 937 g observed; 46 094 g predicted) but equation 4.9 under-predicted sediment loss from the batter site by a factor of ≈0.5 (44 898 g observed; 23 414 g predicted). These equations predicted sediment loss from the cap site to be ≈2.0 times larger than that from the batter site. RUSLE predictions (Evans & Loch 1996) showed that sediment loss from the cap site would be 1.9 times greater than that from the batter site. There is excellent agreement between model predictions. It appears that parameters for this model and the RUSLE similarly reflect the differences in surface treatment between the two sites. However, the observed sediment loss from the batter site during the high intensity event on 9 December 1993 was similar to that observed on the cap site, a factor of ≈2.0 times greater than that predicted by the models. Slopes develop such that for average conditions most of the erodible material is removed leaving material which is below an entrainment threshold (Henderson 1966). After a slope has been exposed for a while most of the transportable material will have been removed. The remaining material will not be removed by small storms but only transported during large storms. This results in dramatically increased transport rates for larger erosion events.

It appears that for higher intensity storms on the cap and batter site the total sediment loss per unit runoff increases by an order of magnitude compared to losses for lower intensity storms (table 4.1), and that bedload is the major contributor to this increase, particularly on the batter site. This is observable for both high intensity events monitored on the batter sites (09 December 1993, I_{10} = 119 mm h^{-1} and 18 March 93, I_{10} = 84 mm h^{-1}). Although based on limited data points and further research is required for confirmation, it appears that for the 0.207 m/m batter slope a threshold discharge may have been reached above which the effect of slope outweighed the effect of surface treatment, and had a greater influence on sediment loss, resulting in a reduced sediment loss ratio between the two sites in contrast to that derived by Evans and Loch (1996).

4.2.2 Derivation of DISTFW Rainfall-Runoff Model Parameters

Parameters were fitted to observed rainfall and runoff for the monitored rainfall events using DISTFW-NLFIT (method described in section 3.2).

Parameter values were fitted to observed hydrographs for observed rainfalls for individual monitored events and to four hydrographs for each site simultaneously. The fitted hydrographs for the individual events are given in appendix B and the fitted and observed hydrographs for the multiple events are given in appendix C. Fitted parameter values are given in table 4.2. Parameters could not be fitted for the batter site event on 22 February 1993, therefore data for an event on 21 February 1993 were used.

Not all catchments on the soil site contribute flow to the hydrographs. The NLFIT .FW input files were configured accordingly.

For five events on the soil site, e_m was fixed at 1.21. This is a reasonable minimum to use when cross-sectional data are unavailable. The value of 1.16 for e_m, derived using limited cross-sectional data for the soil site (Evans pers com), seems to support the selection of 1.21. Also, for five events on the soil site, Sphi tried to be fitted to a zero value and was fixed at 0.001 when fitting parameters. Except for kinematic wave parameters for the event on 22 December 1994, the fitted parameter values for the soil site were fairly consistent. The batter site parameter values were also reasonably consistent. The cap site events had the greatest variation between parameter values.

Table 4.2 Fitted mean DISTFW hydrology model parameters. Standard deviations are given in brackets.

Cap site Date	c_r ($m^{(3-2e_m)}\ s^{-1}$)	e_m	Sphi (mm $h^{-0.5}$)	phi (mm h^{-1})
16 Nov 93	2.94 (0.46)	1.32 (0.05)	10.6 (1.92)	1.02 (6.46)
09 Dec 93	68.0 (35.3)	2.11 (0.15)	0.18 (14.2)	29.0 (27.9)
10 Dec 93	4563 (5087)	3.58 (0.39)	2.84 (1.49)	0.57 (5.53)
21 Feb 94	10.5 (4.91)	1.65 (0.11)	0.62 (4.30)	4.81 (16.8)
Simultaneous fit 16 Nov 93, 09 Dec 93, 10 Dec 93 and 21 Dec 94[b]	7.11 (1.28)	1.58 (0.57)	5.31 (0.58)	8.80 (3.01)
Willgoose & Riley (1993)	4.47	1.66	3.85	6.5
Soil site Date				
30 Nov 94	1.50 (1.08)	1.21[a] (0.15)	0.001 (48.7)	47.5 (126)
22 Nov 94	37.9 (53.9)	2.00 (0.39)	0.66 (1.20)	70.3 (3.74)
17 Jan 95	1.38 (1.85)	1.21[a] (0.28)	0.001 (203)	61.2 (30.5)
19 Jan 95	3.57 (1.39)	1.21[a] (0.09)	0.001 (11.8)	59.3 (4.63)
25 Jan 95	4.50 (1.89)	1.36 (0.11)	8.48 (0.84)	61.2 (3.09)
10 Feb 95	3.28 (0.09)	1.29 (0.09)	0.001 (0.17)	48.0 (0.63)
18 Feb 95	1.04 (0.37)	1.21[a] (0.12)	0.001 (290)	81.7 (76.2)
Simultaneous fit 30 Nov 94, 22 Dec 94 19 Jan 95 and 10 Feb 95[b]	1.25 (0.08)	1.21[a] (0.02)	7.54 (0.33)	47.2 (0.21)
Batter site Date				
21 Feb 93	19.9 (3.98)	1.97 (0.08)	1.56 (0.80)	19.5 (5.02)
18 Mar 93	15.7 (3.95)	1.83 (0.09)	1.54 (0.87)	52.7 (5.54)
16 Nov 93	5.63 (0.85)	1.47 (0.05)	7.09 (0.57)	12.2 (1.52)
09 Dec 93	5.01 (1.27)	1.50 (0.08)	0.0001	15.7 (0.91)
Simultaneous fit 21 Feb 93, 18 Mar 93,16 Nov 93 and 09 Dec 93[b]	6.71 (0.65)	1.54 (0.03)	5.48 (0.36)	16.3 (0.93)

a e_m for these events were fixed at 1.21 (Willgoose pers com 1997).
b Adopted site parameter values.

For the simultaneously fitted multiple events the kinematic wave parameters are comparable for the cap and batter site and Sphi is similar for all sites. The cap and batter parameters are similar to those adopted by Willgoose and Riley (1993) (table 4.2).

Parameter compatibility analysis of the simultaneously fitted parameters using COMPAT (section 3.2.1) indicated that the kinematic wave parameters, c_r and e_m, were not independent of each other (fig 4.4). The ellipses for the cap and batter site overlapped and therefore the parameter values are considered not to be statistically different. However, the soil site ellipse did not overlap the cap and batter site ellipses, therefore the parameters values were considered to be statistically different from the cap and batter site parameter values. The difference is likely to be due to the different surface roughness conditions on the soil site due to ripping and vegetation. The infiltration parameters were considered to be statistically different for all sites as none of the ellipses overlapped (fig 4.5). However, the Sphi value for the cap (5.31 ± 0.58) and batter (5.48 ± 0.36) site can be considered to be similar even though the long-term infiltration rate, phi, is different.

Two sets of parameters were selected for SIBERIA landform evolution modelling (chapter 5). The first set are representative of a landform with no surface treatment ie unvegetated and unripped. This first set of parameters were the simultaneously fitted parameters for multiple storms on the cap site (tables 4.2 and 4.3) since these were in good agreement to those adopted by Willgoose and Riley (1993) (table 4.2). The second set of parameters are representative of a landform that has surface treatment such as vegetation and surface ripping. The second set of parameters were the parameters simultaneously fitted for multiple storms on the soil site (tables 4.2 and 4.3) which resulted in good agreement between predicted and observed hydrographs (appendix C).

Table 4.3 DISTFW parameters selected for SIBERIA landform evolution modelling. The cap site parameters are representative of a landform with no surface treatment such as ripping or vegetation. The soil site parameters are representative of a landform with surface treatment (ripping and vegetation).

	c_r	e_m	Sphi	phi
Cap site	7.11 ± 1.28	1.58 ± 0.57	5.31 ± 0.58	8.80 ± 3.01
Soil site	1.25 ± 0.08	1.21 ± 0.02	7.54 ± 0.33	47.2 ± 0.21

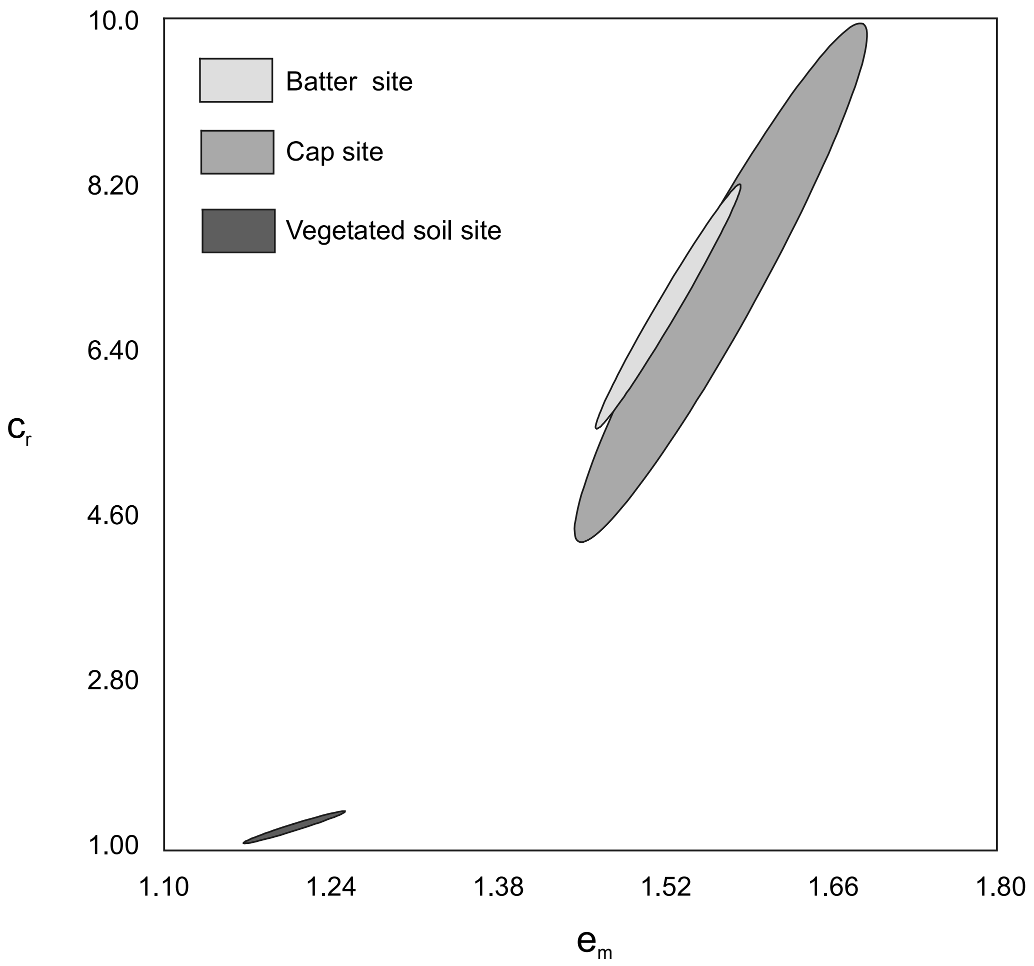

Figure 4.4 95% compatibility regions for simultaneously fitted kinematic wave parameter values for the study sites derived using monitoring data – (1) batter site, (2) cap site and (3) vegetated soil site

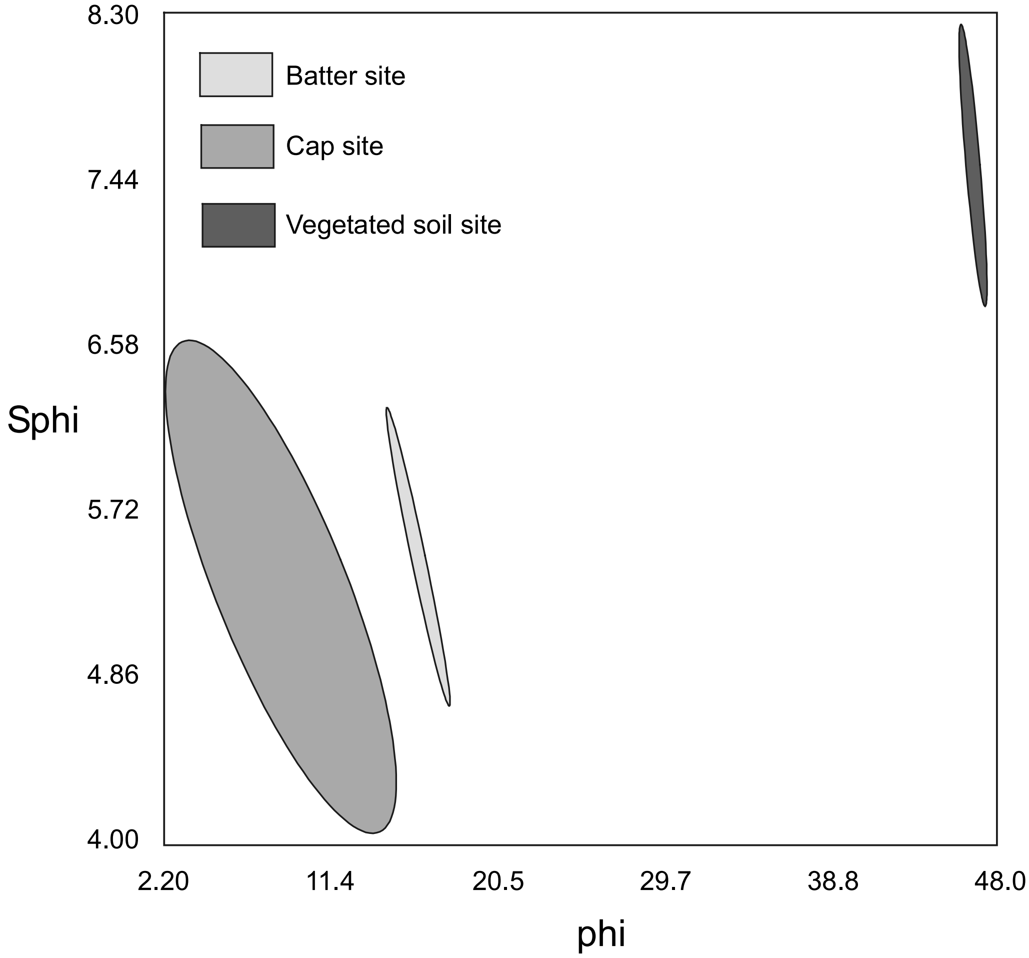

Figure 4.5 95% compatibility regions for simultaneously fitted infiltration parameter values for the study sites derived using monitoring data – (1) batter site, (2) cap site and (3) vegetated soil site

PREDICT (section 3.2.1) was used to test how well the adopted parameters predicted runoff hydrographs (figs 4.6 and 4.7). The adopted parameters for the cap site were used to predict runoff from the cap site for an event which occurred on 03 January 1995. Although the observed hydrograph volume was under-predicted, event runoff was well predicted with all observations falling within 90% prediction limits (fig 4.6).

The second set of adopted parameters (soil site), representing a vegetated and ripped landform, was used to predict runoff from the soil site for an event which occurred on 10 January 1996 (George 1996). This event was not used in the parameter fitting process. For this event the hydrograph volume was largely over-predicted and discharge was poorly predicted (fig 4.7). This may have resulted from the difficulty in predicting infiltration parameters. This does not mean that the second set of adopted parameters are inadequate for modelling or design purposes. Over-predicting hydrograph volume indicates that the infiltration parameter values are under-predicted. This may have resulted from the complexities of the soil site surface (vegetation and ripping on the low slope 0.012 m/m). It may be that no event data were collected where long-term infiltration was achieved. Using under-predicted infiltration parameter values in the modelling process may over-predict the amount of discharge, which will result in an over-prediction of sediment loss. Therefore, using the adopted parameters will over-predict erosion, for some rainfall events, resulting in conservative design of erosion control structures on rehabilitated landforms.

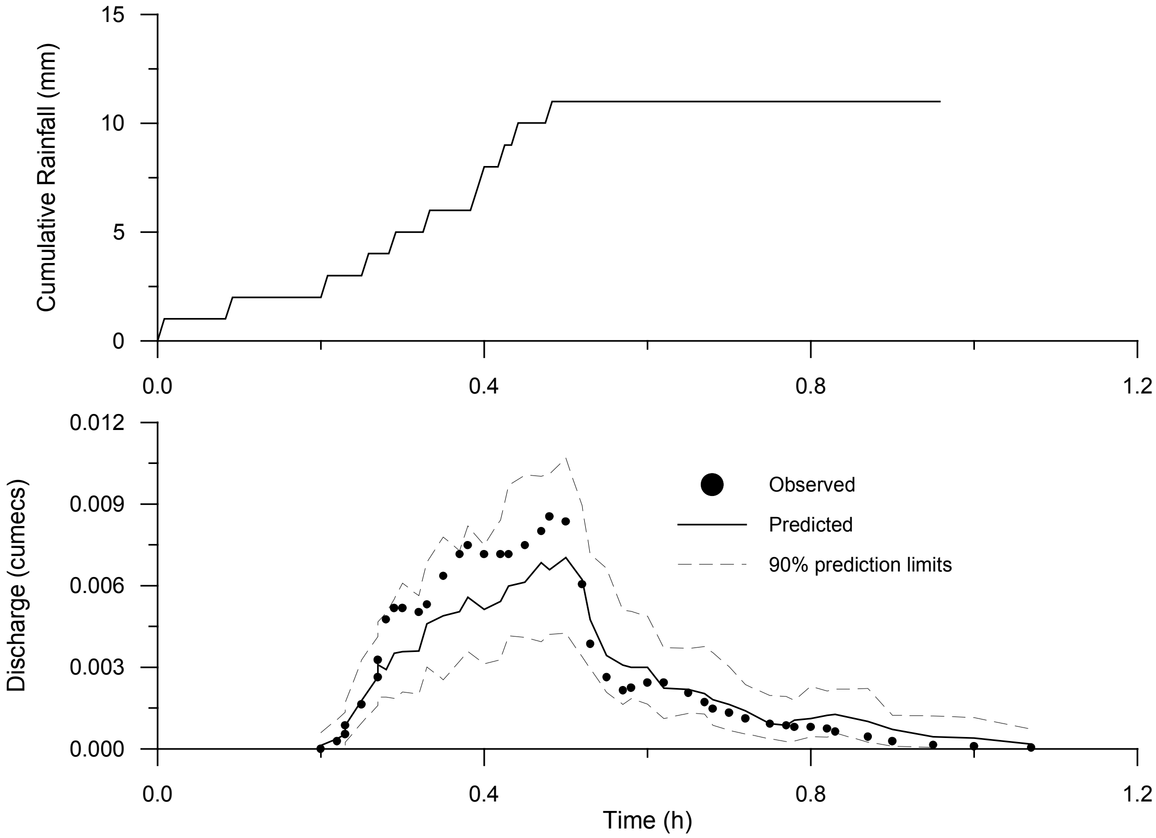

Figure 4.6 Rainfall for the cap site event on 03 January 1995 and hydrograph predicted using adopted parameter values for an unvegetated and unripped landform (cap site). Parameter values are $c_r = 7.11$, $e_m = 1.58$, Sphi = 5.31 and phi 8.8. 90% predition limits are shown.

4.3 Overview

This study highlights the difficulty of deriving sediment transport and hydrology model parameter values for a site. It was fortunate that the study area was in the wet/dry tropics and it was predictable when rain would occur so a monitoring program could be established. However, over a three year monitoring period only 28 full data sets from four sites were collected. The nature of the models require that discrete event data of rainfall, discharge and total sediment loss data are collected. Water level sensors can be used to monitor discharge when an observer is not present but the sensors need to be carefully calibrated and must not be heat-sensitive as this will result in errors. Suspended sediment data are the most difficult to collect as an observer needs to be present at the start of an event to collect runoff samples. Bedload can be collected at the completion of an event. For many of the storms where data sets were incomplete it was the suspended sediment data that were missing. For this type of discrete sampling, the automatic sediment sampler available for this study was inadequate and therefore not used. If the sampling process is commenced at the first runoff the sampler will start and continue to sample the event even if rainfall ceases and discharge stops after a short time. The sampler will continue its cycle resulting in empty sample bottles and will not restart if a larger event with substantial runoff follows soon after. The variable nature of events, ie time of event, is also a problem as for a long event the settings on the sampler may result in only the rising stage of the hydrograph being sampled.

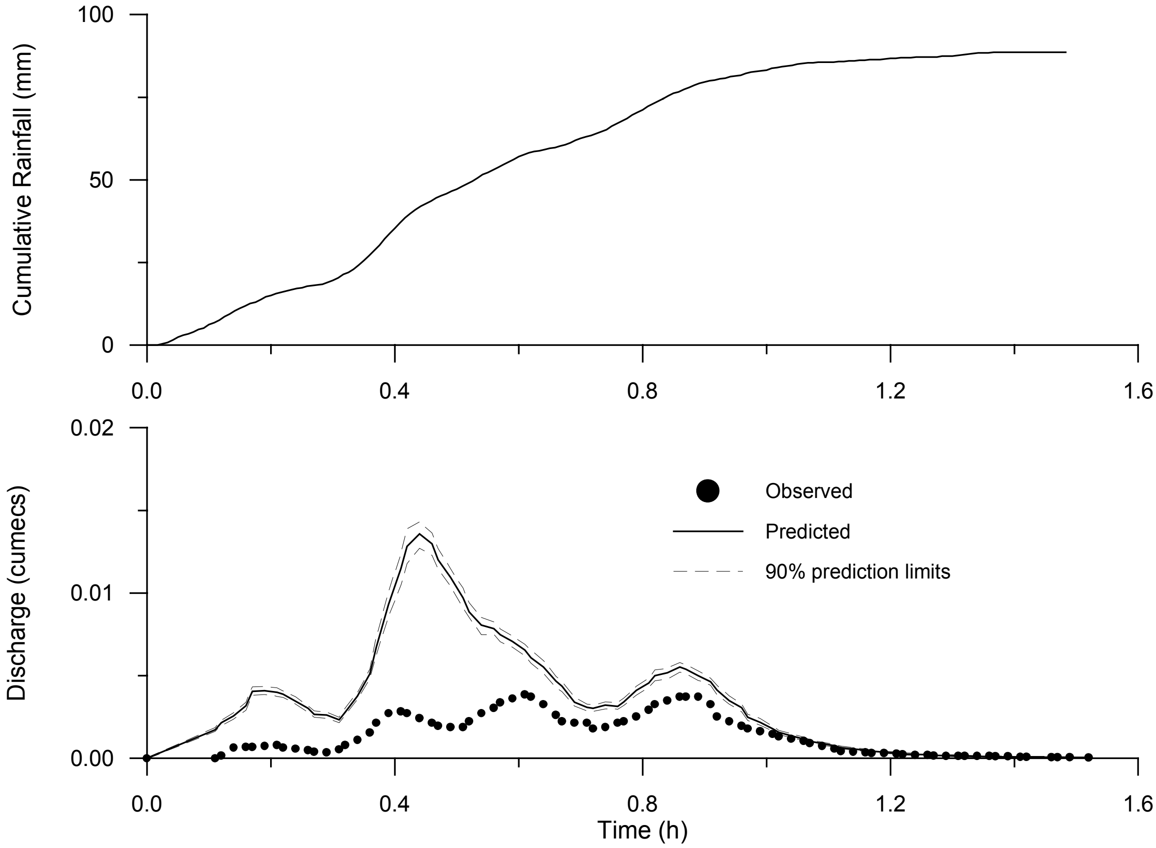

Figure 4.7 Rainfall for the soil site event on 10 January 1996 and hydrograph predicted using adopted parameter values for a vegetated and ripped landform (soil site). Parameter values are $c_r = 1.25$, $e_m = 1.21$, Sphi = 7.54 and phi 47.2. 90% predition limits are shown.

For this study it was important when fitting the sediment transport model that a broad range of events were used and that high sediment loss events were well predicted. Observations indicate that one high sediment loss event may remove more than ten times the amount of sediment that is removed during a low intensity event. Therefore, based on site experience, representative events were selected for parameter derivation. There was difficulty in fitting the model using batter site data as there may be a threshold discharge above which the effects of slope outweigh surface properties resulting in observed sediment losses twice that predicted. The following significant sediment transport equations (4.8 and 4.10) were adopted for landform evolution modelling:

$T_{cap} = 5.79\ S^{0.69} \int Q^{1.59}\, dt$ ($r^2 = 0.92$; df = 10; $p < 0.001$) (for an unvegetated site without surface amelioration)

$T_{soil} = 10.4\ S^{0.69} \int Q^{1.59}\, dt$ ($r^2 = 0.92$; df = 10; $p < 0.001$) (for a vegetated site with surface amelioration, ie ripping)

The adopted DISTFW parameter values are summarised in table 4.3.

The cap site parameters values are good predictors of events. The soil site parameters may over-predict discharge for some rainfall events which will result in conservative design of erosion control structures.

5 Landform modelling using SIBERIA

Design of rehabilitated post-mining landforms should be incorporated in mine planning and to achieve this, there is a need to be able to predict the surface stability of the final landforms. Willgoose and Riley (1993) addressed the application of the landform evolution model SIBERIA (Willgoose et al 1989) to the prediction of the long-term erosional stability of the proposed ERARM post-mining landform by using SIBERIA to model the evolution of a final landform design developed in 1987 (Unger & Milnes 1992). This modelling used parameters derived for unvegetated areas of waste rock using a combination of rainfall simulation and monitoring data. Willgoose (1995) considered that the most important limitation of the Willgoose and Riley (1993) study which could not be addressed because of data availability was 'that it was not possible to allow for the reduction by vegetation of the erodibility of the containment structure'.

The presence of vegetation may affect the input parameters for SIBERIA as vegetation reduces the erosivity of rain by causing the dissipation of kinetic energy on contact with foliage and reducing flow velocity of runoff. These effects of vegetation reduce soil loss and are dependent on height and continuity of foliage, root density and the thickness of ground cover (Morgan 1986). An erosion model such as the RUSLE incorporates a cover factor that accounts for the vegetation effect.

In a sensitivity study Willgoose (1995) used tabulated values of erosion-vegetation correlations for the Universal Soil Loss Equation (USLE) (Wischmeier & Smith 1978) to examine the effect of vegetation cover on erosion. Erosion predictions, using these correlations, for the above-grade landform were compared with the predictions of Willgoose and Riley (1993). The erosion rate of a surface with a fully developed vegetation undergrowth and canopy was predicted to be about 6% of the erosion rate from an unvegetated surface. Willgoose (1995) considered that the rate could increase to 75% where the undergrowth is not fully developed. The most important contributor to reduction in erosion rate was undergrowth. Simulations with SIBERIA indicated that over the 1000 year lifetime the maximum depths of erosion would reduce from 8.8 m for the unvegetated state to 5.4 m for the vegetated state and that the depth of deposition would reduce from 5.4 m to 2.2 m. The extent of valleys created by erosion would be substantially reduced by vegetation with the length of the longest valley being reduced by a factor of four.

The aim of this chapter is to assess the effect of vegetation and surface ripping on simulations of landform evolution by SIBERIA by use of site-specific data. The sediment transport model and DISTFW Rainfall-Runoff model parameterised using monitoring data from natural storm events on the unvegetated, unripped cap site and the vegetated, ripped soil site (chapter 4) were used to derive input parameters for the SIBERIA model. A gully initiation threshold (CIF threshold—chapter 3) was not determined for this study. Therefore, in this study, an arbitrary CIF coefficent (Willgoose 1995) of 0.0003 was used in the simulations to initiate a nominal gully erosion rate on steep batter slopes but not elsewhere, as has been observed on the WRD. The original study of Willgoose and Riley (1993) used a CIF coefficient of 0.0 which gives a CIF <1 resulting in no variation in erodibility across the WRD. In this study, SIBERIA simulations of the WRD landform evolution were conducted as follows:

1. Using the SIBERA input parameter values derived in this study for the unvegetated, unripped cap site with a CIF coefficient of 0.0 resulting in no gully erosion rate.

2. Using the SIBERIA input parameter values derived in this study for the unvegetated, unripped cap site with a CIF coefficient of 0.0003 making gully erosion rates possible on the steep batter slopes.
3. Using the SIBERIA input parameter values derived by Willgoose and Riley (1993) for unvegetated, unripped areas of the WRD with a CIF coefficient of 0.0003 which makes gully erosion rates possible on the steep batter slopes.
4. Using the SIBERIA input parameter values derived in this study for the vegetated and ripped soil site with a CIF coefficient of 0.0003 making gully erosion rates possible on the steep batter slopes.

In discussions in this chapter the above will be referred to as Case 1, Case 2, Case 3 and Case 4.

5.1 Input parameter derivation

The methods of parameter derivation are described in section 3.3 – SIBERIA parameter derivation, and should be referred to when reading the following sub-sections.

5.1.1 Discharge area relationships

The fitted discharge area relationship (equation 3.14), derived for the most extreme 1 in 2 year event, for an unvegetated, unripped landform based on cap site hydrology model parameters is:

$$q_p = 0.000145\, A^{0.83} \; (r^2 = 0.99) \text{ where } A \text{ is in m}^2 \tag{5.1}$$

The relationship fitted by Willgoose and Riley (1993) was:

$$q_p = 0.000114\, A^{0.88} \; (r^2 = 0.9986) \tag{5.2}$$

The fitted discharge area relationship (equation 3.14) for a vegetated and surface ripped landform based on soil site hydrology model parameters is:

$$q_p = 0.000006\, A^{0.90} \; (r^2 = 0.96) \tag{5.3}$$

The acceptable range for m_3 values is 0.5 to 1.0 (Willgoose et al 1991a). The values derived here, 0.83 and 0.90, fall within that range. The coefficients derived in equations 5.1 to 5.3 are not explicitly used in SIBERIA modelling. However, the difference in the value of the coefficient in equation 5.1 and 5.3 suggests that the effect of vegetation and ripping under these conditions is to reduce peak runoff for a 1 in 2 year event by >24 times/unit area. This demonstrates the important hydrological effects of vegetation and ripping.

5.1.2 Long-term runoff series

The selected DISTFW Rainfall-Runoff model parameters for the cap site (section 4.3) were used to create a runoff series from (1) an unvegetated, unripped landform and (2) a vegetated and ripped landform using the method described in section 3.3.2.

A rainfall event recorded on 21 January 1991 (Willgoose & Riley 1993) was used as input to generate runoff from the 1.6 km^2 catchment (fig 3.2) for the 1773 nodes DTM version of DISTFW. The kinematic wave parameter, c_r, was fitted for the 10 sub-catchment version for both the unvegetated (cap site) and vegetated and ripped (soil site) case. The fitted values were 2.15 ± 0.71 m$^{(3-2e_m)}$ s^{-1} and 0.60 ± 0.03 m$^{(3-2e_m)}$ s^{-1} for the unvegetated, unripped and vegetated, ripped case respectively. The fitted hydrographs, using these values, for the unvegetated, unripped case and the vegetated, ripped case are shown in figures 5.1 and 5.2.

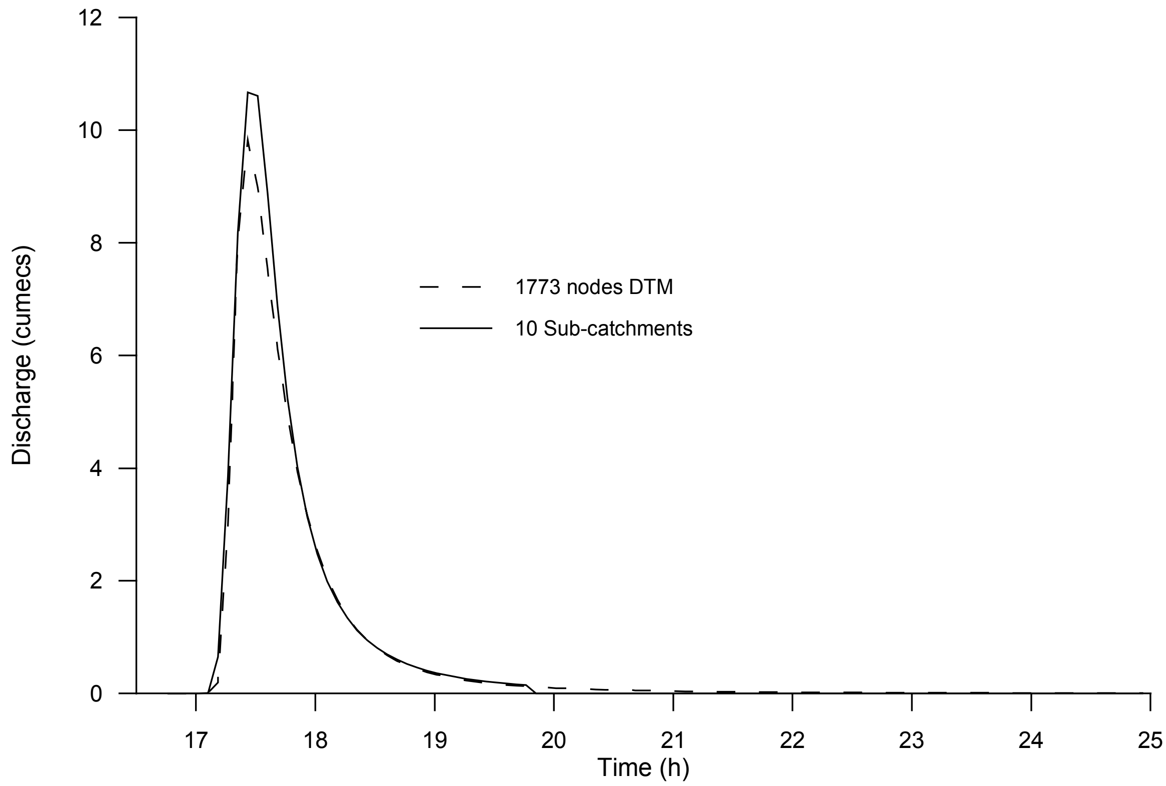

Figure 5.1 Calibration of the 10 sub-catchment runoff model to the output of the 1773 nodes DTM runoff predictions for the event on 21 January 1991 for the unvegetated and unripped case

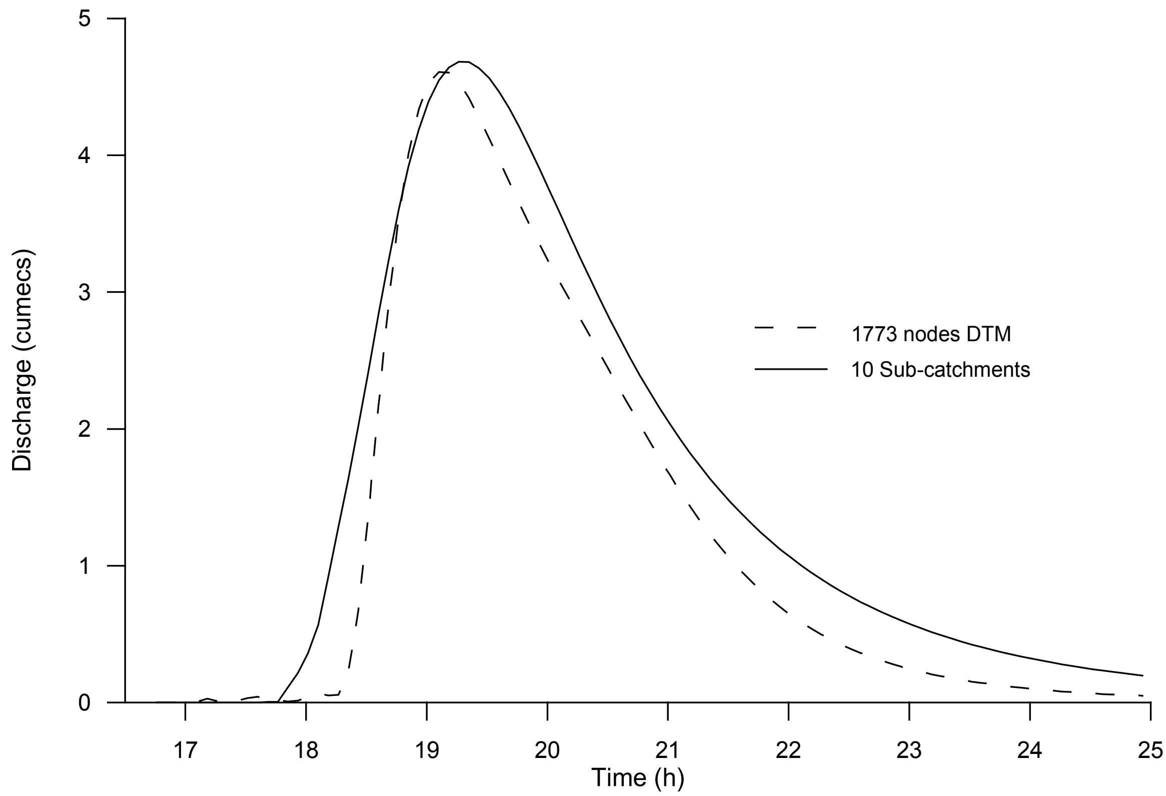

Figure 5.2 Calibration of the 10 sub-catchment runoff model to the output of the 1773 nodes DTM runoff predictions for the event on 21 January 1991 for the vegetated and ripped case

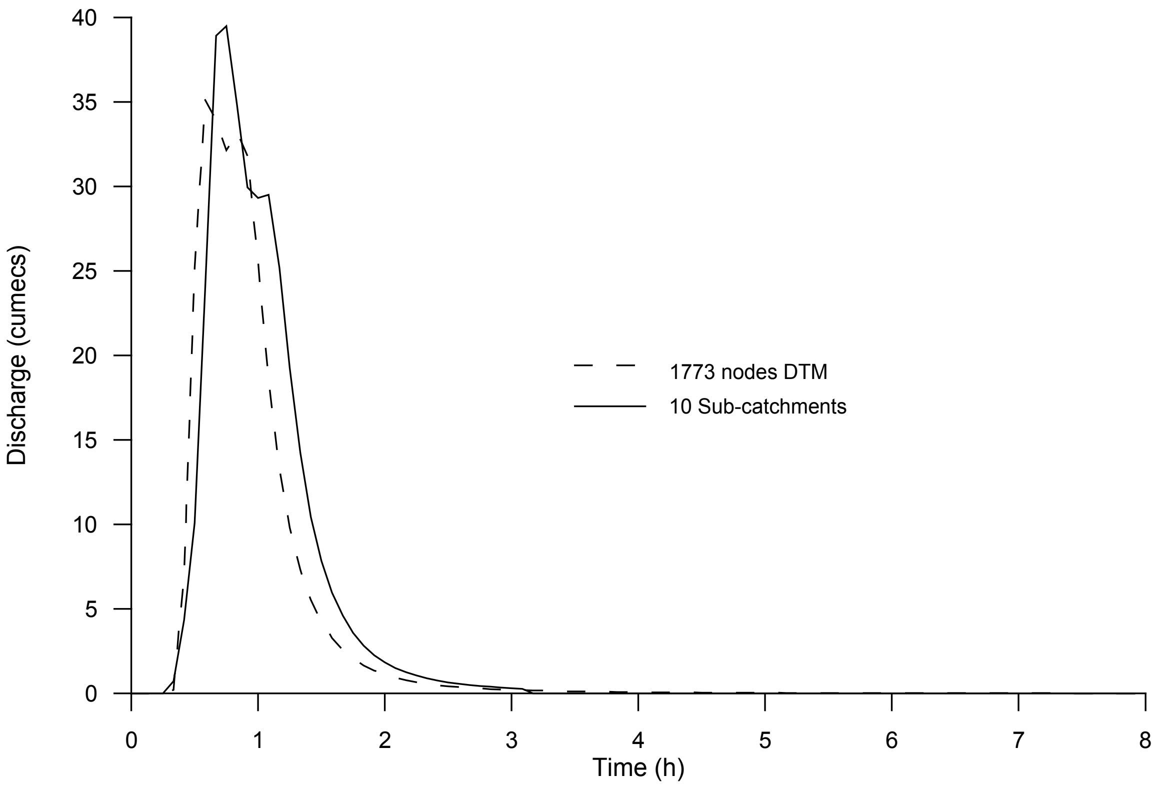

Figure 5.3 Calibration of the 10 sub-catchment runoff model to the output of the 1773 nodes DTM runoff predictions for the event on 10 January 1996 for the unvegetated and unripped case

The modelling by Willgoose and Riley (1993) used a rainfall event recorded on 21 January 1991. Therefore, to test how robust the modelling process was, a rainfall event recorded on 10 January 1996 (George 1996) was used as input to fit c_r for the unvegetated, unripped case (cap site). The fitted hydrograph, using $c_r = 2.15 \pm 0.71$ m$^{(3-2e_m)}$ s^{-1}, is shown in figure 5.3. The hydrograph for the 1773 nodes DTM compares closely with the 10 sub-catchments hydrograph, which indicates that the model is robust for other rainfall events. There is a difference in peak discharges for the hydrographs in figures 5.1 and 5.3 but total discharge is similar and this is important since total discharge is used in equations 4.8 and 4.10 to determine annual sediment loss.

The c_r parameter values derived here, an Sphi value of 0.001 mm h$^{-0.5}$ (conservative – see section 3.3.2) and the e_m and phi values selected in section 4.3, were used to generate annual runoff from the 1.6 km^2 catchment for the unvegetated and unripped case and the vegetated and ripped case for several years of the Jabiru rainfall record (Willgoose & Riley 1993) (table 5.1).

5.1.3 Average sediment loss rate

The annual runoff was used in equations 4.8 and 4.10 to determine annual sediment loss. This was converted to volume by dividing by the bulk density of the surface material (1.85 Mg m^{-3}, cap site unvegetated; 1.68 Mg m^{-3}, soil site vegetated and ripped) (table 5.1).

Note: the losses given in table 5.1 are for a slope 1 m/m. For this part of the analysis, a slope S = 1 m/m was assumed and a slope correction is required at a later stage. The SIBERIA model applies the true slopes of the nodes during the simulations.

The annual sediment losses were used to derive a long-term average sediment loss rate (q_s in equation 3.3) (table 5.1).

Table 5.1 Long-term average soil loss, uncorrected for node scale and slope, from a 1.6 km^2 catchment on the ERARM waste rock dump

		Unvegetated case – Equation 4.8 (n_1 = 0.69)		Vegetated case – Equation 4.10 (n_1 = 0.69)	
Year	Rainfall (mm)	Soil loss mass rate (Mg y^{-1} x 10^5)	Soil loss volume rate (m^3 y^{-1} x 10^4)	Soil loss mass rate (Mg y^{-1} x 10^4)	Soil loss volume rate (m^3 y^{-1} x 10^3)
1972	1163	8.15	44.0	3.54	21.0
1973	1353	10.5	56.7	13.5	80.3
1974	1604	5.92	32.0	2.26	13.5
1975	1642	11.7	63.0	14.0	83.3
1977	928	5.58	30.2	2.72	16.2
1978	1467	10.1	54.3	2.55	15.2
1979	1193	6.04	32.6	0.27	1.6
1980	1663	10.2	55.0	4.79	28.5
1984	2082	18.2	98.2	32.9	196
1986	1145	3.24	17.5	0	0
1987	1277	6.29	34.0	1.57	9.4
1988	1135	6.55	35.2	5.13	30.5
1989	1152	5.39	29.2	0.50	3.0
Average uncorrected soil loss volume rate (q_s) (m^3 y^{-1})			44.8 x 10^4		38.3 x 10^3

The final SIBERIA input parameter, β_1, was determined using the following equation

$$\beta_1 = \frac{q_s}{\beta_3^{m_1} A^{m_1 m_3}} \tag{5.4}$$

assuming $\beta_3 = 1$ (note that values of β_3 calculated in equations 5.1–5.3 were not used), where A is the area of the 1.6 km^2 catchment in m^2 (1 595 700 m^2) and applying the slope correction of equation 3.15

$$\frac{1}{(DTM\ spacing)^{n_1}} = \frac{1}{30^{n_1}}$$

All derived SIBERIA input parameters (equations 3.3 and 3.4) are given in table 5.2.

Table 5.2 Derived SIBERIA input parameters

	Parameter			
Treatment	β_1[a]	m_1	m_3	n_1
Unvegetated, unripped	0.27 x 10^{-3}	1.59	0.83	0.69
Willgoose & Riley (1993)	0.28 x 10^{-3}	1.68	0.88	0.69
Vegetated, ripped	0.50 x 10^{-5}	1.59	0.90	0.69

a Slope correction equation (3.15) has been applied.

5.2 Topographic evolution simulation

The derived SIBERIA input parameters (table 5.2) were used to model the evolution of the proposed above-grade landform option for rehabilitation of the ERARM (Unger & Milnes 1992) for the four cases given above. This landform proposal (fig 5.4) encapsulates tailings from Pit 1 above ground in the present tailings dam with a cap of waste rock. The void left after mining Pit 3 is completed will eventually fill with water becoming a water body.

SIBERIA (Version 7.05) was run on a Sun Ultra-1 Sparc workstation for the equivalent of 1000 years for the above-grade option using the derived parameters (table 5.2). Using these zero year parameters assumes that the initial surface conditions remain constant throughout the simulation period and there is no temporal change in parameters due to soil formation or ecosystem development and there is no spatial variation in parameter values over the DTM area due to surface treatment of the WRD or the undisturbed land surface. The results are presented three-dimensionally based on a 30 m grid with vertical exaggeration. Figure 5.4 shows the as-constructed landform at zero years.

Figure 5.5 shows the landform, for Case 2 (above), at 500 y and 1000 y. Figure 5.6 shows the landform, for Case 3, at 500 y and 1000 y. Figure 5.7 shows the landform, Case 4, at 500 y and 1000 y.

5.2.1 Unvegetated and unripped landform

For Case 2 simulations (fig 5.5), at 500 y there has been considerable material movement in the central depression area (see fig 5.4 for location descriptions and orientation) resulting in large erosion valleys with sediment from the valleys being deposited as fans at the outlet of the valleys. There has also been valley development and subsequent deposition on the steep batters adjacent to pit 3, Retention Pond 1 (RP1) and the tailings dam area (TDA).

By 1000 y, the length of valleys had increased by up to a factor of two over the length at 500 y, more valleys had developed, particularly on the steep batters on the western side, and upstream extension and branching of valleys had commenced.

5.2.1.1 Erosion and deposition

Case 1 simulations allowed a comparison between modelling results using the input parameters derived here and the results of Willgoose and Riley (1993). The original study by Willgoose and Riley (1993) with no gully erosion rates (CIF coefficient = 0.0) on batters found that at 1000 y the maximum valley depth was 7.7 m with 6.1 m maximum deposition and at 500 y the maximum valley depth was 5.7 m, 74% of the 1000 y erosion depth. Case 1 simulations found that at 1000 y the maximum valley depth was 5.6 m with 4.3 m maximum deposition. At 500 y the maximum valley depth was 5.5 m, 98% of the 1000 y erosion depth and 3.4 m maximum deposition.

At 1000 y for Case 2 the maximum valley depth was 7.6 m with the maximum deposition being 14.8 m. At 500 y the maximum valley depth was 7.3 m, 95% of the 1000 y depth, and the maximum deposition was 12.0 m, 81% of the 1000 y deposition.

For both Case 1 and Case 2 simulations, by 500 y both erosion and deposition have almost reached their maximum indicating that sediment movement is most rapid in the early years which agrees with the fluvial geomorphological rate law proposed by Graf (1977).

Case 3 simulations of landform evolution at 500 y and 1000 y are shown in figure 5.6. At 1000 y for the unvegetated, unripped case the maximum valley depth was 11.2 m with the maximum deposition being 9.1 m. At 500 y the maximum valley depth was 5.8 m, 52% of the 1000 y depth, and the maximum deposition was 6.8 m, 75% of the 1000 y deposition. The erosion incision using the Willgoose and Riley (1993) parameter values is greater than the incision modelled using the parameter values derived in this study. This is because Willgoose and Riley (1993), using rainfall simulator data, derived higher values for m_1 and m_3 (table 5.2), the product of which is proportional to erosion incision (Willgoose & Loch 1996).

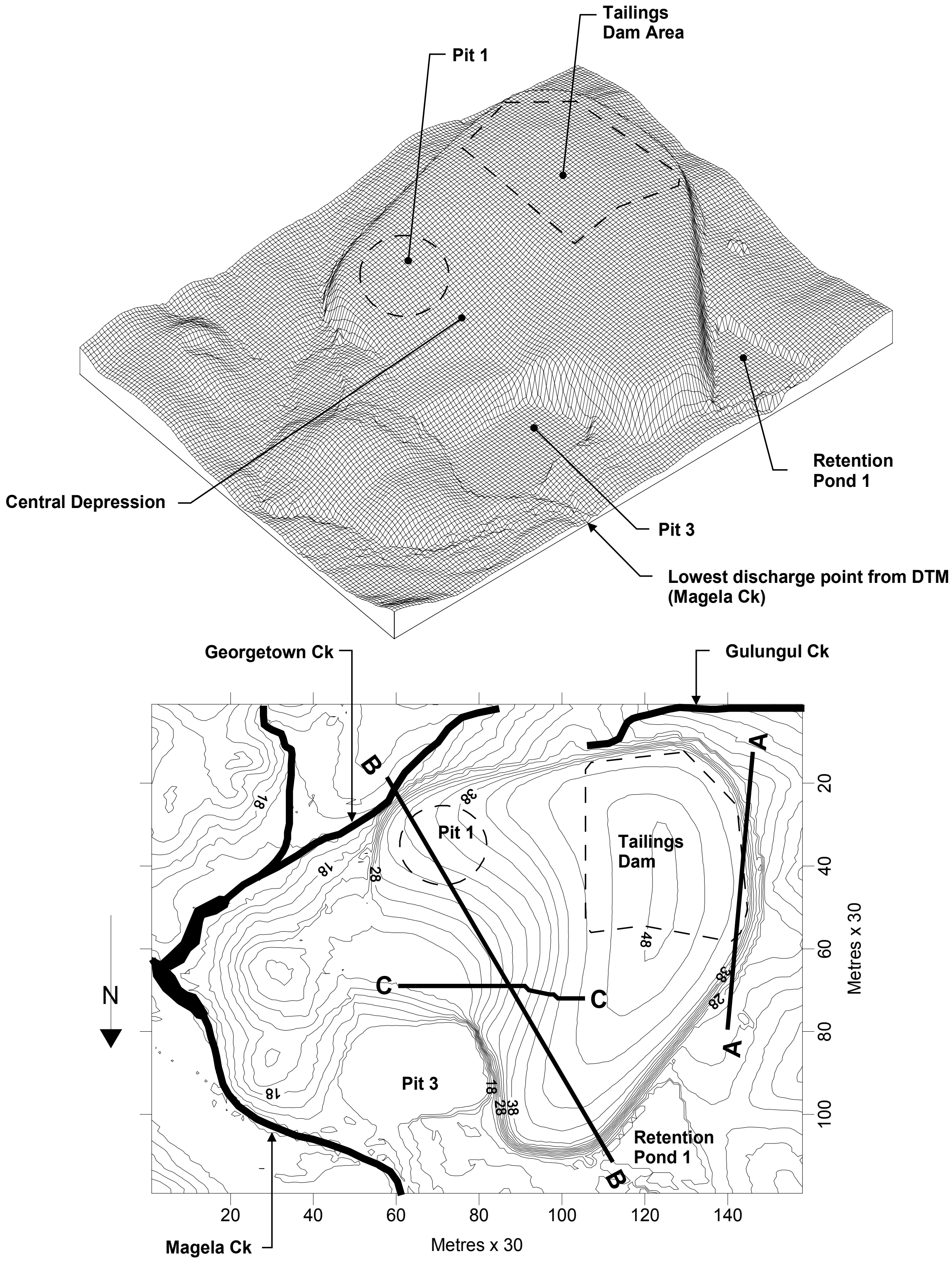

Figure 5.4 Top: 3-D representation of the above-grade landform option at zero years.
Bottom: Contour plan of the above-grade option. Contour intervals are 2 m. DTM spacing – 30 m.

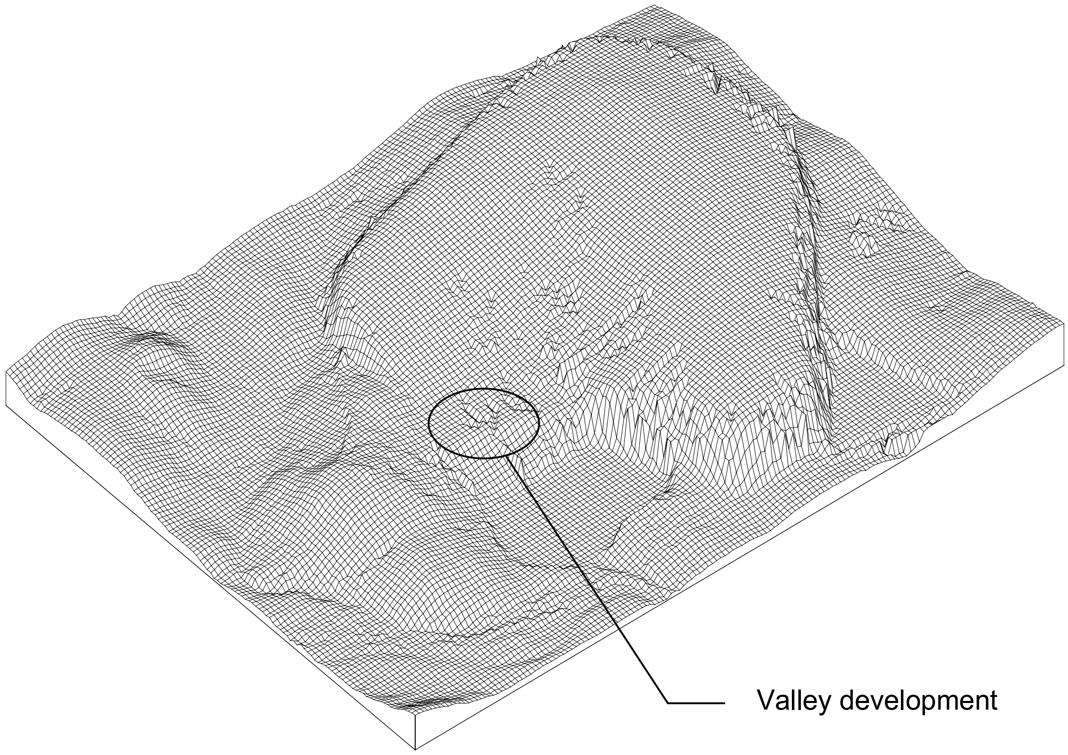

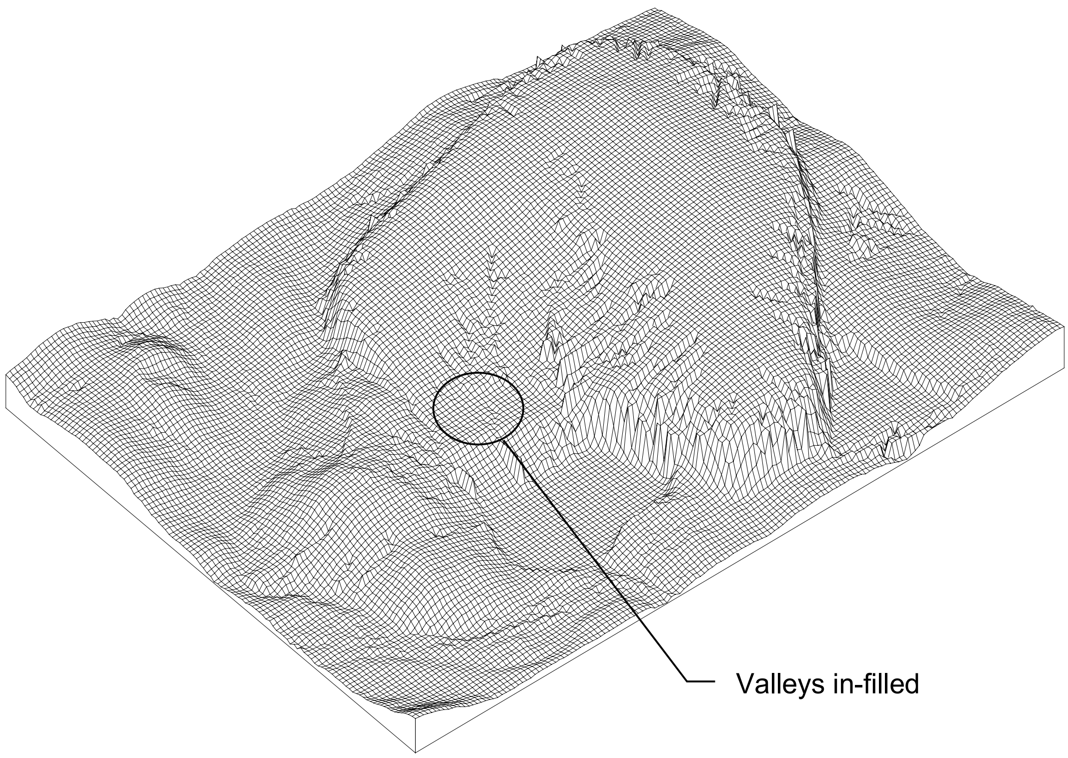

Figure 5.5 SIBERIA simulations of the above-grade option, unvegetated and unripped condition (Case 2), at 500 y (Top) and 1000 y (Bottom). DTM spacing – 30 m.

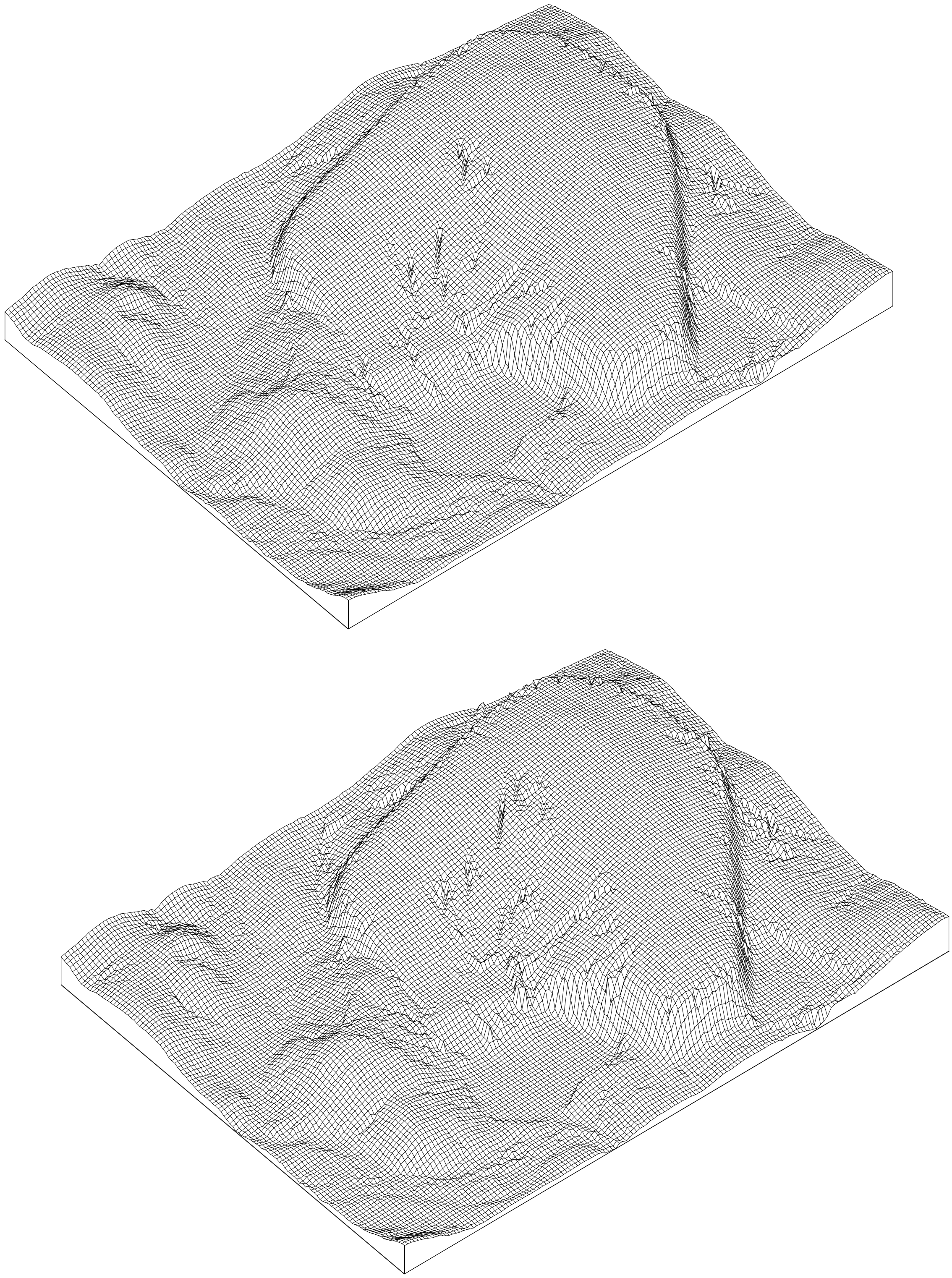

Figure 5.6 SIBERIA simulations of the above-grade option at 500 y (Top) and 1000 y (Bottom) for the unvegetated and unripped condition using the parameters derived by Willgoose and Riley (1993) (Case 3) (table 5.2). DTM spacing – 30 m.

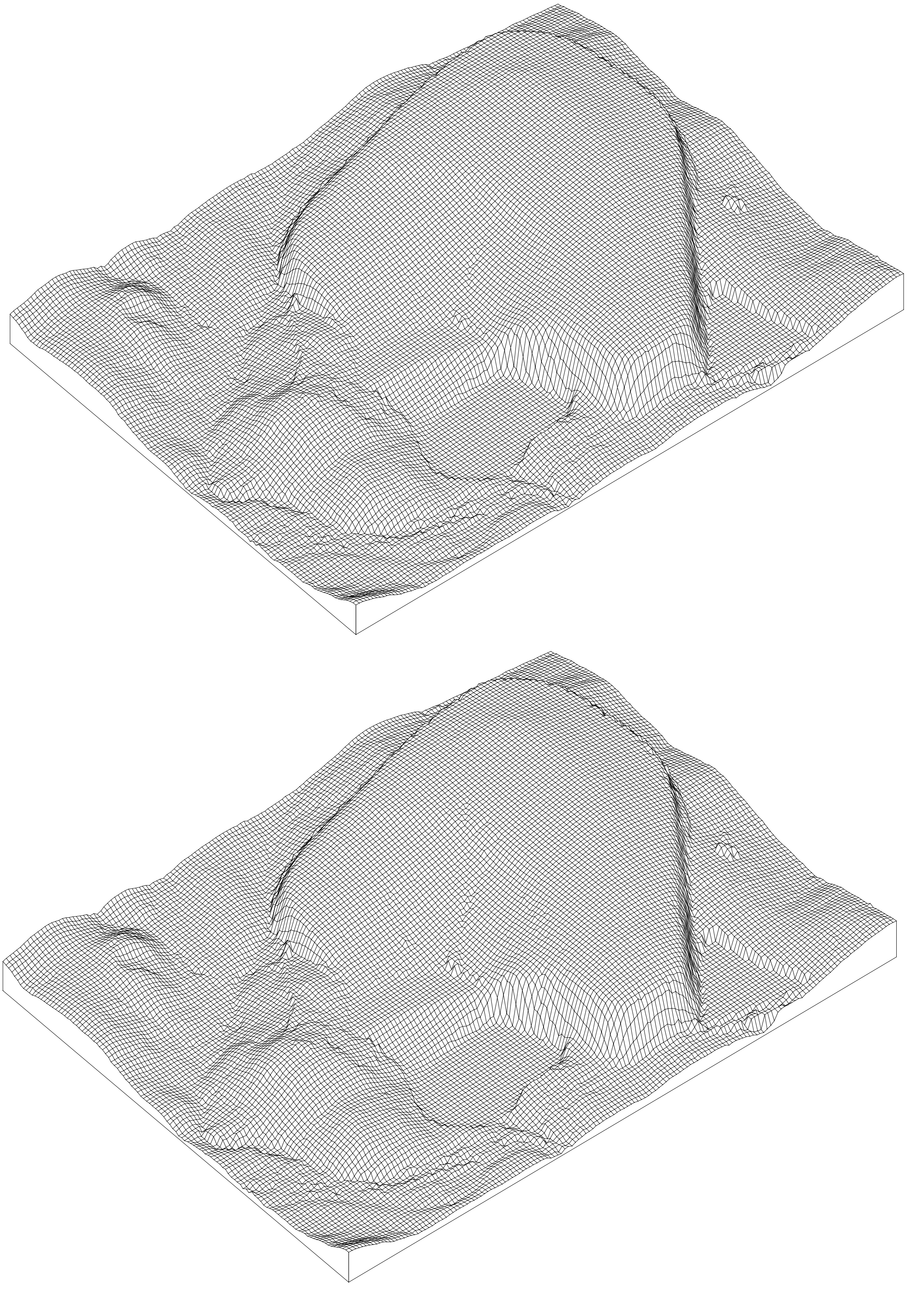

Figure 5.7 SIBERIA simulations of the above-grade option, vegetated and ripped condition (Case 4), at 500 y (Top) and 1000 y (Bottom). DTM spacing – 30 m.

A plot of the initial elevations at zero years minus the 1000 y elevations for Case 2 simulations (fig 5.8) shows erosion positive and deposition negative. This figure clearly shows that major sites of erosion are in the central depression and on the steep batter slopes adjacent to pit 3, RP1 and the TDA.

Comparison of figure 5.5 with figure 5.6 shows that the results obtained using both sets of parameters are similar with respect to valley and fan distribution. The valleys on the steep batter slopes appear to be numerous and long. One valley on the steep batter slope above pit 3 is approximately 400 m long (fig 5.5). The valleys in the central depression are in some cases discontinuous. Erosion is concentrated in localised valleys with little sheet erosion from interfluve areas (fig 5.8). Deeper incision can be seen in figure 5.6 compared with figure 5.5.

Maximum deposition for the two studies is not similar (14.8 m here; 9.1 m Willgoose & Riley (1993) parameters). Depths of deposition of this magnitude have occurred at only a few locations at the outlet of valleys on the steep batter slope between pit 3 and RP1 (figs 5.5 and 5.6). The fans do not appear to extend far past the edge of the slope and are possibly back-filling the valleys. The depth of deposition is controlled by the nature of SIBERIA simulations and slope geometry. Where erosion occurs on the very steep batter slopes, sediment is deposited at the outlet of the valley against the steep batter slope reaching a level higher than the lowest point of the valley at the outlet. There appears to be little transport past the outlet. Jewell and Adhikary (1996) observed large scale depths of deposition into an open pit resulting from erosion caused by water. For simulations using the parameters derived in this study there is less incision than when the Willgoose and Riley (1993) parameters are used. Therefore, since there is less incision valley outlets would be at a higher level on the steep slopes for this study than for the Willgoose and Riley (1993) study resulting in the greater depths of deposition predicted in this study.

On the flatter slopes in the central depression above pit 3, there is a fan which is ≈440 m long with a maximum height of ≈9 m (fig 5.5). The amount of material in the fan is ≈70 290 Mg, which is an average deposition rate of 70 Mg y^{-1} from this one valley. This fan and associated valley runs from the top of the waste rock dump in an easterly direction toward the lower flat section of the central depression above pit 3 (figs 5.4 and 5.5). A section through the valley and fan (fig 5.9) shows aggrading deposition and in-filling of the valley during the 1000 y simulation. The slope of the original surface (0 y) was ≈0.027 m/m. For this valley it appears that vertical incision has ceased by 500 y and that there is only head wall retreat from 500 y to 1000 y.

5.2.1.2 Simulated landform evolution and natural landform evolution

At 500 y multiple valleys had developed on the lower part of the central depression above pit 3 producing a large fan at the outlet. At 1000 y these valleys had filled in and the fan appears to have stabilised (fig 5.5). SIBERIA was run using time steps of 0.5 y, 0.05 y, 0.005 y and -0.5 y. Using annual runoff in the sediment transport equation (equations 4.8 and 4.10) calibrates SIBERIA so that one time step is equal to one simulated year. The model can also be calibrated using runoff for different time periods but this calibrates the model so that one time step is equal to that period of time. By setting the time step parameter value in SIBERIA simulations to, for example, 0.5 the simulated change in elevation is calculated each 0.5 of a simulated time period equal to the time period for which runoff was generated. In this study a time step of 0.5 simulates 0.5 y. The negative time step causes an adaptive timestepping algorithm to be used to determine the step size (Willgoose 1992). There was an insignificant difference in output for each of the time steps. This indicates that the in-filling of the valleys was a real feature of the SIBERIA simulations and not an anomaly arising from timestepping error propagation in the model. This demonstrates the dynamic nature of SIBERIA.

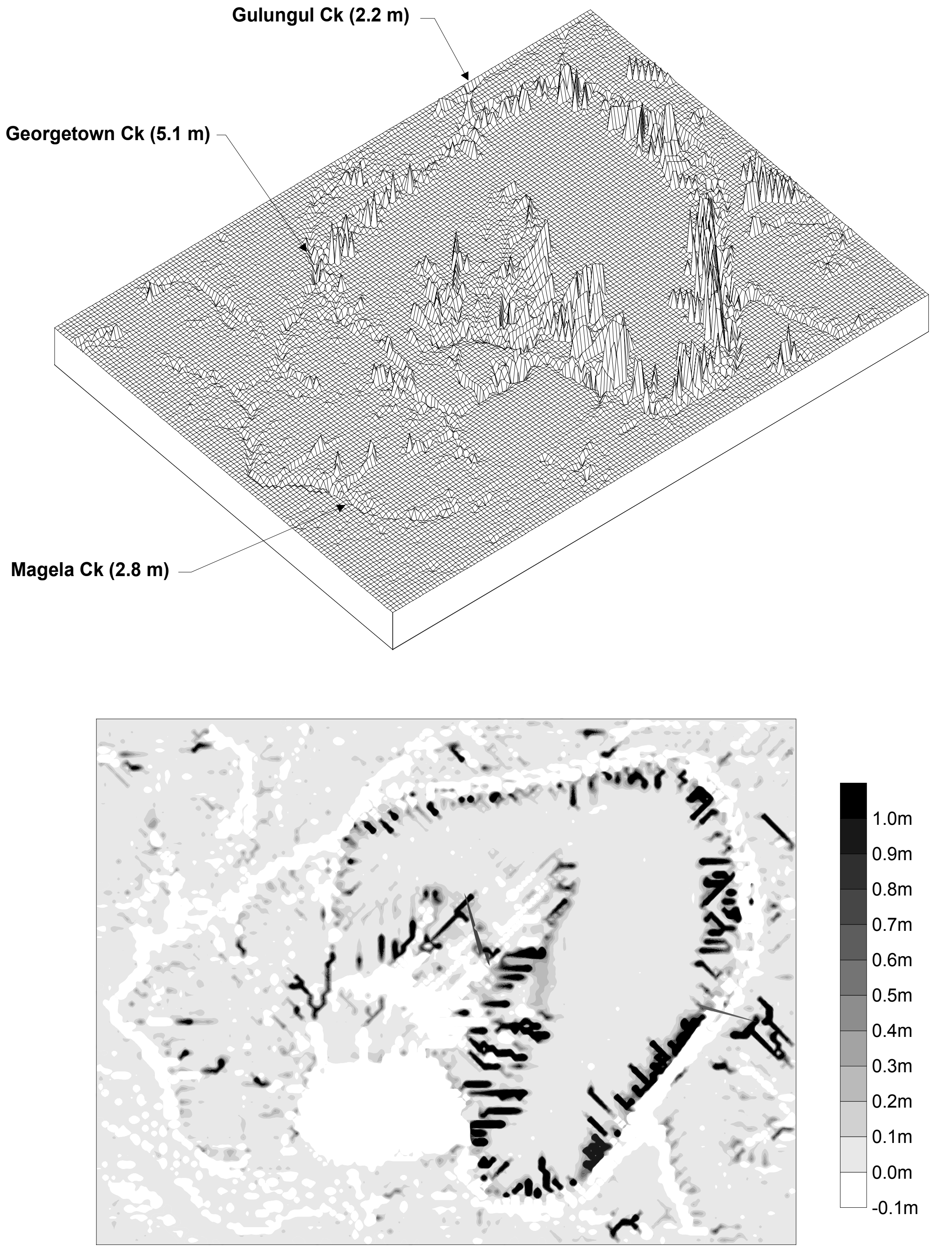

Figure 5.8 Top: Above-grade option, Case 2 simulations (unvegetated, unripped): Erosion (upward) and deposition (downward) at 1000 y. Maximum depth of deposition into streams within the DTM is shown in brackets. Bottom: Contours of erosion with >1 m = black. Shading scale is in m.

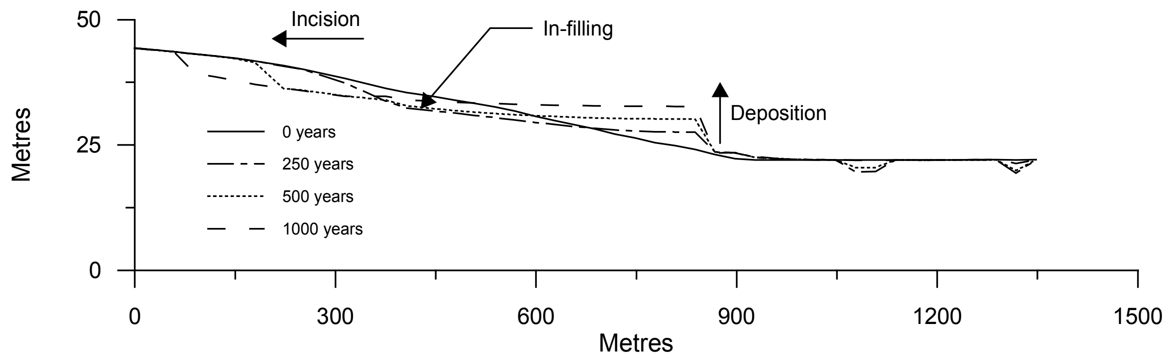

Figure 5.9 Section C-C through a valley and depositional fan (Case 2 simulations) running east to west from the top of the landform to the central depression above pit 3. Incision, aggradation and back-filling are visible.

The processes of valley in-filling has been observed in nature and described by Schumm and Hadley (1957). This description is applied to the SIBERIA simulations as follows:

1. A valley develops in the low-sloped section of the central depression area above pit 3 (fig 5.5).
2. The valley migrates upstream and branches develop (fig 5.5–500 y). At this stage the lower valley is very efficient in sediment transport.
3. Upstream channel migration and branching continues on to the steeper slope above, sediment delivery to the valleys on the lower slope is increased and deposition commences in the lower reaches of the initial valleys above pit 3.
4. As sediment is transported from the steeper slope to the lower slope aggradation occurs until the valleys are in-filled. Figure 5.5 at 1000 y shows discontinuous valleys on the steeper upstream slope and the initial valleys on the lower slope above pit 3 have been in-filled.

Scott and Erskine (1994) observed retrenching of fluvial or wet fans near Sydney as a result of a large storm. Sediment re-entrainment from fans is not clear in these SIBERIA simulations. The input parameters for these SIBERIA simulations are based on a long-term average sediment loss determined using a runoff series from a rainfall record. The parameters do not change throughout the simulation and the averaging of the sediment loss reduces the effect of a large scale storm. The fluvial sediment transport rate equation (equation 3.3) predicts the volume of material removed (erosion) from a node point on the DTM per time interval (one year). During the same time interval, sediment from upstream nodes is deposited at the node. The net change in volume (and node elevation) is the difference between erosion in a downstream direction and deposition from an upstream direction. The main influence on sediment transport would be a change in slope between nodes resulting from a change in elevation of the nodes. Eckis (1928) as cited in Schumm (1977) suggested that for dry fans formed by ephemeral flows, trenching would take place as sediment yield from a source area decreased. For the initial conditions applied in these simulations it is likely that the sediment source will be continuous throughout the 1000 y simulation period. Remobilisation of sediment on the fans and trenching has not been simulated because (1) a large scale erosive event has not been incorporated ie. average condition parameters have been used and (2) for these conditions input parameters remain constant which precludes the simulation of a bedrock layer resulting in simulation of a continuous upstream source of sediment.

The valley form modelled here (fig 5.9) has been observed in nature in many parts of the world and is described as a channelless valley or, in tropical Africa, a *dambo*. *Dambos* are of the form of many headwater valleys in areas of low relief (Thomas 1994) such as on the low slopes of the central depression of the WRD (fig 5.4). The typical *dambo* is associated with highly seasonal savanna climates which conforms to the climate of the study area. SIBERIA, as it was run in this study, was not used to directly model climate seasonality, however, the long-term runoff series used to parameterise the SIBERIA sediment discharge equation was based on seasonal rainfall data. Parameter values may thus reflect climatic seasonality. Confirmation of this is outside the scope of this study and is not investigated further. Thomas (1994) cites Balek and Perry (1973) and Balek (1977) in his review as concluding that *dambos* were mainly fed by direct rainfall. In these natural systems there is little contribution to downstream base flow in the Dry season. They constitute zero-order basins and may be filled with colluvium/alluvium varying in depth from <1 m to <10 m. In areas of high relief, such as on the steep batter slopes of the WRD, *dambos* are known as hillslope hollows with the distinction between the two based on gradient.

The form of the eroded hillslope simulated by SIBERIA on the steep batter slopes has been identified in nature on the west coast of North America (Reneau et al 1986, Reneau et al 1989). Reneau et al (1989) cited the nomenclature of Hack and Goodlett (1960) and Hack (1965) in describing the morphology of these areas as follows: noses – areas of convex-out contours; hollows – areas of concave-out contours; and side slopes – areas of straight contours. Reneau et al (1989) described the hollows as lacking stream channels with predominantly subsurface runoff but with seasonally saturated overland flow. By predicting the formation of these in-filled valleys, SIBERIA has modelled features which have occurred in nature under similar climatic and morphological conditions as in the study area. Reincision of valley fill resulting in discontinuous gullies within valleys has been identified in nature (Melville & Erskine 1986). Reincision of valley fill was not observed in the SIBERIA simulations which may be due to the resolution of the model which is a minimum node area of 900 m^2. Notwithstanding, these results strengthen confidence in SIBERIA that it is a model which accurately simulates natural processes.

It appears that eroded material is transported much further on the low slopes with approximate linear profiles (Toy & Hadley 1987) than on the steep slopes and that deposition occurs at the base of both types of slopes. On the steep batters, the transition from the low, upper cap slope to the steep batter slope to the low slope at the base of the batter gives a complex convexo-concave profile (Toy & Hadley 1987). Deep incision occurs at the upper slope transition and deep deposition occurs at the lower slope transition. East et al (1988) measured erosion from batter slopes of the WRD at ERARM using erosion pins and found that ground loss incorporating settlement was least at the base of the plots. This indicates that erosion was greatest from the upper slope.

5.2.1.3 Impact on Magela, Georgetown and Gulungul Creeks

Deposition has been simulated as occurring along most of Gulungul and Georgetown Creeks and a large portion of Magela Creek. The line of the streams, represented by deposition downward, can be seen in figure 5.8 in the three dimensional view. Analysis of the grid file on which figure 5.8 is based indicates that over the 1000 y simulation period deposition has reached a depth of 2.8 m in Magela Creek, 2.2 m in Gulungul Creek and 5.1 m in Georgetown Creek. These depths of deposition are in isolated locations.

Along a 200 m reach of Georgetown Creek, near a WRD batter, the average depth of deposition is 2.4 m around the maximum of 5.1 m. As a conservative estimate this represents deposition of approximately 19 000 Mg of sediment in this reach of Georgetown Creek over the 1000 y simulation period. Since deposition by 500 y may be as much as 81% of that at 1000 y, as much as 15 400 Mg of sediment may be deposited in this reach by 500 y.

East et al (1985) considered that the sediment transport capacity of Gulungul and Georgetown Creek would be sufficient to remove material far in excess of that normally produced by erosion, but did not quantify the amount. East et al (1985) also considered that sediment transport within Georgetown Creek, downstream of the mine, would be complicated because of the backflow relationship of the stream within Magela Creek during high flows resulting from cyclonic conditions. Under these conditions of high rainfall, high flow and intensive erosion there would be little or no flow from Georgetown Creek to Magela Creek resulting in reduced transport capacity and deposition of sediment within the Georgetown Creek system. The biological and physical impact of this deposition is uncertain.

The estimates of deposition should be treated with caution as the mode in which SIBERIA was run did not model fluvial transport in the streams within the DTM. Therefore these figures represent what is deposited during the simulated time period without further transport in the streams or flushing during high flow events.

5.2.2 Vegetated and ripped landform

Sediment movement is not obvious on the landform for Case 4 simulations (fig 5.7). However, there is some evidence of valley development in the central depression and on the steep batter slopes. Minor deposition is visible above pit 3 on the 1000 y output. At 1000 y for the vegetated and ripped case the maximum valley depth was 2.4 m with the maximum deposition being 4.8 m. At 500 y the maximum valley depth was 1.4 m, 58% of the 1000 y depth, and the maximum deposition was 2.8 m, 58% of the 1000 y deposition. For the vegetated and ripped condition, incision and deposition proceeded at a fairly constant rate indicating that simulated processes are almost linear with time.

By 1000 y on the vegetated and ripped surface (fig 5.10) valleys have formed but the maximum depth of these are only 32% of the maximum depth (7.6 m) of those formed on the unvegetated, unripped surface. The valleys are mostly located at the top of the steep batter slope and there is some minor incision in the central depression (fig 5.7).

The effect of vegetation and ripping on landform evolution at 1000 y is clearly seen when figure 5.8 and figure 5.10 are compared. The vertical scales on these figures are the same and these plots of initial elevations at zero years minus the 1000 y elevations clearly show where erosion and deposition occurs on both the unvegetated, unripped and vegetated, ripped sites. These figures are not comparable with those of the sensitivity study of Willgoose (1995) as he used cover factors for vegetated surfaces only (ignoring ripping), whereas the only site available for this study was the ripped and vegetated soil site. Willgoose (1995) found that fully developed vegetation cover reduced the erosion rate to 6% of the unvegetated state ie the results of Willgoose and Riley (1993).

A change in mass of the DTM during the 1000 y simulation period can be determined by subtracting the volume of the landform at zero y from the volume at 1000 y. The product of this difference and the bulk density of the material gives the change in mass. For the vegetated and ripped case (Case 4 simulations), the change in mass of the DTM of the landform was 13.6 Mg over the 1000 y simulation period compared with a change in mass of the DTM of 544 Mg for the unvegetated, unripped case (Case 2 simulations).

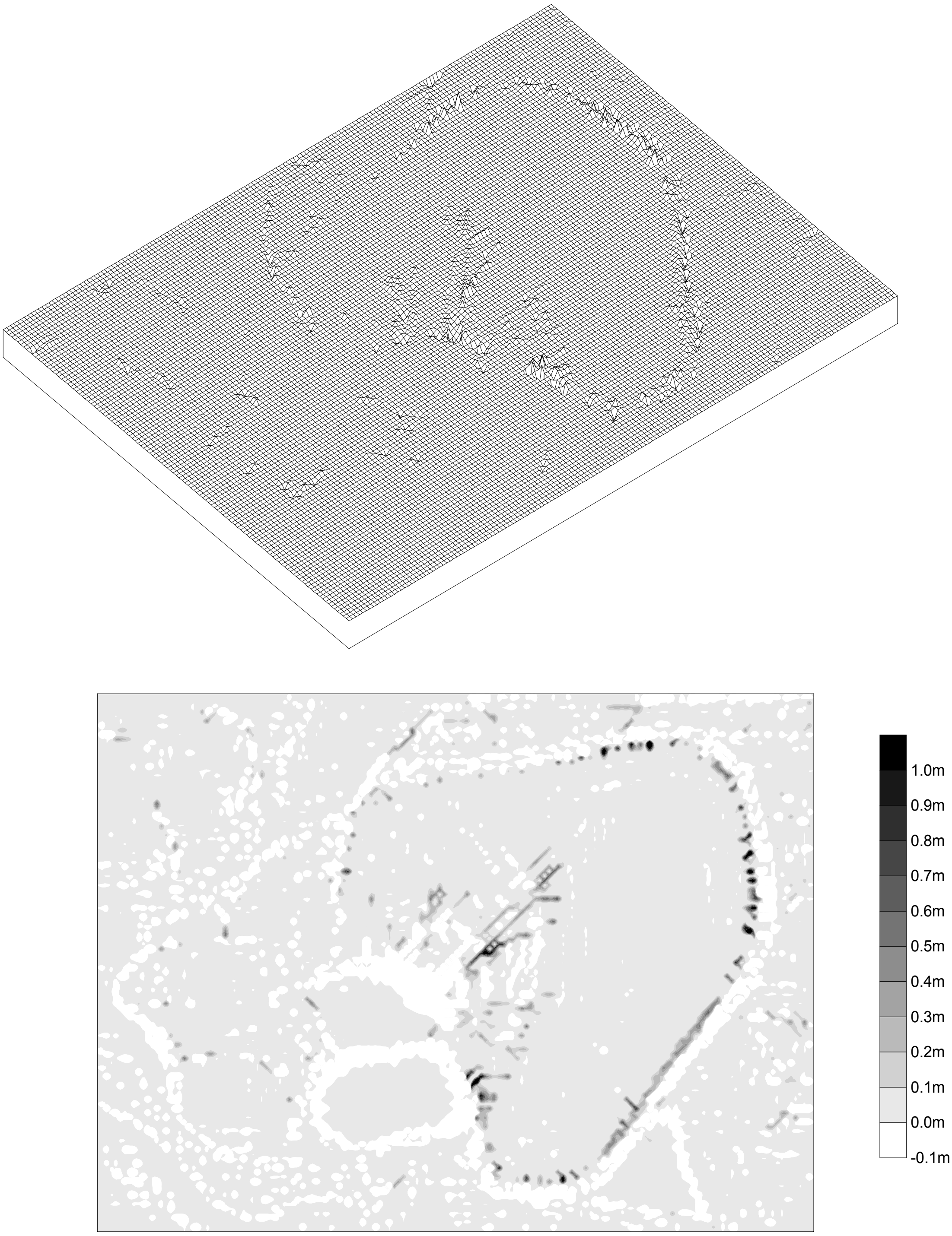

Figure 5.10 Top: Above-grade option, Case 4 simulations (vegetated and ripped): erosion (upward) and deposition (downward) at 1000 y. Bottom: Contours of erosion with >1 m = black. Shading scale is in m.

The change in mass for the fully vegetated and ripped case was 2.5% that of the unvegetated and unripped case. Change in mass of the DTM is used to compare the difference between the unvegetated, unripped case and the vegetated, ripped case and should not be interpreted as a net loss from the system as it is not a true representation of sediment movement from the DTM into Magela Creek (fig 5.4). There is large scale sediment redistribution within the DTM for the unvegetated, unripped case as described above where simulations show a loss of approximately 70 Mg y^{-1} of sediment from one valley.

As stated above the mode in which SIBERIA was run did not model fluvial sediment transport or flushing in the streams within the DTM and which are not part of the landform. Therefore the sediment load leaving the DTM via the streams is not modelled. The change in mass of the DTM may only be an indication of sediment loss from a small number of nodes on the boundary of the DTM.

5.2.2.1 Tailings containment implications

Sections through the landform (figs 5.11 and 5.12) (locations of sections are shown in fig 5.4) show the effect of vegetation and ripping on incision.

Section A-A (fig. 5.11) is taken through the TDA across the top of the steep batter slope. For the Case 4 simulations the maximum valley incision is 2.2 m at a maximum width of ≈60 m which gives a side slope of the valley of about 0.067 m/m perpendicular to the direction of flow. This is a broad valley with gently sloping walls that will not impact on the tailings if, for example, a 5 m deep layer of waste rock was used to cap the tailings dam. With respect to the thickness of the tailings cap, a final decision has not yet been made. The deepest incision for the Case 2 simulations (fig 5.11) is ≈5 m, with a maximum width of ≈60 m. This is also a broad valley with sloping side walls of about 0.179 m/m slope. This valley would just breach the tailings at 1000 y in this area.

Section B-B (fig 5.12) taken through the central depression shows the incision and deposition for the Case 2 simulations. The large fan in the central depression area is ≈5.7 m high and ≈150 m wide with side slopes of about 0.08 m/m at this point. The rate of deposition on this fan, stated above, is 70 Mg y^{-1}. A fan is also visible near RP1 where material has been dumped at the base of the batter at the outlet of a valley. This section shows that much material is eroded and deposited in the central depression resulting in numerous valleys and fans in this area. This indicates that there is much movement of material within the landform catchment. For the Case 4 simulations, section B-B (fig 5.12) shows only minor roughening of the surface ie deposition and erosion ≈0.5–1.0 m deep.

5.3 Discussion

SIBERIA input parameters for the proposed above-grade rehabilitated landform at ERARM were derived using natural storm data. For an unvegetated, unripped state, SIBERIA simulations showed that at 1000 y numerous valleys and fans had formed on the landform. Major valley formation occurred at the transition from low to high slopes at the top of the batter slopes and major deposition occurred at the transition from high to low slopes at the base of the batter. Transport of sediment at the base of the batters was not extensive. The fans on low slopes in the centre of the landform were generally longer than those on the steep batter slopes. Simulations show valleys forming and later being in-filled, a process which has been identified in nature. This indicates that SIBERIA is dynamic and models natural processes.

Erosion incision was quicker in the early years as the maximum depth of erosion at 500 y for the unvegetated, unripped case was 95% that of the maximum depth at 1000 y. It appears that

SIBERIA simulated stabilisation of vertical incision at about 500 y, and continued retreat of valley head walls and an increase in the number of valleys from 500 y to 1000 y. The predicted maximum deposition (14.8 m) was over 50% (9.1 m) greater than that predicted using the Willgoose and Riley (1993) parameters (Case 3 simulations).

It is important to note that Case 2 simulations of the unvegetated, unripped WRD showed a change in mass of the DTM of 0.54 Mg y^{-1} which does not adequately reflect the large movement of material within the DTM area. From one valley alone on the cap of the WRD the erosion rate was 70 Mg y^{-1}. Estimated sediment movement into creek catchments within the DTM area from SIBERIA simulations in this study showed that conservatively 19 000 Mg of sediment could be input into Georgetown Creek over a 1000 y period.

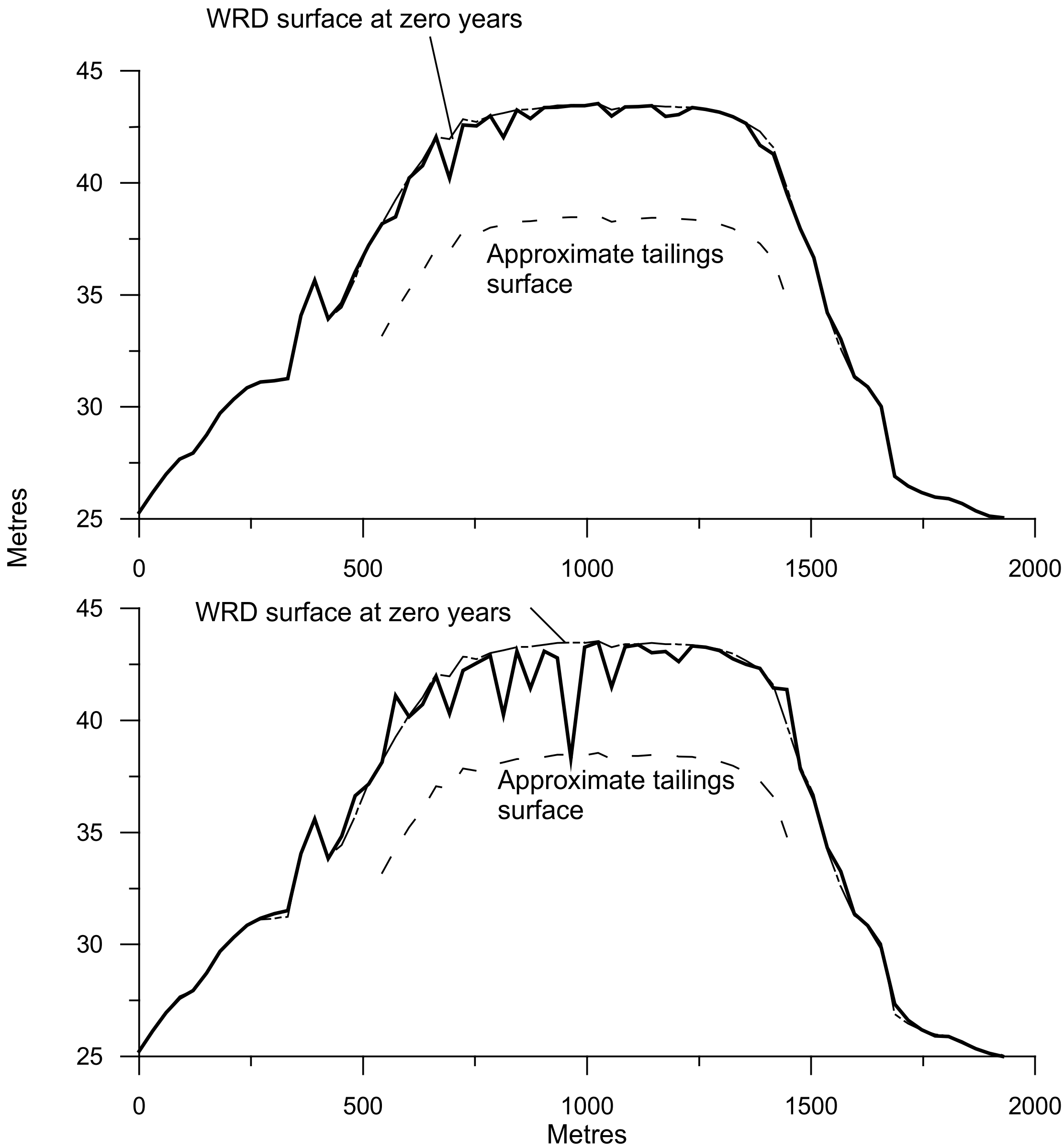

Figure 5.11 Section A-A through the landform (see fig. 5.4). Top: Case 4 simulations (vegetated and ripped) at 1000 y; Bottom: Case 2 simulations (unvegetated and unripped) at 1000 y.

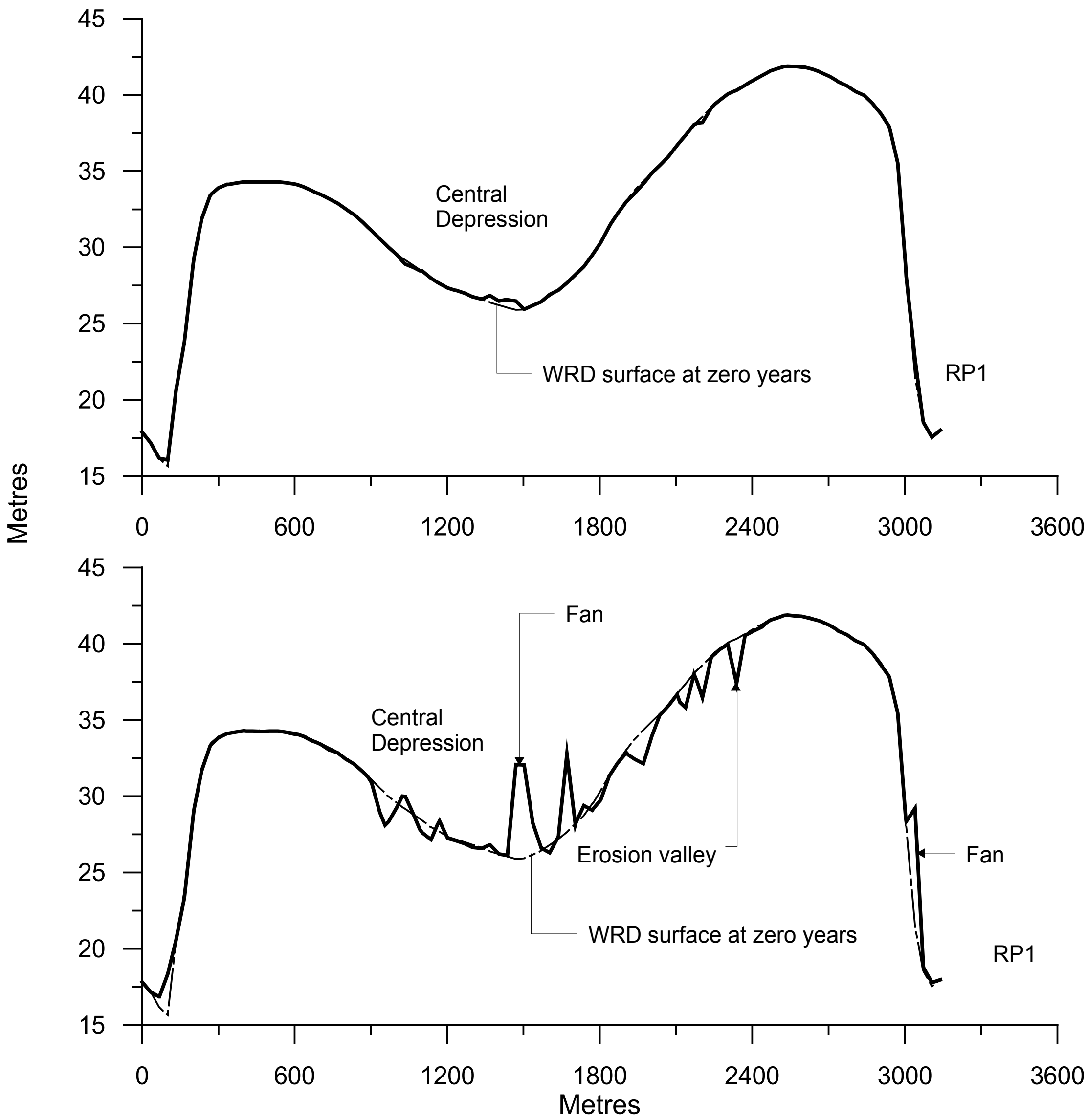

Figure 5.12 Section B-B through the landform (see fig. 5.4). Top: Case 4 simulations (vegetated and ripped) at 1000 y; Bottom: Case 2 simulations (unvegetated and unripped) at 1000 y.

Further research is required to define the fate of that sediment, and assess the impact of sediment deposition on streams, particularly Georgetown Creek, where backflow relationships with Magela Creek will reduce sediment transport capacity in Georgetown Creek resulting in deposition within the system.

For the vegetated and ripped condition, SIBERIA simulations predicted that sediment movement would occur in similar locations as those for the unvegetated, unripped state, but at a much reduced scale.

The results of the simulations were predictable due to a knowledge of erosion processes and the knowledge that vegetation reduces runoff and erosion. The modelling gives results which are qualitatively similar to those intuitively expected, which supports the validity of the modelling process. However, this novel study quantifies the effect of these surface treatments on the post-mining landform evolution process allowing optimum design of landforms. For example, section A-A (fig 5.11) shows that the maximum erosion depth in the TDA for the vegetated and ripped condition is 2.2 m. This allows erosion estimates to be refined such that a more precise depth of waste rock capping on the tailings could be determined. For the example used here under conditions of stable vegetation and ripping, based on the refined erosion estimate, a confident reduction of 2 m depth of capping material could be made. This equates to a volume of approximately 2 Mm^3 of waste rock material which would not have to be placed over the 1 km^2 tailings dam. If a 10 m^3 bucket loader was used to spread the waste rock at a cost of \$1.50 m^{-3}, this reduction in depth represents a saving of approximately \$3 000 000. The design has been optimised resulting in both protection of the environment and cost reduction.

It should be noted that the SIBERIA modelling process can be further refined. These refinements are discussed in chapter 6 – Conclusions and further investigation.

6 Conclusions and further investigation

In broad terms, the major achievements of this project are:

- documentation of the process of data collection, parameter derivation and modelling of rehabilitated landform design which can be incorporated in mine planning;
- assessment of the effects of vegetation and surface amelioration on simulated landform evolution of the rehabilitated landform at ERA Ranger Mine.

To incorporate rehabilitated landform modelling in mine planning, site-specific rainfall, runoff and sediment loss data are required to parameterise a total sediment loss equation and the DISTFW rainfall-runoff model. These models are then used to derive an average annual sediment discharge from a landform to parameterise the SIBERIA model sediment discharge equation. Once this is completed SIBERIA can be used to simulate the topographic evolution of a landform over a specific time period incorporating various rehabilitation strategies such as revegetation and surface ripping. Little previous work has been done on the practical application of the models to the process of rehabilitated mining landform design. This study is applied research and there are major advances in knowledge resulting from the documentation of methods of collection, reduction and analysis of real mine site data; the presentation of the techniques of derivation of model parameters from the data; the application of the models to a mining environment; and the discussion of issues arising during the process.

Specific conclusions arising from the research are presented and areas of further investigation are discussed.

6.1 Conclusions

The collection of rainfall, runoff and sediment loss data and model parameterisation is a complex and difficult process. The main technique of data collection used was natural rainfall event monitoring. To parameterise models used in the SIBERIA landform simulation process for various mine site conditions, it is necessary to collect complete sets of rainfall, runoff, suspended sediment and bedload sediment for rainfall events at representative sites.

Data sets were collected from sites with the following surface treatments: (1) a surface with no treatment (eg. ripping or rock mulch) and no vegetation (cap site – 0.028 m/m slope); (2) a surface with a large percentage of large competent rock fragments similar to a rock mulch (batter site – 0.207 m/m slope); (3) a surface that had been ripped and vegetated (soil site – 0.012 m/m slope); and (4) a ripped surface that had well established vegetation approximately 10 years old (fire site). A single soil loss equation was derived that was applicable to all sites (except the fire site). This resulted in one parameter value representing cover and conservation practices which could be adjusted depending on slope of the study site. Runoff was the major control in the soil loss prediction relationship for specific sites.

Hydrological parameters (kinematic wave and infiltration) that were derived for the DISTFW model were derived for each site excluding the fire site. Statistical compatibility analysis of these parameters showed that the parameter sets for each surface treatment were statistically different reflecting the effects of these treatments. This shows that the differences between the surface treatments, such as vegetation, ripping and rock mulching, can be quantified in terms of hydrology model parameters, and these differences are statistically significant. The results highlight the importance of predicting an accurate hydrograph as this is the controlling factor when using the sediment loss equation discussed here.

Difficulties were experienced with respect to monitoring of natural rainfall events. However, the location of the study site (the wet/dry tropics) was an advantage with respect to monitoring. In the wet/dry tropics it is predictable that rain will occur during a Wet season which allows a monitoring program to be established. The nature of the models require that discrete event rainfall, discharge and total sediment loss data are collected. To achieve this an observer must be present at each site for the duration of the event to collect the complete data set. Over the three year monitoring period for this study, only 28 full data sets from four sites were collected. Suspended sediment data are the most difficult to collect as an observer needs to be present at the start of an event to collect runoff samples containing suspended sediment. Bedload can be collected at the completion of an event. For many of the storms where sediment data sets were incomplete it was the suspended sediment data that were missing.

The natural rainfall event data were used to fit the following sediment transport equations (4.8 and 4.10) which were adopted for landform evolution modelling using SIBERIA:

$T_{cap} = 5.79\ S^{0.69} \int Q^{1.59}\, dt$ ($r^2 = 0.92$; $p < 0.001$) (for an unvegetated site without surface amelioration)

$T_{soil} = 10.4\ S^{0.69} \int Q^{1.59}\, dt$ ($r^2 = 0.92$; $p < 0.001$) (for a vegetated site with surface amelioration, ie ripping)

A small number of high sediment loss events were recorded on the cap and batter sites. It is important that event data used to fit sediment transport equations are representative of the range of events that occur during a Wet season. It was observed in this study that the minority high intensity events removed ≈70% of the total sediment lost during all the reported events.

Parameterisation of the SIBERIA discharge area relationship demonstrated the important hydrological effect of vegetation and ripping with peak runoff from an unvegetated and unripped site an order of magnitude greater than from a vegetated ripped site for a 1 in 2 year rainfall event. For an unvegetated, unripped state with gully erosion rates on steep batter slopes, SIBERIA simulations showed that at 1000 y the landform was dissected by localised erosion valleys with fans at the outlets of most valleys. Major valley formation occurred at the transition from low to high slopes at the top of the batter slopes and major deposition occurred at the transition from high to low slopes at the base of the batter. The fans on low slopes in the centre of the landform were generally longer than those on the steep batter slopes. Simulations show valleys forming and later being in-filled. SIBERIA modelled stabilisation of vertical incision at about 500 y, and continued retreat of valley head walls and an increase in the number of valleys from 500 y to 1000 y. The eroded hillslope forms simulated by SIBERIA have been observed in nature and described as zero-order drainage basins occurring in highly seasonal savanna climates such as the climate of the study site.

For the vegetated and ripped condition, with gully erosion rates on steep batter slopes, SIBERIA simulations predicted that sediment movement would occur in similar locations as those for the unvegetated, unripped state, but at a much reduced scale. The modelling gives results which are qualitatively similar to those intuitively expected as a result of the effect of vegetation on runoff and erosion, which supports the validity of the modelling process.

However, this novel study quantifies the effect of these surface treatments on the post-mining landform evolution process allowing optimum design of landforms. For example, this quantitative analysis showed that maximum erosion depth in the TDA for the vegetated and ripped condition is 2.2 m. Therefore, based on these results, a more precise depth of waste rock capping on the tailings could be determined. A reduction of 2 m depth of cap material over the tailings, if it could be proven to be safe, equates to a volume of 2 Mm^3 per km^2 of waste rock material saving. If a 10 m^3 bucket loader was used to spread the waste rock at a cost of \$1.50 m^{-3}, this reduction in depth represents a saving of \$3 000 000 per km^2.

6.2 Further investigation

There are a number of issues related to the SIBERIA modelling process which require further investigation. These issues are discussed in the following.

1. The data used for the simulations in this study were for a landform with surfaces that were (1) unvegetated and unripped and (2) vegetated and ripped. These data reflect the condition of the landform at zero years. The SIBERIA simulations conducted were based on constant parameter values reflecting these initial conditions with no change during the simulation period or any spatial variation of surface conditions such as vegetation, ripping or rock mulching of the landform. For example, it has been recognised that rip lines only maintain their integrity for periods of approximately five years, but this effect was not incorporated in the simulations. Temporal and spatial changes in parameter values resulting from weathering, soil forming processes, ecosystem development and varying rehabilitation strategies were also not incorporated in the modelling process. Research is needed that can identify the effect on input parameters of these processes so that SIBERIA can be run incorporating temporal and spatial changes including stream transport.

2. The SIBERIA simulations in this study were based on the assumption that the surface conditions, ie vegetation and ripping, were the same for all surface slopes. Apart from the batter site, the sites available for this study had surface slopes <0.03 m/m and the batter site data were not used for SIBERIA modelling. These limited slopes resulted in difficulty in deriving a slope exponent for the sediment transport model. It is commonly recognised that there is a positive correlation between sediment loss and slope and in this study, on the 0.207 m/m batter slope, a possible runoff threshold was identified above which there was an increase in erosion rate. Therefore data should be collected from a range of sites with different slopes to confirm the sediment transport model slope exponent.

3. In this study, SIBERIA was run in a mode which did not reflect climate seasonality. However the long-term runoff series, which was used to derive SIBERIA input parameters, was derived using seasonal rainfall data. The resulting eroded hill-slopes simulated were similar to features recognised in nature which form in areas of highly seasonal climate. It should be investigated to what extent model parameters reflect climate seasonality.

4. Validation is an important part of modelling. The landform evolution of Mancos Shale badlands in Utah, USA, has been interpreted using a drainage basin simulation model (Howard 1997). Although the simulations and field interpretation of erosional history were consistent, Howard (1997) considered that process rate laws and model parameters were not validated and that long-term process observations would be valuable in the

validation process. In the case of SIBERIA modelling, studies in the following areas have been developed to validate model predictions (Willgoose & Loch 1996):

a) Monitoring erosion and runoff from a mine site abandoned 40 years ago to collect data to test if SIBERIA can simulate the erosional features on the abandoned site;

b) A gully has been deliberately triggered on the WRD at ERARM. The growth of the gully will be monitored to qualitatively test development rates and compare these rates with those simulated by SIBERIA;

c) Using DTM data from a natural catchments in Arnhem Land Australia, near the mine site, to test SIBERIA's ability to simulate natural landscape formation and to predict the depth of erosion on the cap layer of the rehabilitated landform.

There are other areas of study which may be necessary. Nevertheless, this study has provided the practitioner with a method, comprehensively documented, that can be used to incorporate landform evolution modelling in mine planning and has quantified the effects of surface treatments on landform evolution which can be used as a basis for more accurate design. Application of the methods described in this study will result in more cost efficient mining practices and greater protection of the environment.

Appendix A.1 Constant width plot input file bat18_3o.fw

```
Data file is for a rainfall simulation plot (plot version)
RUM 93 batter large scale plot  Monitoring
18/3/93 1745hrs
PLOT
# No of elements, No of reservoirs, no of u/S elements
   10        0        1
# No of U/S element draining into D/S elements
#
# zero time (hrs), timestep (minutes), time of duration of storm (hrs)
#
0. 0.1  2.
# --------------------------------------
#  OUTPUT PARAMETERS
# --------------------------------------
# no of pts for output discharge,psteps
1 1
# subareas at which discharge requested
10
#  maximum discharge on output graph
0.002
#
INCIDENCES
  0  1  2  3  4  5  6  7  8  9
PARAMETERS
# Kind of element
  0
#  No Area Length   U/S    D/S   SWSupply Gamma Sorpt Phi GWsupply
#              Elevation Elevation
# ------------------------------------------------------------------
  1  60.03  3.765   9.2    8.4    1.0    1.0  1.0  1.0   1.0
  2  60.03  3.765   8.4    7.5    1.0    1.0  1.0  1.0   1.0
  3  60.03  3.765   7.5    6.7    1.0    1.0  1.0  1.0   1.0
  4  60.03  3.765   6.7    5.9    1.0    1.0  1.0  1.0   1.0
  5  60.03  3.765   5.9    5.1    1.0    1.0  1.0  1.0   1.0
  6  60.03  3.765   5.1    4.4    1.0    1.0  1.0  1.0   1.0
  7  60.03  3.765   4.4    3.6    1.0    1.0  1.0  1.0   1.0
  8  60.03  3.765   3.6    2.9    1.0    1.0  1.0  1.0   1.0
  9  60.03  3.765   2.9    2.1    1.0    1.0  1.0  1.0   1.0
  10 60.03  3.765   2.1    1.3    1.0    1.0  1.0  1.0   1.0
#  Hillslope and Channel conveyances
#  ------------------------------------
#    1st set are hillslope conveyances
#    2nd set are  channel  conveyances
#  ------------------------------------
#  Element No, No of conveyances
#  CR, EM, CONVEY
```

```
#
CONVEYANCES
1 2
0.158       1.      0.
0.158       1.      1000.
#
#  Parameter Multpliers
#  Ch-CR  Ch-EM  SWSupply SWGamma Sorptivity   Phi  GWSupply  timing(sec)
MULTIPLIERS
  7.8    1.33    0.03      0.375  0.00001     6.5     1000.    0.0
1
0.0 0.0
# -------------
# No of pluvios
# -------------
RAINFALL #1
   1
CUMPLUVIO bat18_3o.rf
1.00 1.00 1.00 1.00 1.00 1.00 1.00 1.00 1.00 1.00
# --------------------------------
#  No of known initial flows at stations
# --------------------------------
INITIALQ
title line 1
title line 2
title line 3
   1
# stations at which flows known and initial flow (cumecs)
  10 0.0
#  No of stations with known inflows
INFLOWQ NONE
#  Hydrograph to calibrate with (no of values)
CALIB #1 bat18_3o.ro
END
```

Appendix A.2 Rainfall input file bat18_3o.rf

```
#    3 lines of titles
RUM93 monitoring
Batter site, large scale plot
Rainfall 17:46:30hrs 18/03/93
#    number of data points
     23
# time      rainfall
#  (h)      (mm)
0           0
0.008333       1
0.016667       1
0.025       2
0.033333       2
0.041667       3
0.05           4
0.058333       5
0.066667       5
0.075       6
0.083333       7
0.091667       8
0.1            9
0.108333       11
0.116667       12
0.125       13
0.133333       14
0.4         14
0.408333       15
0.625       15
0.633333       16
1.383333       16
2           16
```

Appendix A.3 Runoff input file bat18_3o.ro

```
#    3 lines of titles
RUM93 monitoring
Batter site, large scale plot
Runoff 17:46:30hrs 18/03/93
#    number of data points
     101
# time       runoff
#  (h)       (m³s⁻¹)
0            0
0.05         0
0.058333     0.00046
0.066667     0.001647
0.075        0.003181
0.083333     0.004727
0.091667     0.007187
0.1          0.00988
0.108333     0.011657
0.116667     0.011199
0.125        0.01191
0.133333     0.007624
0.141667     0.00699
0.15         0.009459
0.158333     0.007624
0.166667     0.006321
0.175        0.005
0.183333     0.004003
0.191667     0.003093
0.2          0.002529
0.208333     0.002093
0.216667     0.001647
0.225        0.001383
0.233333     0.00121
0.241667     0.001048
0.25         0.000945
0.258333     0.000755
0.266667     0.000678
0.275        0.000564
0.283333     0.000525
0.291667     0.00046
0.3          0.000424
0.308333     0.000364
0.316667     0.00034
0.325        0.00034
0.333333     0.000308
0.341667     0.000308
0.35         0.000278
0.358333     0.000278
0.366667     0.000221
0.375        0.000221
0.383333     0.000194
0.391667     0.000194
0.4          0.000169
0.408333     0.000169
0.425        0.000169
0.433333     0.000169
0.441667     0.000144
0.45         0.000144
0.458333     0.000121
0.466667     0.000144
0.475        0.000121
0.483333     0.000121
0.491667     0.000144
0.5          0.000144
0.508333     0.000121
0.516667     0.000121
0.525        0.000144
0.533333     0.000121
0.541667     0.000144
0.55         0.000144
0.558333     0.000121
0.566667     0.000144
0.575        0.000121
0.583333     0.000144
0.591667     0.000169
0.6          0.000144
0.608333     0.000144
0.616667     0.000169
0.625        0.000169
0.633333     0.000194
0.641667     0.000194
0.65         0.000221
0.658333     0.000249
0.666667     0.000249
0.675        0.000249
0.683333     0.000249
0.691667     0.000249
0.7          0.000278
0.708333     0.000278
0.716667     0.000249
0.725        0.000278
0.733333     0.000249
0.783333     0.000249
0.791667     0.000221
0.8          0.000194
0.833333     0.000194
0.841667     0.000169
0.866667     0.000169
0.875        0.000144
0.941667     0.000144
0.95         0.000121
1.016667     0.000121
1.025        9.9E-05
1.125        9.9E-05
1.133333     8.3E-05
1.358333     8.3E-05
1.366667     6.4E-05
1.383333     6.4E-05
2.0          0
```

Appendix A.4 Output plot file bat18_3n.prt

```
>>> Nlfit Version 2.07g <<<
+--------------------------------------------------------------------+
!                                                                    !
+--------------------------------------------------------------------+

 Model identification string: FW MODEL V3.0
 Posterior moments file is bat18_3n.pmf

 ******************************************************************
 No of fitted parameters =  4, No of observations =  101
 Observation range: Minimum =    1
                    Maximum =  101

 Number of explicitly censored observations =    0
 All observed responses less than        0.     were censored
 All observed responses less than or equal to -1.0e20 are flagged as MISSING and were censored

 Residual mean=  -0.10020E-01

 Gauss-Marquardt method: Marquardt lambda=      0.

 Convergence monitor=  0.337791E-02

 Fitted parameter     Current       Change about current value
  #   Name             value         delta                t stat
  1   Cr              15.6806     -0.781283E-02  -0.197589E-02
  2   em          1.82945     -0.213318E-03  -0.237722E-02
  3   Sorptivity       1.53704      0.170886E-02  0.195514E-02
  4   Phi          52.7281     -0.102595E-01  -0.185241E-02

 Correlation matrix of fitted parameters:
  1.00000
  0.97369   1.00000
 -0.15253  -0.25186   1.00000
  0.04548   0.10074  -0.93143   1.00000

 Durbin-Watson statistic=    0.7815   Serial correlation=  0.6093

 ******************************************************************
 Maximized log-likelihood is  794.773
 Derivative status: Forward difference with 0.100E-05 std dev perturbation

Gauss-Marquardt method: Marquardt lambda =        0.

 Summary of posterior distributions
 Model parameters:
 Fit#  Name       Transform       Mean       Std dev     Untransformed
 ----------------------------------------------------------------------
   1  Cr                None         15.6806       3.95408             15.6806
   2  em                None         1.82945      0.897344E-01        1.82945
  **  Cs                None        0.300000E-02                       0.300000E-02
  **  Gamma             None        0.375000                       0.375000
   3  Sorptivity None         1.53704       0.874035              1.53704
   4  Phi               None         52.7281       5.53844             52.7281
  **  Cg                None         1000.00                       1000.00
  **  (Disabled)        None        0.100000E-03                       0.100000E-03
  **  Timing #1         None        0.100000E-03                       0.100000E-03
  **  InitWet #1        None        0.100000E-03                       0.100000E-03

  Fit  Response        Parameter       Mean        Std dev
   #    # Name          Type  #
 -----------------------------------------------------------------
  **   1 18/03/93     Lambda           0.
```

```
 **   1                K       0.100000E-02
*****************************************************************
               +-----------------------------------------------+
               !  Response equation number= 1  Name: 18/03/93    !
               +-----------------------------------------------+
 Performance indices for untransformed response data
             Observed      Predicted
     Mean     0.1373E-02     0.1340E-02
   Std dev     0.2754E-02     0.2697E-02

Coefficient of determination = 0.926 (adjusted coefficient of determination = 0.924)
Coefficient of efficiency    = 0.926
Residual mass coefficient    = 0.982
*******************************************************************
 >>>> Error vs predicted response plot <<<<
Mean= 0.33615E-04 Variance= 0.58295E-06 Std dev= 0.76351E-03 Skew=  -1.079 Skew std error= 0.240

Residual versus predicted response plot
    ..............................................................................
   4.357                             +                          .
      .                     +                                 .
      .                                                       .
      .                                                       .
      .                +                                      .
   1.766                       +        +        +                .
      .          +      +   +                          +      .
      .        +  +  +                                        .
      .***222+++-+++--------------------------------------------------------------+----+.
      .  +                                                    .
  -0.825      +                                                 .
      .       +                                               .
      .                                                       .
      .                                                       .
      .                                                       .
  -3.416                                                        .
      .                                         +             .
      .                                                       .
      .                                                   + .
      !........!........!........!........!........!........!........!........!..........
     0.0     13.4     26.8     40.2     53.6     66.9     80.3     93.7    107.1
                                   X-axis multiplier= 0.10000E-03


>>> Time series plot of observed and predicted values for response 1 <<<

Time            Response                          O = observed; P = predicted
Step  Observed     Predicted   Difference         |----------i---------i---------i---------i---------i|
   1      0.          0.           0.             |O                                       |
   2      0.      0.95288E-03 -0.95288E-03         |O--P                                          |
   3  0.46000E-03  0.16736E-02 -0.12136E-02       |-O----P                                       |
   4  0.16470E-02  0.15756E-02  0.71378E-04       |------O                                      |
   5  0.31810E-02  0.22789E-02  0.90211E-03       |---------P  O                                  |
   6  0.47270E-02  0.33042E-02  0.14228E-02       |-------------P     O                            |
   7  0.71870E-02  0.45367E-02  0.26503E-02       |------------------P         O                  |
   8  0.98800E-02  0.65531E-02  0.33269E-02       |--------------------------P            O        |
   9  0.11657E-01  0.10981E-01  0.67617E-03       |---------------------------------------------P  O  |
  10  0.11199E-01  0.11372E-01 -0.17306E-03       |----------------------------------------------OP   |
  11  0.11910E-01  0.11916E-01 -0.60582E-05       |-------------------------------------------------O |
  12  0.76240E-02  0.11815E-01 -0.41908E-02       |-------------------------------O-----------------P |
  13  0.69900E-02  0.10092E-01 -0.31021E-02       |----------------------------O------------P        |
  14  0.94590E-02  0.82691E-02  0.11899E-02       |-----------------------------------P    O         |
  15  0.76240E-02  0.65607E-02  0.10633E-02       |---------------------------P   O               |
  16  0.63210E-02  0.51526E-02  0.11684E-02       |---------------------P    O                 |
  17  0.50000E-02  0.41321E-02  0.86786E-03       |----------------P   O                      |
  18  0.40030E-02  0.33764E-02  0.62663E-03       |-------------P  O                          |
  19  0.30930E-02  0.27836E-02  0.30936E-03       |-----------PO                               |
```

```
20  0.25290E-02  0.23089E-02  0.22015E-03    |---------PO                    |
21  0.20930E-02  0.19280E-02  0.16498E-03    |-------PO                      |
22  0.16470E-02  0.16228E-02  0.24215E-04    |------O                        |
23  0.13830E-02  0.13776E-02  0.53726E-05    |-----O                         |
24  0.12100E-02  0.11796E-02  0.30375E-04    |----O                          |
25  0.10480E-02  0.10185E-02  0.29495E-04    |---O                           |
26  0.94500E-03  0.88633E-03  0.58666E-04    |---O                           |
27  0.75500E-03  0.77696E-03 -0.21963E-04    |--O                            |
28  0.67800E-03  0.68568E-03 -0.76777E-05    |--O                            |
29  0.56400E-03  0.60888E-03 -0.44884E-04    |-OP                            |
30  0.52500E-03  0.54377E-03 -0.18772E-04    |-O                             |
31  0.46000E-03  0.48816E-03 -0.28159E-04    |-O                             |
32  0.42400E-03  0.44035E-03 -0.16348E-04    |-O                             |
33  0.36400E-03  0.39898E-03 -0.34979E-04    |-O                             |
34  0.34000E-03  0.36297E-03 -0.22971E-04    |OP                             |
35  0.34000E-03  0.33146E-03  0.85359E-05    |O                              |
36  0.30800E-03  0.30375E-03  0.42478E-05    |O                              |
37  0.30800E-03  0.27926E-03  0.28741E-04    |O                              |
38  0.27800E-03  0.25752E-03  0.20479E-04    |O                              |
39  0.27800E-03  0.23815E-03  0.39855E-04    |O                              |
40  0.22100E-03  0.22081E-03  0.19396E-06    |O                              |
41  0.22100E-03  0.20524E-03  0.15763E-04    |O                              |
42  0.19400E-03  0.19121E-03  0.27931E-05    |O                              |
43  0.19400E-03  0.17852E-03  0.15478E-04    |O                              |
44  0.16900E-03  0.16702E-03  0.19775E-05    |O                              |
45  0.16900E-03  0.41157E-03 -0.24257E-03    |OP                             |
46  0.16900E-03  0.33119E-03 -0.16219E-03    |O                              |
47  0.16900E-03  0.36962E-03 -0.20062E-03    |OP                             |
48  0.16900E-03  0.29781E-03 -0.12881E-03    |O                              |
49  0.14400E-03  0.27319E-03 -0.12919E-03    |O                              |
50  0.14400E-03  0.29576E-03 -0.15176E-03    |O                              |
51  0.12100E-03  0.30014E-03 -0.17914E-03    |O                              |
52  0.14400E-03  0.27061E-03 -0.12661E-03    |O                              |
53  0.12100E-03  0.23202E-03 -0.11102E-03    |O                              |
54  0.12100E-03  0.20703E-03 -0.86033E-04    |O                              |
55  0.14400E-03  0.20088E-03 -0.56879E-04    |O                              |
56  0.14400E-03  0.20682E-03 -0.62821E-04    |O                              |
57  0.12100E-03  0.21478E-03 -0.93779E-04    |O                              |
58  0.12100E-03  0.21730E-03 -0.96304E-04    |O                              |
59  0.14400E-03  0.21174E-03 -0.67742E-04    |O                              |
60  0.12100E-03  0.19925E-03 -0.78250E-04    |O                              |
61  0.14400E-03  0.18278E-03 -0.38779E-04    |O                              |
62  0.14400E-03  0.16553E-03 -0.21534E-04    |O                              |
63  0.12100E-03  0.15011E-03 -0.29107E-04    |O                              |
64  0.14400E-03  0.13813E-03  0.58666E-05    |O                              |
65  0.12100E-03  0.13025E-03 -0.92467E-05    |O                              |
66  0.14400E-03  0.12623E-03  0.17766E-04    |O                              |
67  0.16900E-03  0.12531E-03  0.43691E-04    |O                              |
68  0.14400E-03  0.12640E-03  0.17598E-04    |O                              |
69  0.14400E-03  0.12842E-03  0.15581E-04    |O                              |
70  0.16900E-03  0.13045E-03  0.38555E-04    |O                              |
71  0.16900E-03  0.13184E-03  0.37156E-04    |O                              |
72  0.19400E-03  0.37518E-03 -0.18118E-03    |OP                             |
73  0.19400E-03  0.32141E-03 -0.12741E-03    |O                              |
74  0.22100E-03  0.36561E-03 -0.14461E-03    |OP                             |
75  0.24900E-03  0.30019E-03 -0.51187E-04    |O                              |
76  0.24900E-03  0.29185E-03 -0.42847E-04    |O                              |
77  0.24900E-03  0.32048E-03 -0.71484E-04    |O                              |
78  0.24900E-03  0.31858E-03 -0.69578E-04    |O                              |
79  0.24900E-03  0.28298E-03 -0.33975E-04    |O                              |
80  0.27800E-03  0.24546E-03  0.32540E-04    |O                              |
81  0.27800E-03  0.22635E-03  0.51649E-04    |O                              |
82  0.24900E-03  0.22589E-03  0.23107E-04    |O                              |
83  0.27800E-03  0.23395E-03  0.44053E-04    |O                              |
84  0.24900E-03  0.23981E-03  0.91867E-05    |O                              |
85  0.24900E-03  0.15799E-03  0.91012E-04    |O                              |
```

```
 86  0.22100E-03  0.14726E-03  0.73743E-04      |O                                   |
 87  0.19400E-03  0.14084E-03  0.53161E-04      |O                                   |
 88  0.19400E-03  0.14043E-03  0.53566E-04      |O                                   |
 89  0.16900E-03  0.14145E-03  0.27547E-04      |O                                   |
 90  0.16900E-03  0.13873E-03  0.30273E-04      |O                                   |
 91  0.14400E-03  0.13590E-03  0.81004E-05      |O                                   |
 92  0.14400E-03  0.10113E-03  0.42865E-04      |O                                   |
 93  0.12100E-03  0.96838E-04  0.24162E-04      |O                                   |
 94  0.12100E-03  0.68728E-04  0.52272E-04      |O                                   |
 95  0.99000E-04  0.65963E-04  0.33037E-04      |O                                   |
 96  0.99000E-04  0.42016E-04  0.56984E-04      |O                                   |
 97  0.83000E-04  0.40602E-04  0.42398E-04      |O                                   |
 98  0.83000E-04  0.18727E-04  0.64273E-04      |O                                   |
 99  0.64000E-04  0.18280E-04  0.45720E-04      |O                                   |
100  0.64000E-04  0.17430E-04  0.46570E-04      |O                                   |
101       0.      0.48127E-05 -0.48127E-05      |O                                   |
                                |----------i---------i---------i---------i---------i|
```

>>>> Residual plots for residual a <<<<
Mean=-0.10072E-01 Variance= 0.19867E-01 Std dev= 0.14095 Skew= -1.570 Skew std error= 0.241
Residual versus predicted response plot

```
    ..........................................................................................
  2.775                      +            +                              .
    .                 +                                              .
    .           +                                                    .
    .                       +                                        .
    .                 +   +             +          +                   .
  0.795+2             +  +                                               .
    .**3   +++ +++ +                                        +      .
    .266222-----------------------------------------------------------------------+----+.
    . 74                                                             .
    .  6                                                             .
 -1.185   +                                                            .
    .                                                                .
    .                                                  +             .
    .                                                                .
    .                                                           + .
 -3.165                                                                .
    .                                                                .
    .       +                                                        .
    .     +                                                          .
    !.........!.........!.........!.........!.........!.........!.........!.........!.........!...........
   0.0     13.4     26.8     40.2     53.6     67.0     80.3     93.7    107.1
                                    X-axis multiplier= 0.10000E-03
```

Cumulative periodogram (assumes constant error variance)

```
    ...........................................
  1.000                    ++++2+++++2++++++.
    .                  ++              .
    .               ++++++               .
    .              +2                  .
    .            +++                    .
  0.763          2+                      .
    .        +                         .
    .        +                         .
    .       +                          .
    .                                  .
  0.526      +                           .
    .                                  .
    .                                  .
    .     +                            .
    .                                  .
  0.288     +                            .
    .                                  .
    .    +                             .
    .  +++                              .
    .2+                                .
```

```
      !.........!.........!.........!.........!...
    0.0       0.1       0.2       0.4       0.5
                   Frequency
```

Hypothesis: errors are time-independent - test statistic = 0.4551
- 5% Exceedance value of test statistic = 0.1943

Plot of standardised residuals against time

```
      .............................................................................................
   2.775    ++                                                          .
      .   +                                                          .
      .  +                                                           .
      .          +                                                   .
      .        ++ ++                                                    .
   0.795            ++                              ++          +   .
      . +    +          2++++       +++++ 2++               + ++++++       +2++  ++++2+++++ ++ .
      .-------++-------------++++2++-----+------------++----2+-+--------++-++-------------------+.
      .                                 ++ +++  ++++          +    +                    .
      .                               ++  ++               + +                     .
  -1.185                                +                                          .
      .                                                                         .
      .        +                                                                 .
      .                                                                         .
      .       +                                                                  .
  -3.165                                                                           .
      .                                                                         .
      .+                                                                         .
      .+                                                                         .
      !.........!.........!.........!.........!.........!.........!.........!.........!...........
    0.0      11.1      22.2      33.4      44.5      55.6      66.7      77.9      89.0
```

Runs test Z-statistic = -7.592 Test statistic for in- or decreasing variance = 0.07
it is distributed as f with 48, 48 dof

Plot of standardised residuals vs N(0,1) variate

```
      .............................................
   2.775                                   +   +.
      .                                       .
      .                               ++     .
      .                                       .
      .                             ++       .
   0.984                              2+        .
      .                       343232          .
      .------------------345454544-----------------.
      .              33442                      .
      .          +323+                          .
  -0.808        ++2+                               .
      .     +                                   .
      .                                        .
      .                                        .
      .    +                                    .
  -2.599    +                                    .
      .                                        .
      .                                        .
      .                                        .
      .   +                                     .
  -4.390+                                        .
      !.........!.........!.........!.........!.....
    -2.5     -1.3     -0.2      1.0      2.1
                   Normal variate
```

Hypothesis: Errors are normally-distributed - test statistic = 0.1822
- 5% Exceedance value of test statistic = 0.0888

>>>> Residual plots for residual a <<<<

Summary of standardised residuals above and below 2.000 standard deviations

```
  Positive outliers      Negative outliers
 Obs no  Std residual   Obs no  Std residual
--------------------------------------------
     7       2.775        2        -4.748
     8       2.589
     6       2.026
```

Autocorrelation function

```
Lag      Autocorrelation         -1.0 -.8 -.6 -.4 -.2 0.0  .2  .4  .6  .8 1.0
    Estimate  95% limits on white noise   |....|....|....|....|....|....|....|....|....|....|
 1   0.613     0.201    -0.201   |              <   |****>**********        |
 2   0.141     0.202    -0.202   |              <   |****>                  |
 3  -0.063     0.203    -0.203   |              <  **|   >                  |
 4  -0.269     0.204    -0.204   |            **<****|   >                  |
 5  -0.384     0.205    -0.205   |          *****<****|   >                 |
 6  -0.239     0.206    -0.206   |             *<****|   >                  |
 7  -0.052     0.207    -0.207   |              <   *|   >                  |
 8   0.040     0.209    -0.209   |              <   |*  >                   |
 9   0.251     0.210    -0.210   |              <   |****>*                 |
10   0.397     0.211    -0.211   |              <   |****>*****             |
11   0.198     0.212    -0.212   |              <   |*****                  |
12  -0.004     0.213    -0.213   |              <    *   >                  |
13  -0.054     0.214    -0.214   |              <   *|   >                  |
14  -0.084     0.216    -0.216   |              <  **|   >                  |
15  -0.078     0.217    -0.217   |              <  **|   >                  |
                                  |.......................|.......................|
```

Note < and > denote approximate 95% limits on the white noise autocorrelation function

Partial autocorrelation function

```
Lag    Partial autocorrelation       -1.0 -.8 -.6 -.4 -.2 0.0  .2  .4  .6  .8 1.0
    Estimate  95% limits on white noise   |....|....|....|....|....|....|....|....|....|....|
 1   0.613     0.201    -0.201   |              <   |****>**********        |
 2  -0.376     0.202    -0.202   |           ****<****|   >                 |
 3   0.090     0.203    -0.203   |              <   |** >                   |
 4  -0.384     0.204    -0.204   |          *****<****|   >                 |
 5  -0.007     0.205    -0.205   |              <    *   >                  |
 6   0.061     0.206    -0.206   |              <   |** >                   |
 7  -0.017     0.207    -0.207   |              <    *   >                  |
 8  -0.001     0.209    -0.209   |              <    *   >                  |
 9   0.305     0.210    -0.210   |              <   |****>***               |
10  -0.003     0.211    -0.211   |              <    *   >                  |
11  -0.169     0.212    -0.212   |              <****|   >                  |
12   0.087     0.213    -0.213   |              <   |** >                   |
13  -0.002     0.214    -0.214   |              <    *   >                  |
14   0.155     0.216    -0.216   |              <   |****>                  |
15   0.037     0.217    -0.217   |              <   |*  >                   |
                                  |.......................|.......................|
```

Note < and > denote approximate 95% limits on the white noise partial autocorrelation function

Appendix A.5 Output posterior moment file bat18_3n.pmf

```
POSTERIOR MOMENTS FILE – VERSION 3.0
FW MODEL V3.0

   10    4  101    0    1    1  0.1000000E-05    0
    1    1    0    0    1    1    0    0    0    0
   0.1568064E+02   0.1829452E+01   0.1537045E+01   0.5272812E+02
   0.3954076E+01
   0.9736893E+00   0.8973438E-01
  -0.1525285E+00  -0.2518574E+00   0.8740346E+00
   0.4548119E-01   0.1007364E+00  -0.9314282E+00   0.5538444E+01
   0.1568064E+02   0.1829452E+01   0.3000000E-02   0.3750000E+00   0.1537045E+01
   0.5272812E+02   0.1000000E+04   0.1000000E-03   0.1000000E-03   0.1000000E-03
    0    0    0    0    0    0    0    0    0    0
   0.1986732E-01
   0.0000000E+00
   0.1000000E-02
```

c_r e_m Cs Gamma Sphi phi Cg (Disabled)

```
Timing #1 InitWet #1
    1
18/03/93
    0    0
   0.5058856E+02
    1  101   0.0000000E+00
 0 0 0 0 0 0 0 0 0 0 0 0 0 0 0 0 0 0 0 0 0 0 0 0 0 0 0 0 0 0 0 0 0 0 0 0 0 0 0 0
 0 0 0 0 0 0 0 0 0 0 0 0 0 0 0 0 0 0 0 0 0 0 0 0 0 0 0 0 0 0 0 0 0 0 0 0 0 0 0 0
 0 0 0 0 0 0 0 0 0 0 0 0 0 0 0 0 0 0 0 0 0
```

Appendix B.1 Batter site

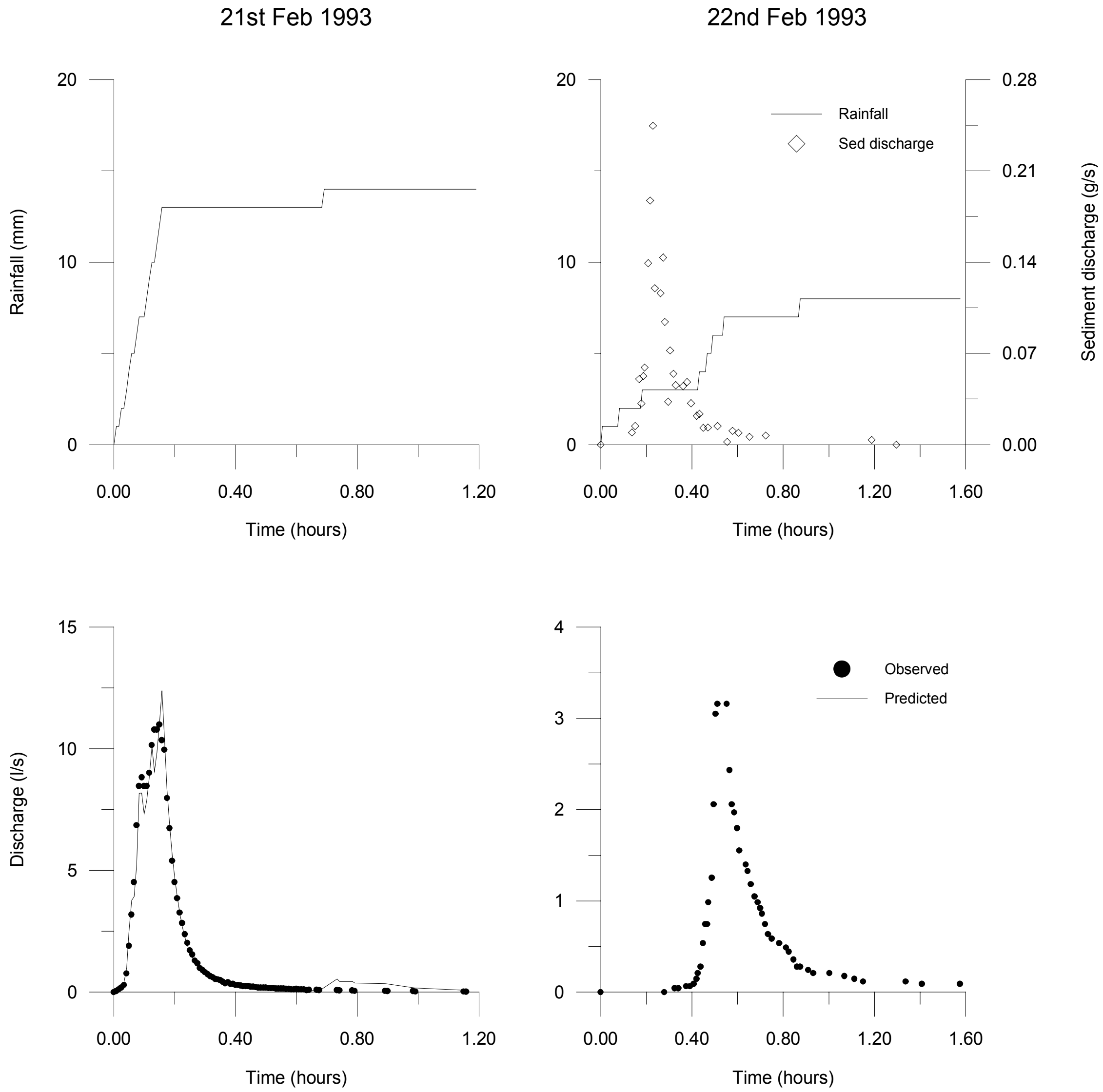

21st Feb 1993 | 22nd Feb 1993

NLFIT input files: bat21_2o.fw, bat21_2o.rf/ro | Did not fit

NLFIT output files: bat21_2n.prt/pmf

Parameter	Mean	St Deviation
c_r	19.9	3.98
e_m	1.97	0.08
Sphi	1.56	0.80
phi	19.5	5.02

Appendix B.1 continued

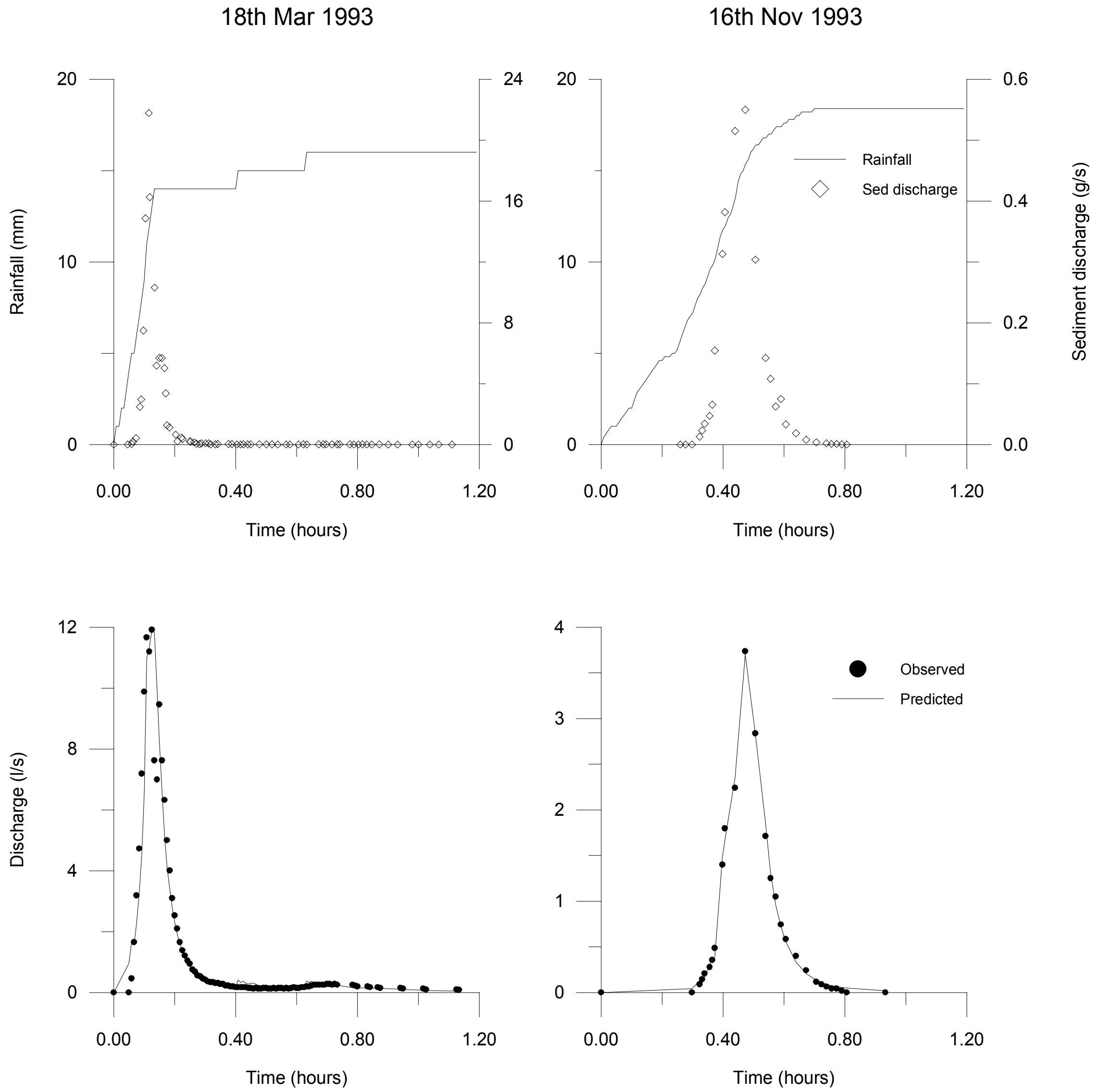

18th Mar 1993

NLFIT input files: bat18_3o.fw, bat18_3o.rf/ro

NLFIT output files: bat18_3n.prt/pmf

Parameter	Mean	St Deviation
c_r	15.7	3.95
e_m	1.83	0.09
Sphi	1.54	0.87
phi	52.7	5.54

16th Nov 1993

NLFIT input files: bat17o11.fw, bat17o11.rf/ro

NLFIT output files: bat17o11n.prt/pmf

Parameter	Mean	St Deviation
c_r	5.63	0.85
e_m	1.47	0.05
Sphi	7.09	0.57
phi	12.2	1.52

Appendix B.1 continued

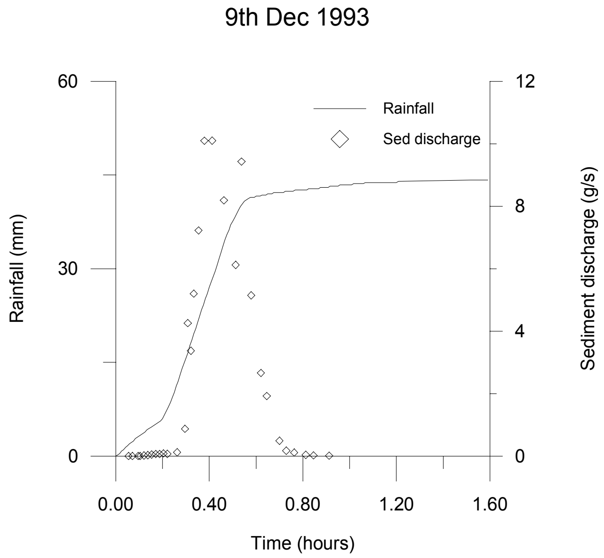

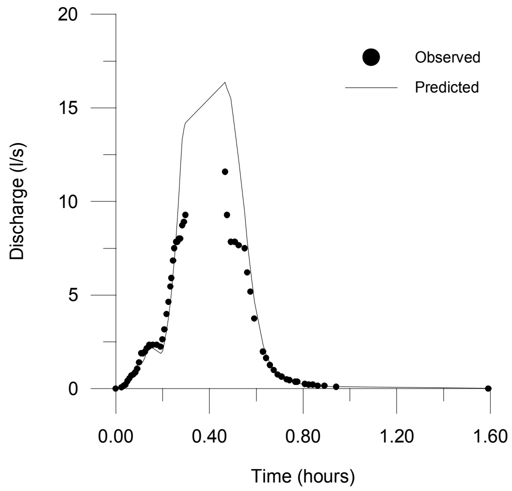

9th Dec 1993

NLFIT input files: bat10o12.fw, bat10o12.rf/ro

NLFIT output files: bat10o12.prt/pmf

Parameter	Mean	St Deviation
c_r	5.01	1.27
e_m	1.50	0.08
Sphi	0.0001	
phi	15.7	0.91

Appendix B.2 Cap site monitoring data

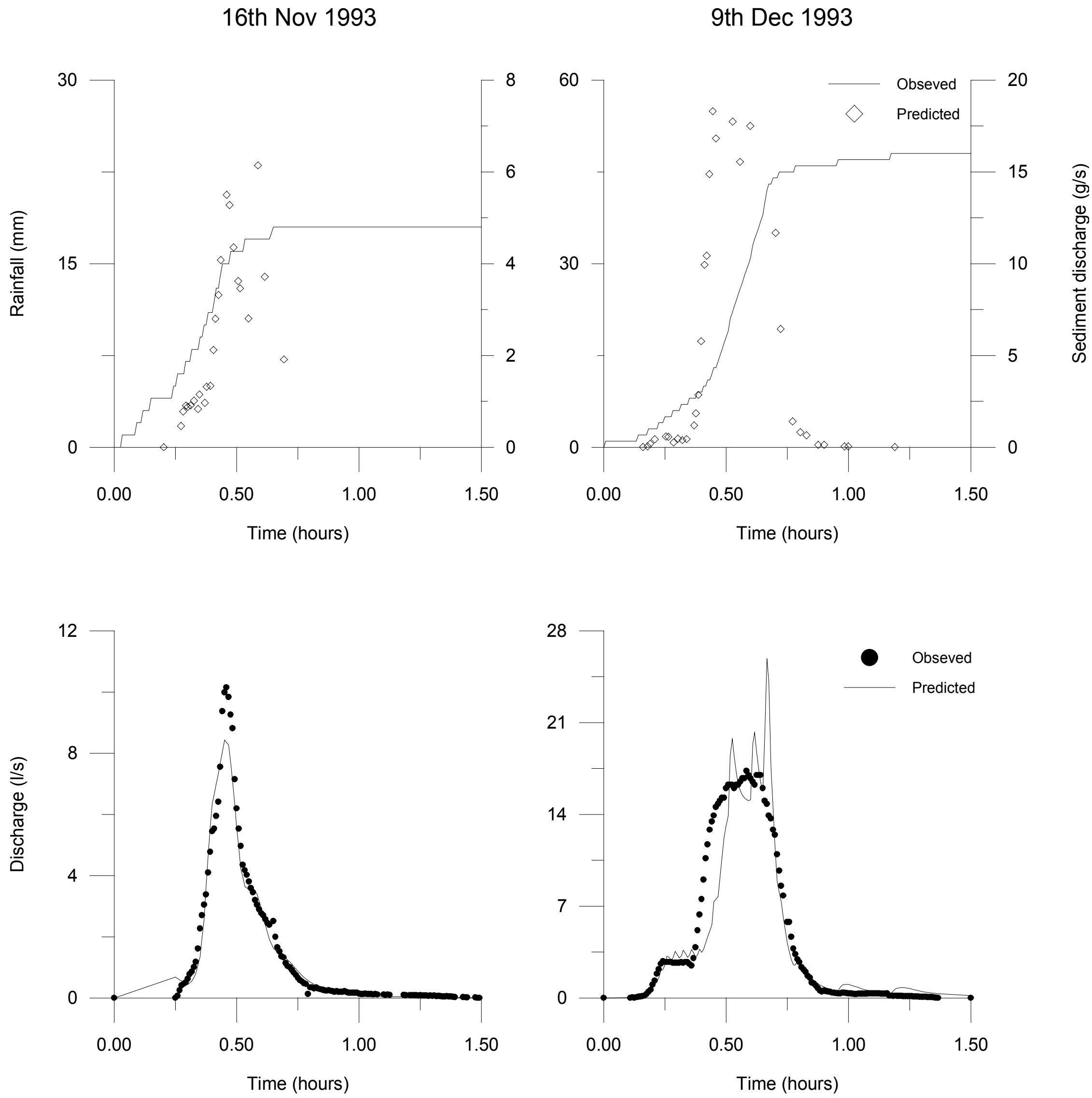

16th Nov 1993

NLFIT input files: cap16_11.fw, cap16_11.rf/ro

NLFIT output files: cap16_11n.prt/pmf

9th Dec 1993

NLFIT input files: cap10_12.fw, cap10_12.rf/ro

NLFIT output files: cap10_12n.prt/pmf

Parameter	Mean	St Deviation	Parameter	Mean	St Deviation
c_r	2.94	0.46	c_r	68.0	35.3
e_m	1.32	0.05	e_m	2.11	0.15
Sphi	10.6	1.92	Sphi	0.18	14.2
phi	1.02	6.46	phi	29.0	27.9

Appendix B.2 continued

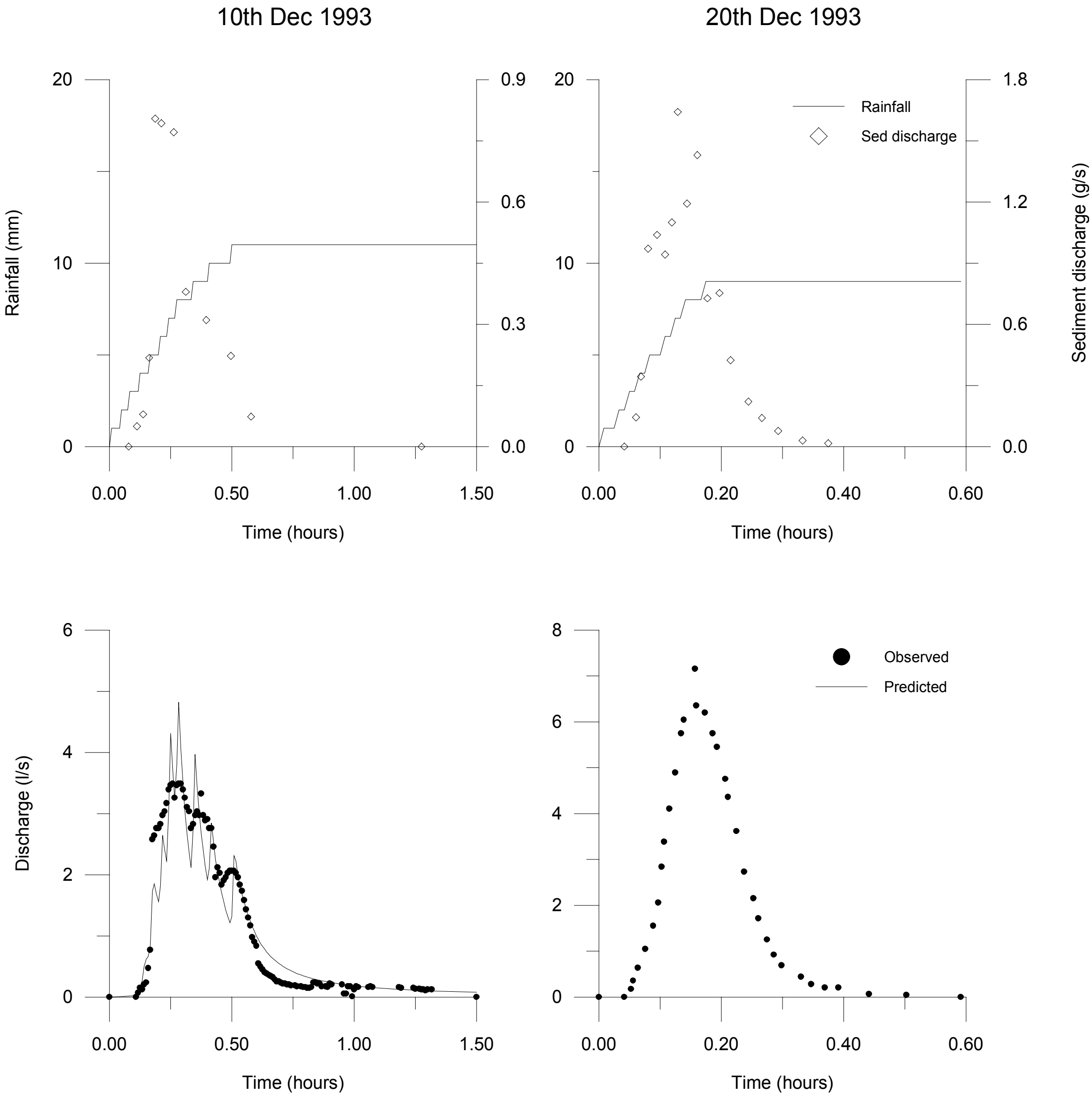

10th Dec 1993 | 20th Dec 1993

NLFIT input files: cap10a12.fw, cap10a12.rf/ro | Did not fit

NLFIT output files: cap10a12.prt/pmf

Parameter	Mean	St Deviation
c_r	4563	5087
e_m	3.58	0.39
Sphi	2.84	1.49
phi	0.57	5.53

Appendix B.2 continued

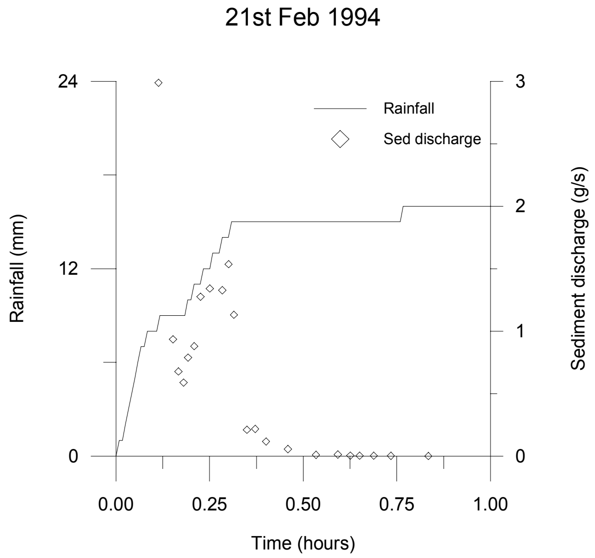

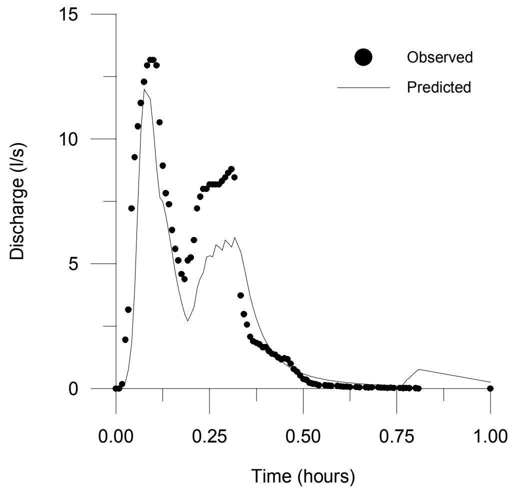

21st Feb 1994

NLFIT input files: cap21o02.fw, cap21o02.rf/ro

NLFIT output files: cap21o02n.prt/pmf

Parameter	Mean	St Deviation
c_r	10.5	4.91
e_m	1.65	0.11
Sphi	0.62	4.30
phi	4.81	16.8

Appendix B.3 Soil site monitoring data

30th Nov 1994 22nd Dec 1994

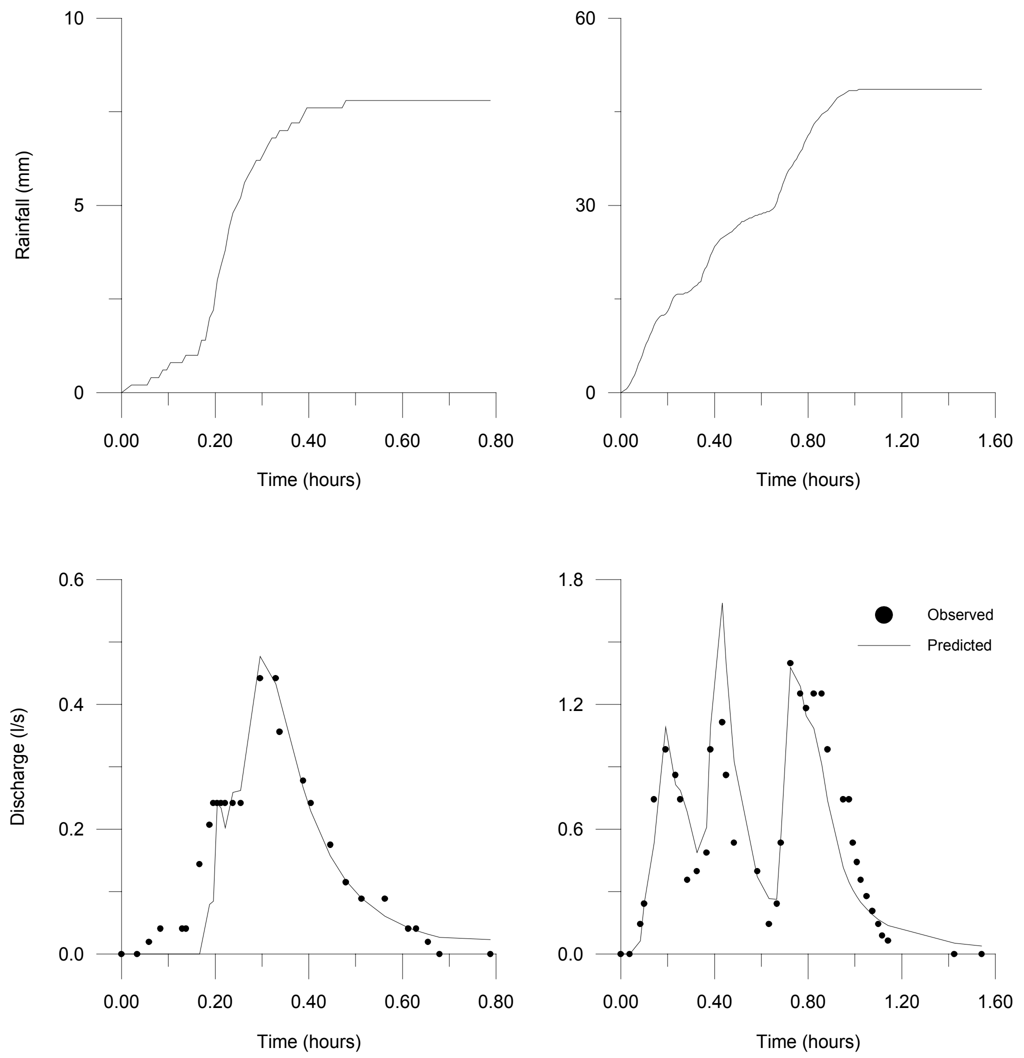

30th Nov 1994

NLFIT input files: so1130.fw, so1130.rf/ro

NLFIT output files: so1130gw.prt/pmf

Parameter	Mean	St Deviation
c_r	1.50	1.08
e_m	1.21	0.15
Sphi	0.001	48.7
phi	47.5	126

22nd Dec 1994

NLFIT input files: so1223.fw, so1223.rf/ro

NLFIT output files: so1223.prt/pmf

Parameter	Mean	St Deviation
c_r	37.9	53.9
e_m	2.00	0.39
Sphi	0.66	1.20
phi	70.3	3.74

Appendix B.3 continued

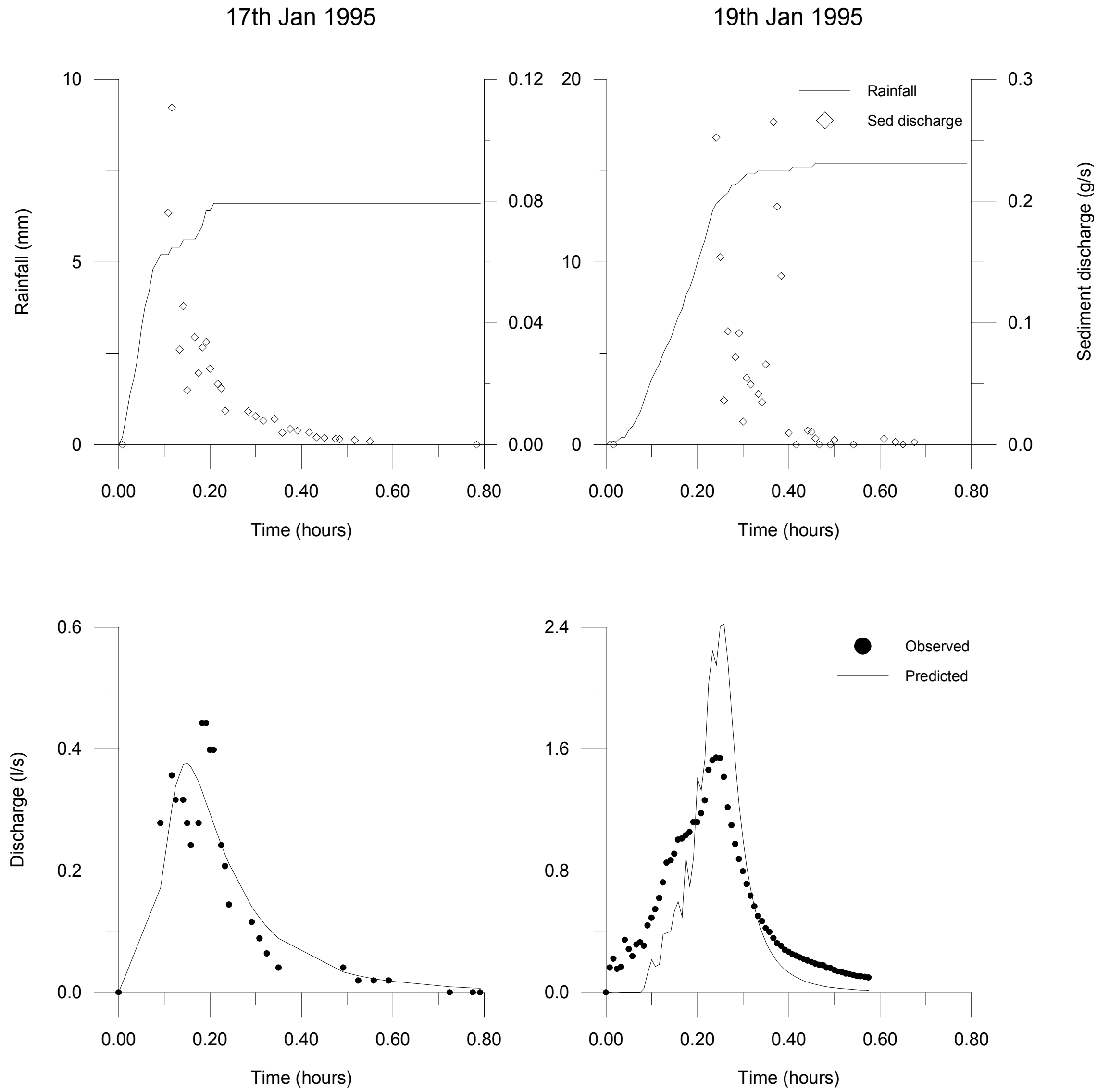

17th Jan 1995

NLFIT input files: so0118.fw, so0118.rf/ro

NLFIT output files: so0118gw.prt/pmf

19th Jan 1995

NLFIT input files: so0120.fw, so0120.rf/ro

NLFIT output files: so0120gw.prt/pmf

Parameter	Mean	St Deviation	Parameter	Mean	St Deviation
c_r	1.38	1.85	c_r	3.57	1.39
e_m	1.21	0.28	e_m	1.21	0.09
Sphi	0.001	203	Sphi	0.001	11.8
phi	61.2	30.5	phi	59.3	4.63

Appendix B.3 continued

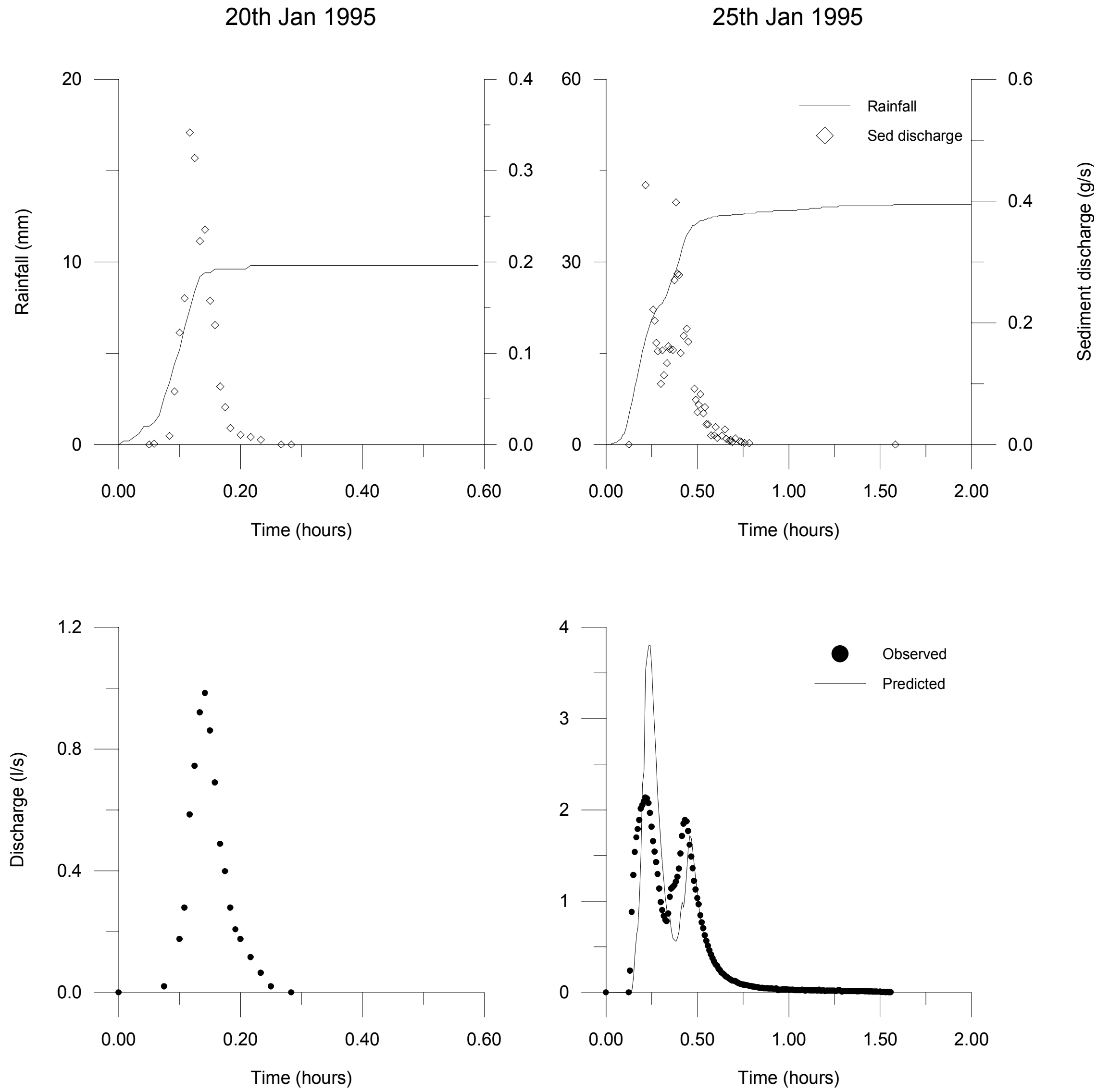

20th Jan 1995

Did not fit

25th Jan 1995

NLFIT input files: so0126.fw, so0126.rf/ro

NLFIT output files: so0126.prt/pmf

Parameter	Mean	St Deviation
c_r	4.50	1.89
e_m	1.36	0.11
Sphi	8.48	0.84
phi	61.2	3.09

Appendix B.3 continued

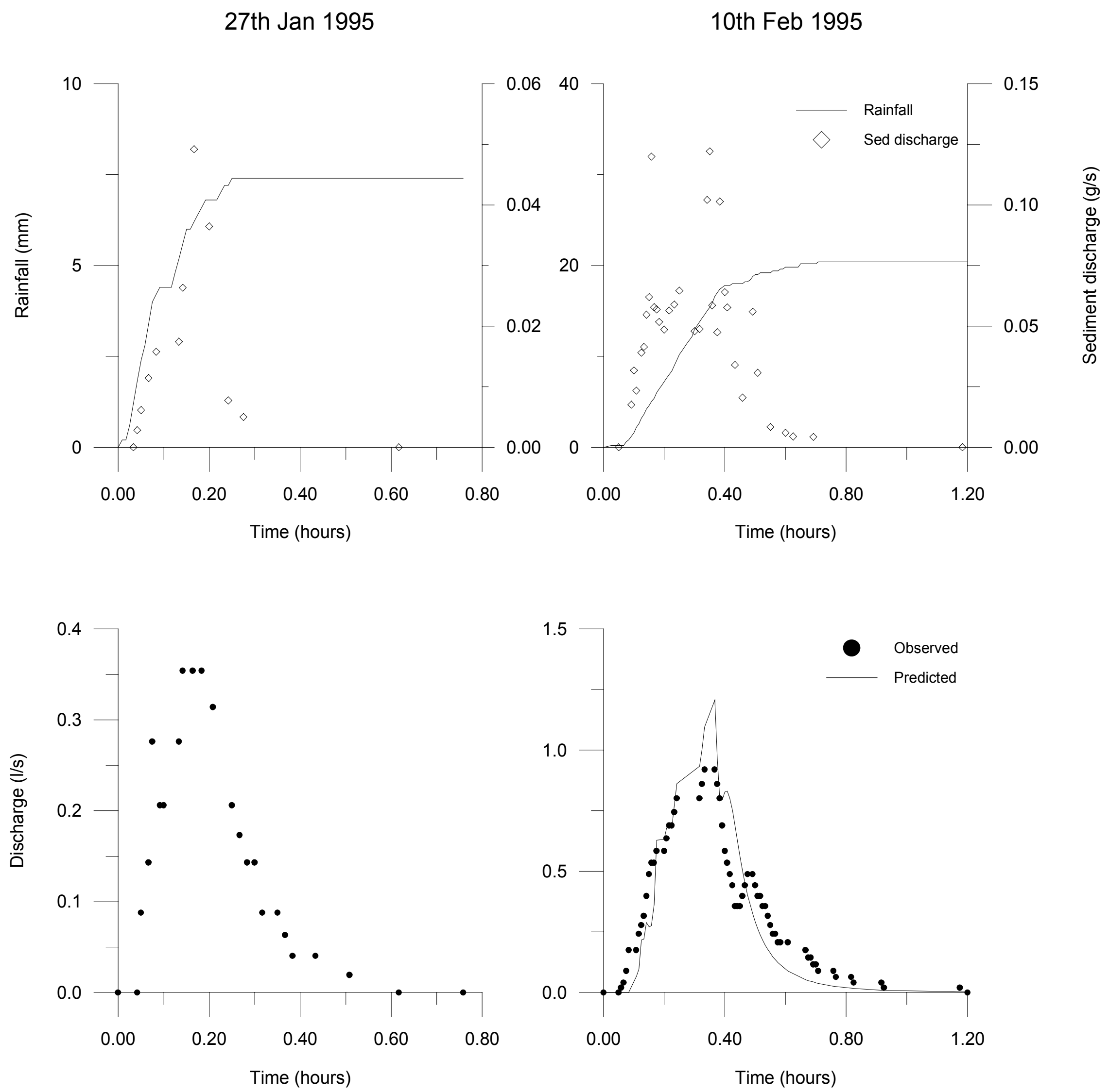

27th Jan 1995

Did not fit

10th Feb 1995

NLFIT input files: so0210.fw, so0210.rf/ro

NLFIT output files: so0210.prt/pmf

Parameter	Mean	St Deviation
c_r	3.28	0.09
e_m	1.29	0.09
Sphi	0.001	0.17
phi	48.0	0.63

Appendix B.3 continued

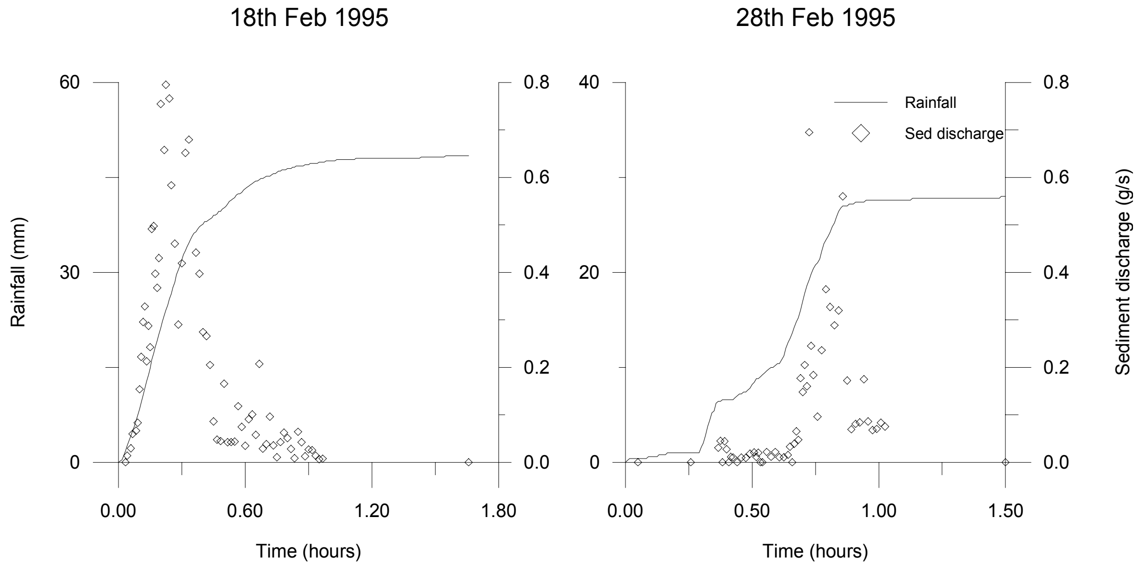

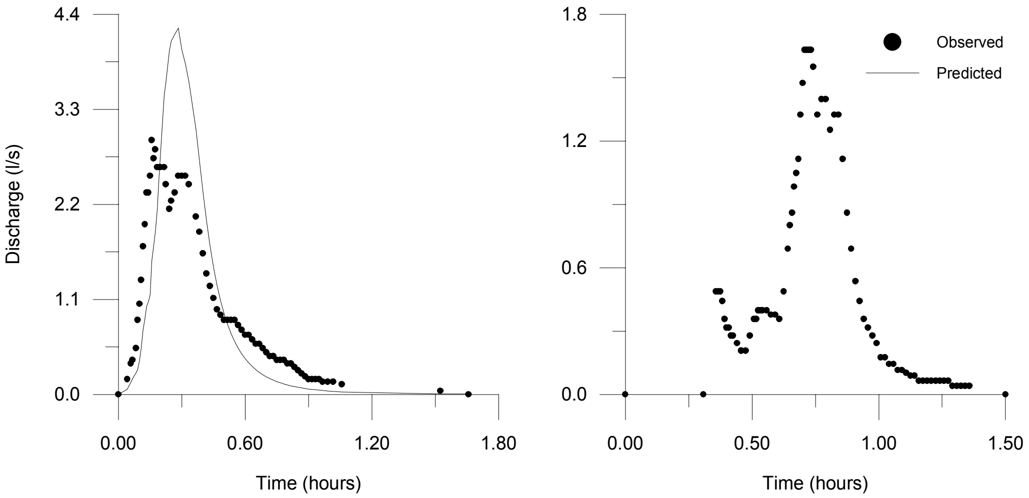

18th Feb 1995 | 28th Feb 1995

NLFIT input files: so0218.fw, so0218.rf/ro | Did not fit

NLFIT output files: so0218gw.prt/pmf

Parameter	Mean	St Deviation
c_r	15.7	3.95
e_m	1.83	0.09
Sphi	1.54	0.87
phi	52.7	5.54

Appendix B.3 continued

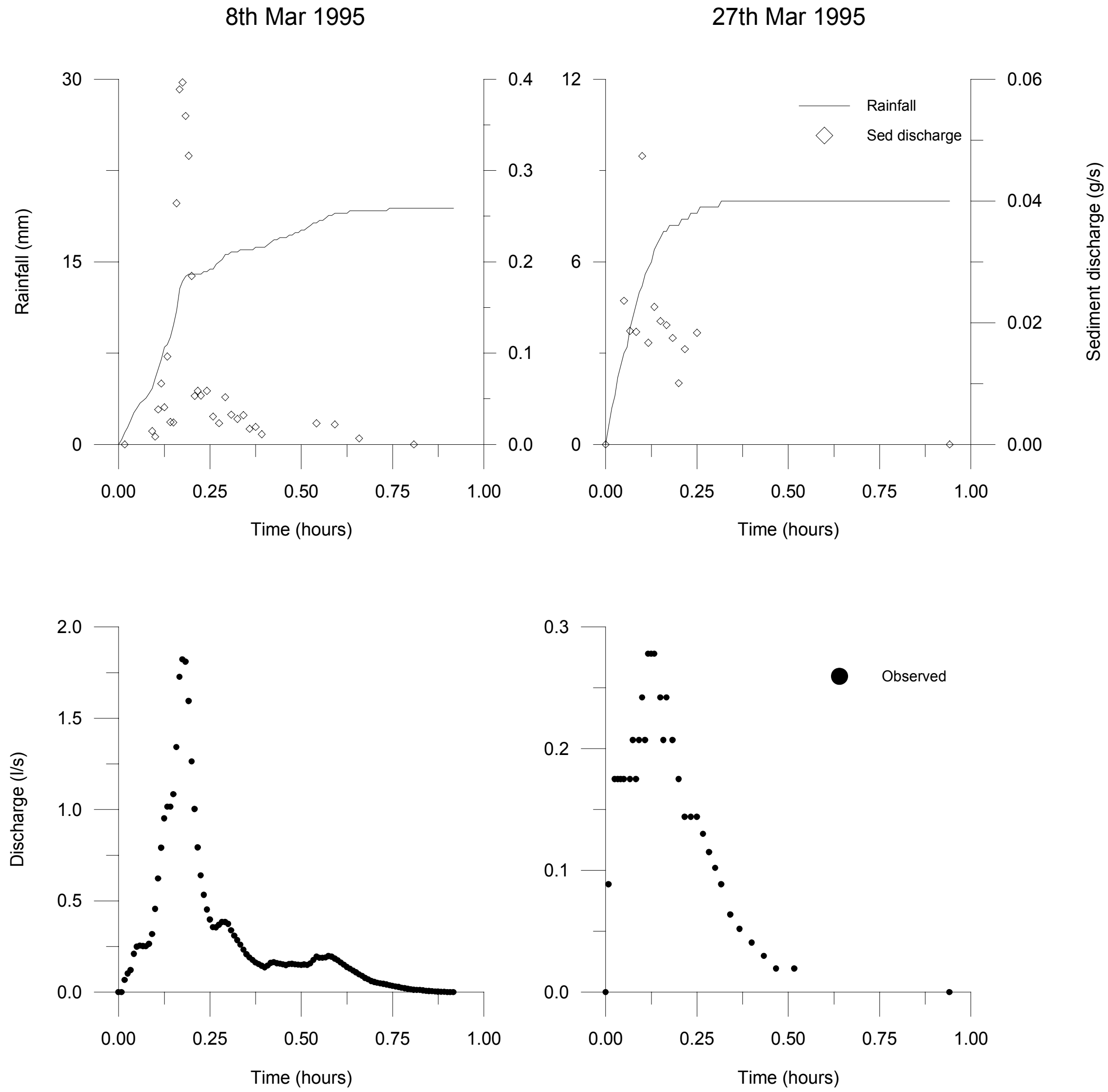

8th Mar 1995

Did not fit

27th Mar 1995

Did not fit

Appendix B.4 Fire site

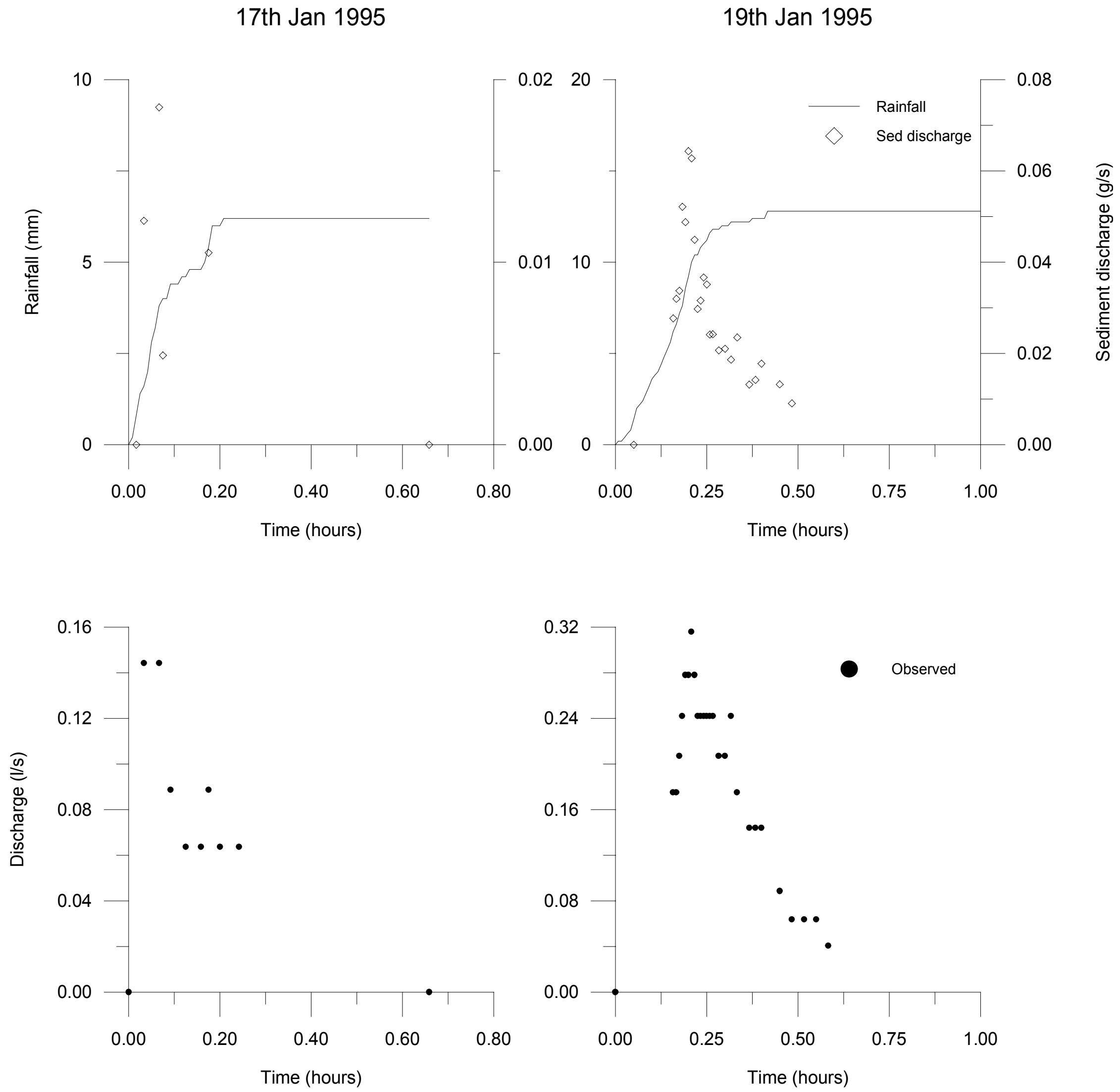

Appendix B.4 continued

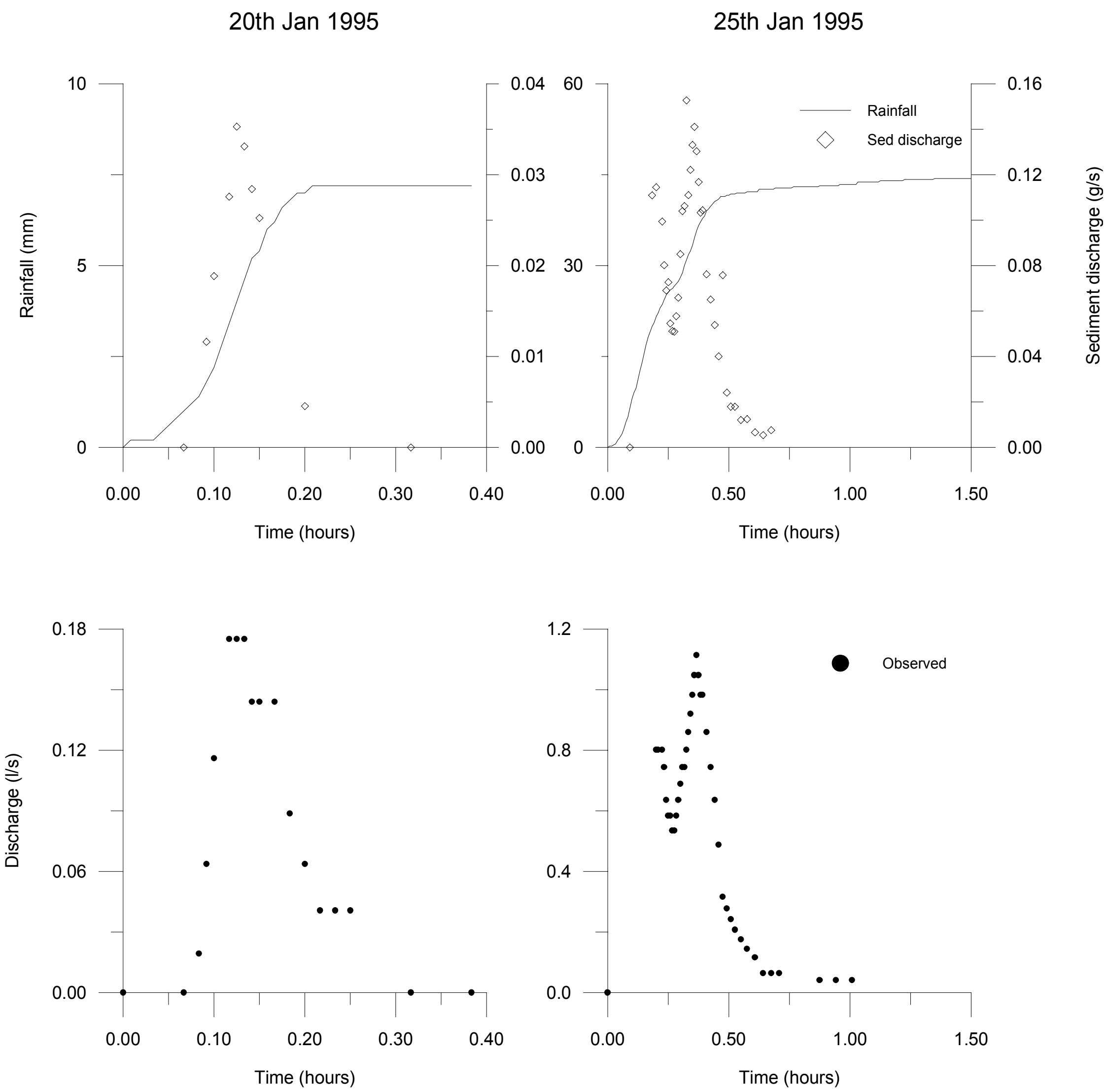

Appendix B.4 continued

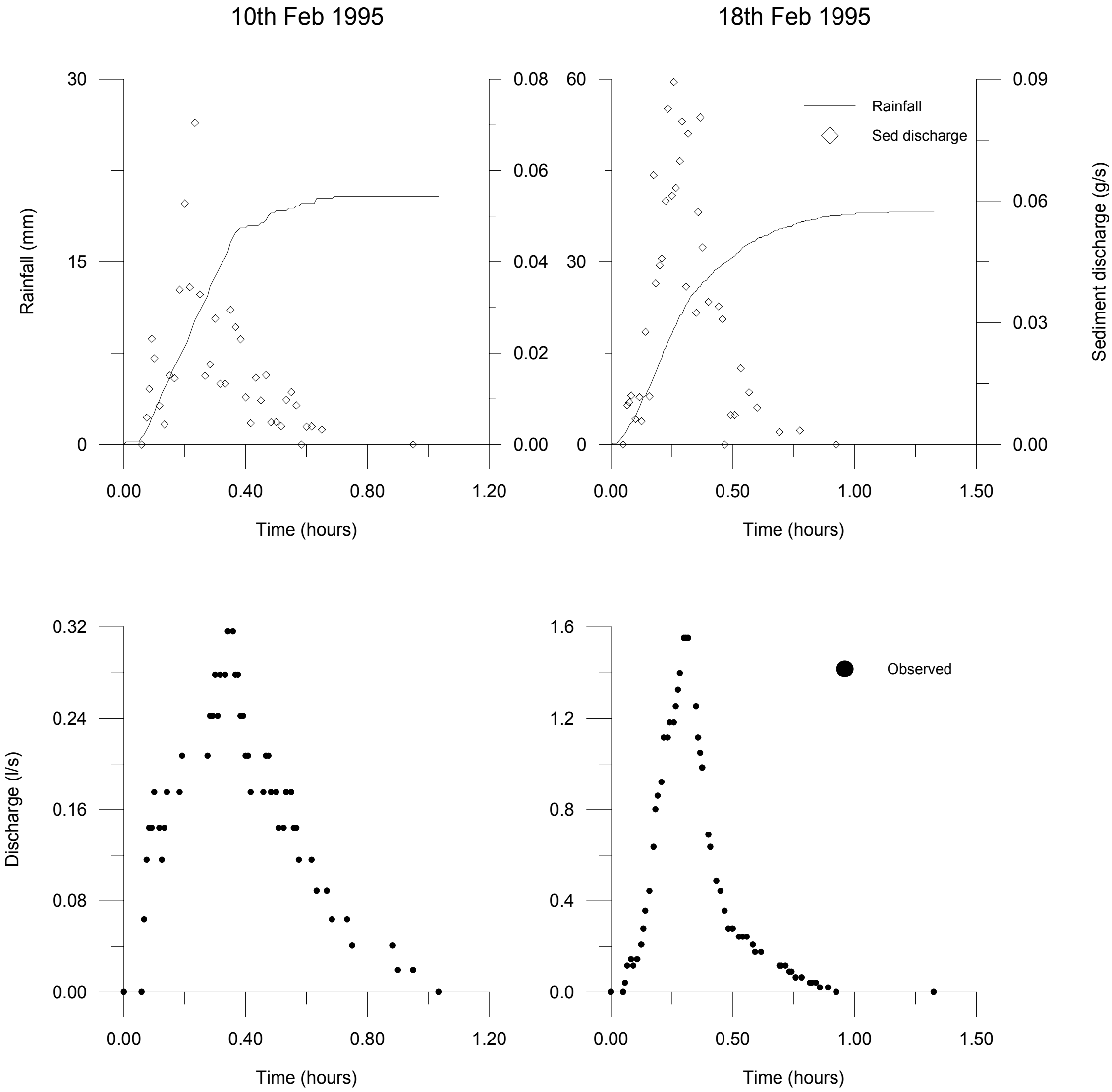

Appendix B.4 continued

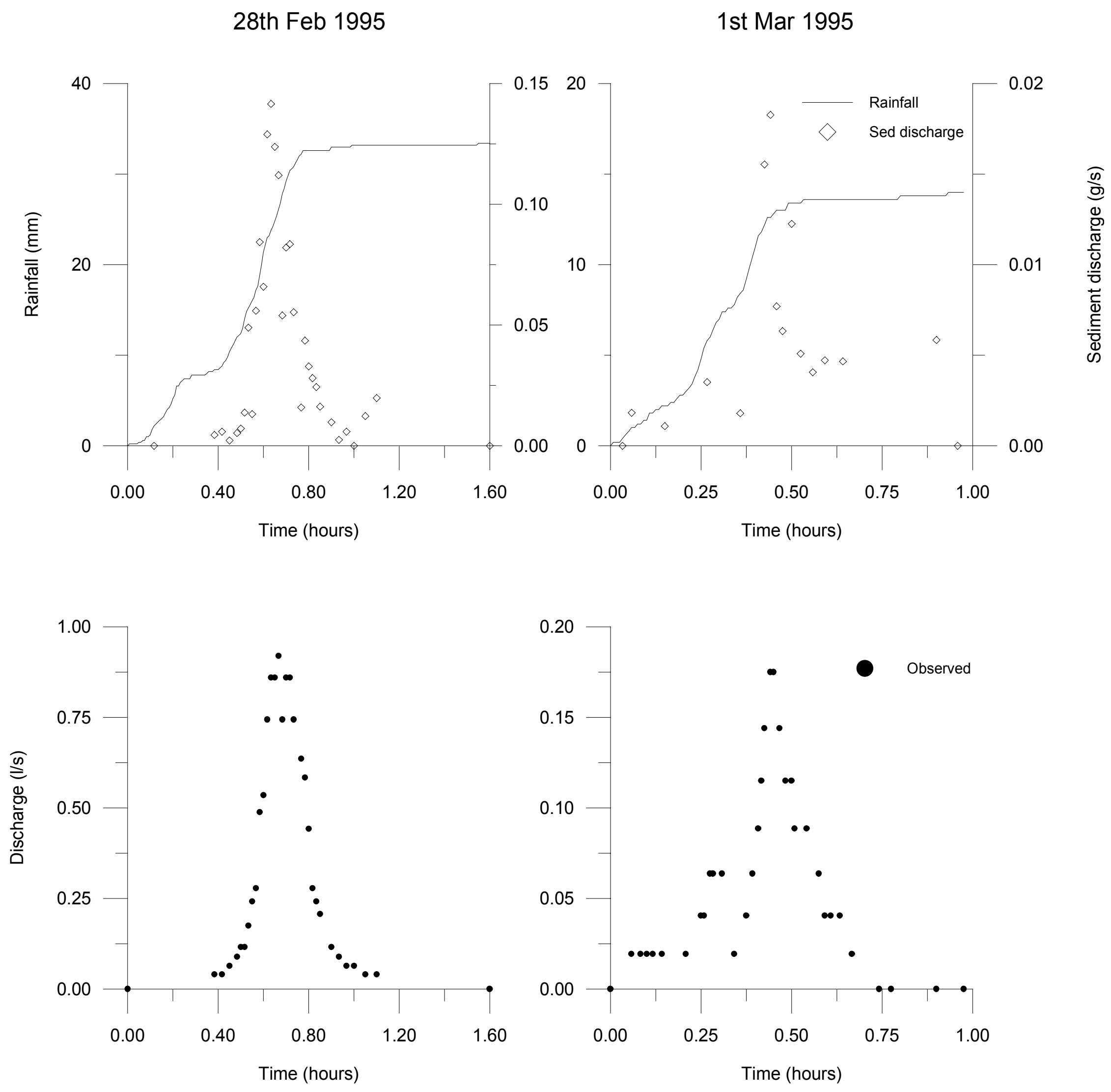

Appendix B.4 continued

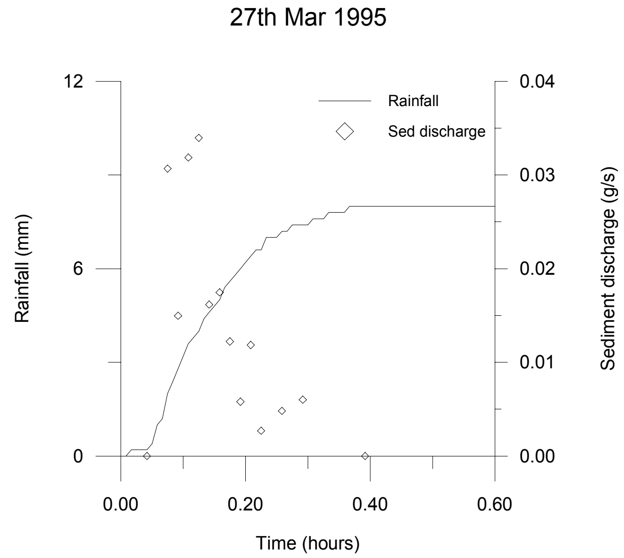

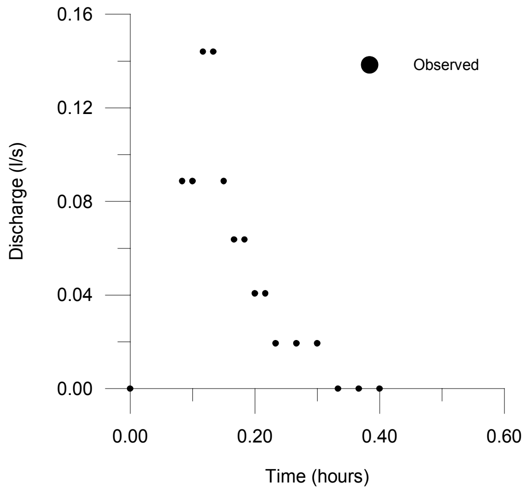

Appendix C Simultaneously fitted hydrographs

Batter site

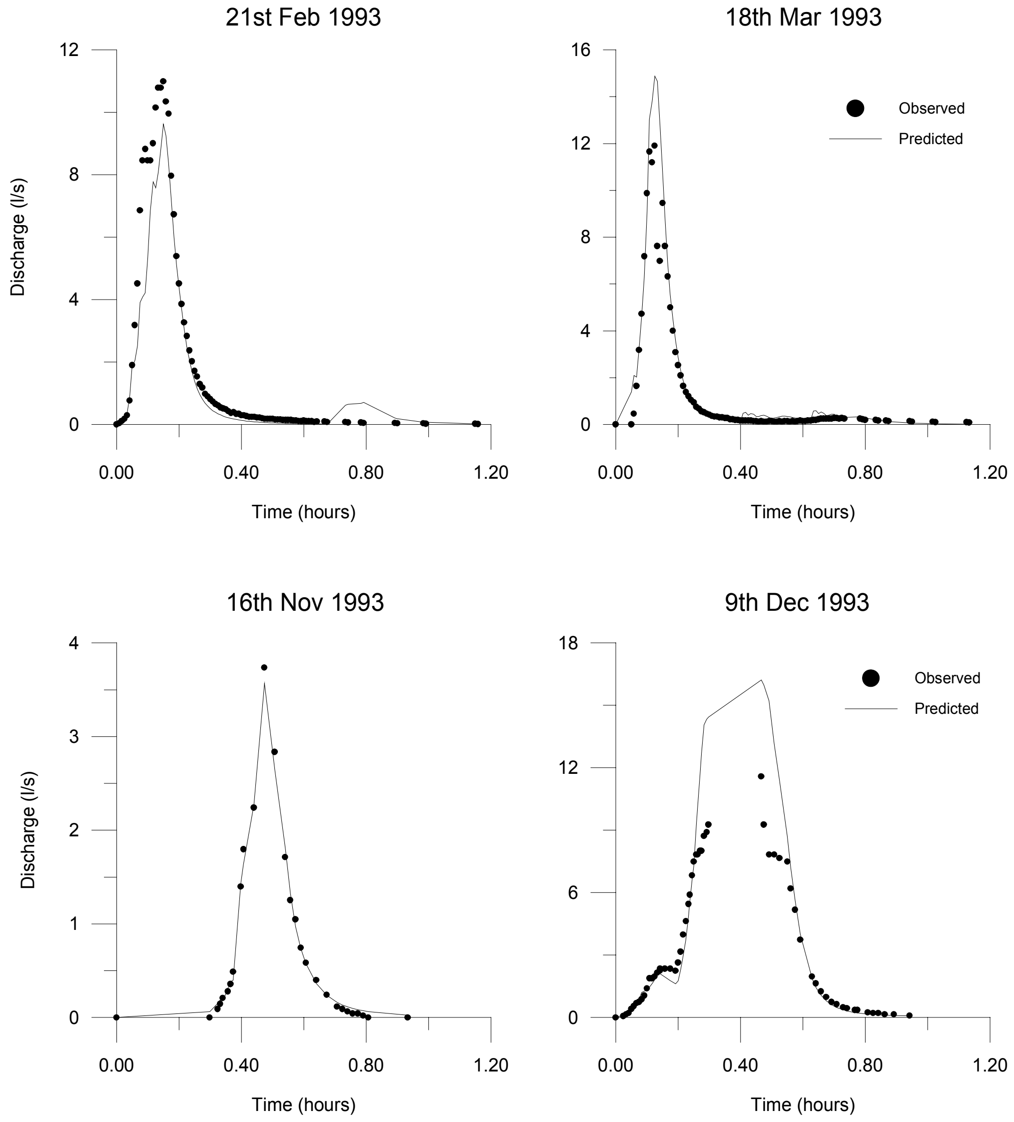

Simultaneous fit - Batter Site

NLFIT input files: b4storm.fw

NLFIT output files: b4storm.prt/pmf

Parameter	Mean	St Deviation
c_r	6.71	0.65
e_m	1.54	0.03
Sphi	5.48	0.36
phi	16.3	0.93

Cap site

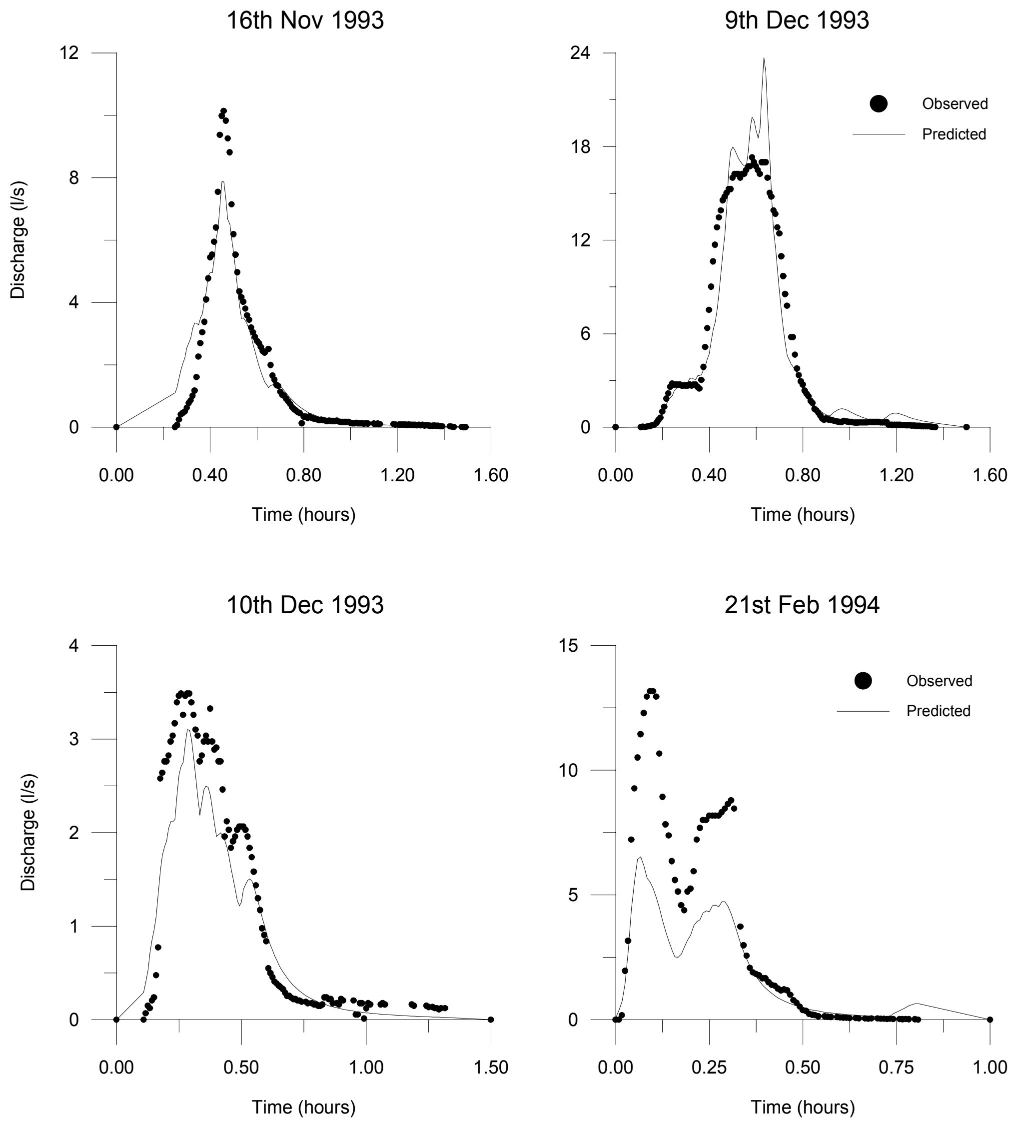

Simultaneous fit - Cap Site

NLFIT input files: cap9394n.fw

NLFIT output files: cap9394n.prt/pmf

Parameter	Mean	St Deviation
c_r	7.11	1.28
e_m	1.58	0.57
Sphi	5.31	0.58
phi	8.80	3.01

Soil site

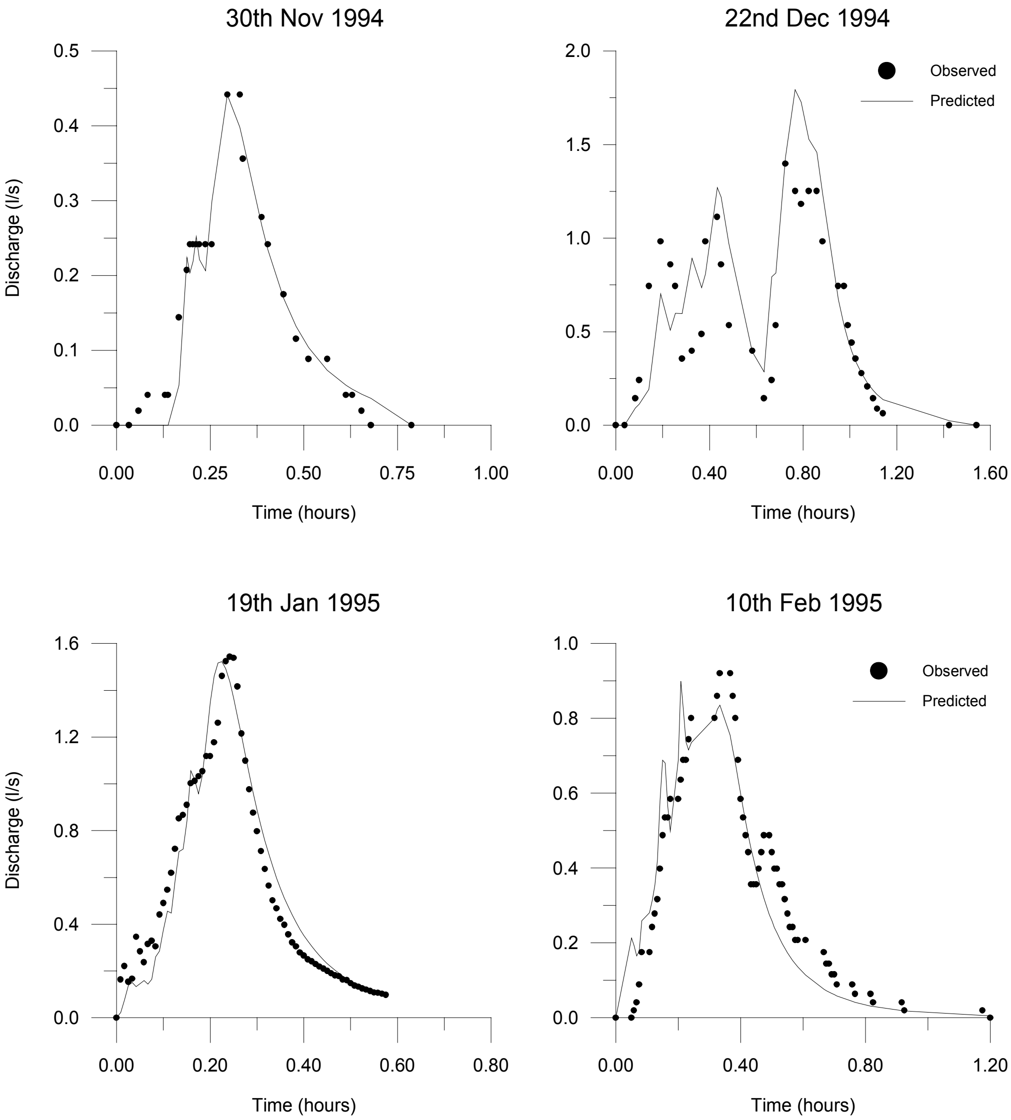

Simultaneous fit - Soil Site

NLFIT input files: 4storm.fw

NLFIT output files: 4stormgw.prt/pmf

Parameter	Mean	St Deviation
c_r	1.25	0.08
e_m	1.21	0.02
Sphi	7.54	0.33
phi	47.2	0.21

References

Agassi M & Levy GJ 1991. Stone-cover and rain intensity: Effects on infiltration, erosion and water splash. *Australian Journal of Soil Research* 29, 565–575.

Arkenstal M, Willgoose GR, Loch RJ & Pocknee C 1994. *Calibration of DISTFW parameters for the QDPI rainfall simulator Oaky Creek,* Research report no 093.04.1994, Department of Civil, Surveying and Environmental Engineering, The University of Newcastle, NSW.

Balek J 1977. *Hydrology and water resources in tropical Africa*. Developments in Water Science 8, Elsevier Scientific Publications, Amsterdam.

Balek J & Perry JE 1973. Hydrology of seasonally inundated African headwater swamps. *Journal of Hydrology* 19, 227–249.

Bos MG, Replogle JA & Clemmens AJ 1984. *Flow measuring flumes for open channel systems*. Wiley, New York.

DRI 1991. *Environmental management for mining in Queensland (Draft)*. Queensland Department of Resource Industries, Brisbane.

East TJ, Cull RF & Duggan K 1985. Surface runoff yields and sediment transport processes near Ranger. In *Alligator Rivers Region Research Institute: Annual research summary 1984–85.* Supervising Scientist for the Alligator Rivers Region, AGPS, Canberra, 99–102.

East TJ, Cull RF, Uren CJ, Curley PM & Unger CJ 1988. Erosional stability of waste rock dump batters at Ranger. In *Alligator Rivers Region Research Institute: Annual research summary 1987–88.* Supervising Scientist for the Alligator Rivers Region, AGPS, Canberra. 122–124.

Eckis R 1928. Alluvial fans of the Cucamonga district, southern California. *Journal of Geology* 36, 225–247.

Edwards K 1987. *Runoff and soil loss studies in NSW.* Technical Handbook 10. Soil Conservation Service of NSW and Macquarie University, Sydney.

Edwards WM & Owens LB 1991. Large storm effects on total soil erosion. *Journal of Soil and Water Conservation* 46, 75–78.

Evans KG 1992. Determination of interrill erodibility parameters for selected overburden spoil types from Central Queensland open-cut coal mines. MSc thesis, The University of Queensland, St Lucia, Queensland.

Evans KG 1997. Runoff and erosion characteristics of a post-mining rehabilitated landform at Ranger uranium mine, Northern Territory, Australia, and the implications for its topographic evolution. PhD thesis, The University of Newcastle, NSW.

Evans KG & Loch RJ 1996. Using the RUSLE to identify factors controlling erosion rates of mine soils. *Land Degradation and Development* 7 (3), 267–277.

Evans KG & Riley SJ 1993a. Large scale erosion plots on the Ranger uranium mine waste rock dump. Natural rainfall monitoring 1992/93 Wet season: Part 1 Hydrology data. Internal report 118, Supervising Scientist for the Alligator Rivers Region, Canberra. Unpublished paper.

Evans KG & Riley SJ 1993b. Large scale erosion plots on the Ranger uranium mine waste rock dump: Natural rainfall monitoring 1992/93 Wet season, Part 2 Sediment loss data. Internal report 131, Supervising Scientist for the Alligator Rivers Region, Canberra. Unpublished paper.

Evans KG & Riley SJ 1993c. Regression equations for the determination of discharge through RBC flumes. Internal report 104, Supervising Scientist for the Alligator Rivers Region, Canberra. Unpublished paper.

Evans KG & Willgoose GR 1994. An experimental study on the effect of vegetation on erosion of the Ranger uranium mine waste rock dump: A proposal. Internal report 164, Supervising Scientist for the Alligator Rivers Region, Canberra. Unpublished paper.

Evans KG, Aspinall TO & Bell LC 1991. Erosion prediction models and factors affecting the application of the Universal Soil Loss Equation to post-mining landscapes in Central Queensland. In *1991 Queensland Coal Symposium Proceedings*. The Australasian Institute of Mining and Metallurgy, Melbourne, 123–132.

Evans KG, Loch RJ, Aspinall TO & Bell LC 1997. Laboratory rainfall simulator studies of selected open-cut coal mine overburden spoils from Central Queensland. *Australian Journal of Soil Research* 35, 15–29.

Evans KG, Saynor MJ & Riley SJ 1996. Ranger uranium mine waste rock dump rainfall simulation experiments 1993: Large scale plots–data. Internal report 209, Supervising Scientist, Canberra. Unpublished paper.

Field WG 1982. Kinematic wave theory of catchment response with storage. *Journal of Hydrology* 55, 279–301.

Field WG & Williams BJ 1983. A generalised one-dimensional kinematic catchment model. *Journal of Hydrology* 60, 25–42.

Field WG & Williams BJ 1987. A generalised kinematic catchment model. *Water Resources Research* 23 (8), 1693–1696.

Finnegan LG 1993. Hydrolic characteristics of deep ripping under simulated rainfall at Ranger uranium mine. Internal report 134, Supervising Scientist for the Alligator Rivers Region, Canberra. Unpublished paper.

Foster GR 1982. Modelling the erosion process. In *Hydrologic modelling of small watersheds*. eds CT Haan, HP Johnson & DL Brakensiek, Monograph No 5, ASAE, Michigan, 297–380.

Foster GR 1987. *User requirements: USDA-Water Erosion Prediction Project (WEPP)*. National Soil Erosion Research Laboratory Report 1, USDA-ARS, W. Lafayette, Indiana.

George EM 1996. Hydrology of ripped surfaces under rainfall simulation: RUM 1993 data and vegetation, sediment and hydrology studies of the fire and soil sites: WRD, RUM 1995–96 Wet season monitoring. Internal report 201, Supervising Scientist, Canberra. Unpublished paper.

Graf WL 1977. The rate law in fluvial geomorphology. *American Journal of Science* 277, 178–191.

Greene RSB, Kinnell PIA & Woods JT 1994. Role of plant cover and stock trampling on runoff and soil erosion from semi-arid wooded rangelands. *Australian Journal of Soil Research* 32, 953–973.

Guy BT, Dickenson WT & Rudra RP 1987. The role of rainfall and runoff in the sediment transport capacity of interrill flow. *Transactions of the American Society of Agricultural Engineers* 30, 1378–86.

Hack JT 1965. *Geomorphology of the Shenandoah Valley, Virginia and West Virginia, and origin of the residual ore deposits*. US Geological Survey Professional Paper 484, Reston.

Hack JT & Goodlett JC 1960. *Geomorphology and forest ecology of a mountain region in the central Appalachians*. US Geological Survey Professional Paper 347, Reston.

Hair JF, Anderson RE, Tatham RL & Black WC 1995. *Multivariate data analysis (4th Edition) with readings*. Prentice Hall, New Jersey.

Hannan JC & Bell LC 1993. Surface rehabilitation. In *Australasian coal mining practice*. Monograph Series No 12, eds AJ Hargraves & CH Martin, The Australasian Institute of Mining and Metallurgy, Melbourne. 233–252.

Henderson FM 1966. *Open channel flow.* Prentice Hall, Englewood Cliffs, New Jersey.

Howard AD 1994. A detachment-limited model of drainage basin evolution. *Water Resources Research* 30, 2261–2285.

Howard AD 1997. Badland morphology and evolution: Interpretation using a simulation model. *Earth Surface Processes and Landforms* 22, 211–227.

Jeffreys JT, Brett J, Aspinall TO, White B, Stevens C & Johnson M 1986. Mine planning. In *Australasian coal mining practice*. Monograph Series No 12, eds AJ Hargraves & CH Martin, The Australasian Institute of Mining and Metallurgy, Melbourne. 174–188.

Jewell RJ & Adhikary DP 1996. Geotechnical stability issues for final voids. In *Post-mining landform stability and design workshop proceedings,* eds LC Bell & RW McLean, Australian Centre for Minesite Rehabilitation Research, Brisbane, 123–136.

Kirkby MJ 1971. Hillslope process-response models based on the continuity equation. In *Slopes form and process*. Institute of British Geographers Special Publication 3, London, 15–30.

Knisel WG 1980. CREAMS. *A field scale model for chemicals, runoff and erosion from agricultural management systems.* Conservation Research Report 26, US Department of Agriculture, Science and Education Administration, Washington.

Kuczera G 1989. An application of Bayesian nonlinear regression to hydrologic modelling. *Advances in Engineering Software* 11 (3), 149–155.

Kuczera G 1994. NLFIT: A bayesian nonlinear regression program suite Version 1.00g. Department of Civil, Surveying and Environmental Engineering, The University of Newcastle, NSW.

Leopold LB, Wolman MG & Miller JP 1964. *Fluvial processes in geomorphology*. Freeman, London.

Loch RJ & Bourke JJ 1994. Effects of vegetation on runoff and erosion. Internal report on rainfall simulator studies, Meandu Mine, Tarong April 1994. Natural Resource Management, Queensland Department of Primary Industries, Toowoomba, unpublished.

Loch RJ & Bourke JJ 1995. Postmining landscape parameters for erosion and water quality control. Internal report on: Effects of vegetation, slope gradient, and time since rehabilitation on runoff and erosion. Results of rainfall simulator studies on 12 m long plots, Goonyella Mine, May 1995. Natural Resource Management, Queensland Department of Primary Industries Toowoomba, unpublished.

Loch RJ & Rosewell CJ 1992. Laboratory methods for measurement of soil erodibilities (K factors) for the Universal Soil Loss Equation, *Australian Journal of Soil Research* 30, 233–248.

Loch RJ, Silburn DM & Freebairn DM 1989. Evaluation of the CREAMS model II. Use of rainulator data to derive soil erodibility parameters and prediction of field soil losses using derived parameters. *Australian. Journal of Soil Research* 27, 563–576.

Lopes VL, Nearing MA, Foster GR, Finker SC & Gilley JE 1989. The water erosion prediction project: erosion process. In *National Water Conference: Proceedings of the Specialty Conference sponsored by the Irrigation and Drainage Division and Water Resources Planning and Management Division of the American Society of Civil Engineers and the Deleware Section of the American Society of Civil Engineers*, ed TA Austin, The American Society of Civil Engineers, New York, 503–510.

Melville MD & Erskine W 1986. Sediment remobilisation and storage by discontinuous gullying in humid southeastern Australia. *International Association of Hydrological Sciences* 159, 277–286.

Meyer LD 1994. Rainfall simulators for soil erosion research. In *Soil erosion research methods*. 2nd edn, ed R Lal, Soil and Water Conservation Society, Ankeny IA, 83–103.

Miller N & Lee O 1989. The water erosion prediction project operational computer program. In *National Water Conference: Proceedings of the Specialty Conference sponsored by the Irrigation and Drainage Division and Water Resources Planning and Management Division of the American Society of Civil Engineers and the Deleware Section of the American Society of Civil Engineers*, ed TA Austin, The American Society of Civil Engineers, New York, 511–515.

Milnes AR 1988. *Rock weathering in the waste rock dumps at the Ranger Project Area*. Focus Report 3 to Ranger Mines Pty Ltd, CSIRO Division of Soils, Adelaide.

Moglen G & Bras RL 1994. *Simulation of observed topography using a physically-based basin evolution model*. Report 340, Ralph M Parsons Laboratory, Department of Civil and Environmental Engineering, MIT, Boston, MA.

Morgan RPC 1986. *Soil erosion and conservation*. Longman Scientific & Technical, England.

Needham RS 1988. *Geology of the Alligator Rivers uranium field, Northern Territory*. Bureau of Mineral Resources Bulletin 224. Canberra.

O'Reagan GJ, Lowell A & Roe P 1991. Computer based design of rehabilitated strip mine landforms. In *1991 Queensland Coal Symposium Proceedings*. The Australasian Institute of Mining and Metallurgy, Melbourne, 141–147.

Packer IJ, Hamilton GJ & Koen TB 1992. Runoff, soil loss and soil physical property changes of light textured surface soils from long-term tillage treatments. *Australian Journal of Soil Research* 30, 389–806.

Pilgrim DH 1987. *Australian rainfall and runoff: A guide to flood estimation.* Volume 1, rev edn, The Institution of Engineers Australia, Canberra.

Philip JR 1969. Theory of infiltration. *Advances in Hydroscience* 5, 215–296.

Phillips M 1991. Reclamation: The use of computer aided design to integrate reclamation and mine planning. In *1991 Queensland Coal Symposium Proceedings*. The Australasian Institute of Mining and Metallurgy, Melbourne, 133–140.

Renard KG, Laflen JM, Foster GR & McCool DK 1994. The Revised Universal Soil Loss Equation. In *Soil erosion research methods*, 2nd edn, ed R Lal, Soil and Water Conservation Society, Ankeny IA, 105–124.

Reneau SL, Dietrich WE, Dorn RI, Berger CR & Rubin M 1986. Geomorphic and palaeoclimatic implications of latest Pleistocene radiocarbon dates from colluvium-mantled hollows, California. *Geology* 14, 655–658.

Reneau SL, Dietrich WE, Rubin M, Donahue DJ & Jull AJT 1989. Analysis of hillslope erosion rates using dated colluvial deposits. *Journal of Geology* 97, 45–63.

Riley SJ 1992. Modelling hydrogeomorphic processes to assess the stability of rehabilitated landforms, Ranger uranium mine, Northern Territory, Australia. Internal report 55, Supervising Scientist for the Alligator Rivers Region, Canberra. Unpublished paper.

Riley SJ & Gardiner B 1991. Characteristics of slope wash erosion on the waste rock dump, Ranger uranium mine, Northern Territory. International Hydrology & Water Resources Symposium, The Institution of Engineers, Australia, National Conference Publication No. 91/92. 295–300.

Riley SJ & Williams DK 1991. Thresholds of gullying, Arnhem Land, Northern Territory, Australia. *Malaysian Journal of Tropical Geography* 22 (2), 133–143.

Rogers RD & Schumm SA 1991. The effect of sparse vegetative cover on erosion and sediment yield. *Journal of Hydrology* 123, 19–24.

Saynor MJ, Evans KG, Smith BL & Willgoose GR 1995. Experimental study on the effect of vegetation on erosion of the Ranger uranium mine waste rock dump. Natural rainfall monitoring data: 1994/95 Wet season erosion and hydrology model calibration. Internal report 195, Supervising Scientist for the Alligator Rivers Region, Canberra. Unpublished paper.

Schumm SA 1977. *The fluvial system*. John Wiley and Sons, New York.

Schumm SA & Hadley RF 1957. Arroyos and the semiarid cycle of erosion. *American Journal of Science* 255, 161–174.

Silburn DM & Loch RJ 1989. Evaluation of the CREAMS model I. Sensitivity analysis of the soil erosion/sedimentation component for aggregated clay soils. *Australian Journal Soil Research* 27, 545–561.

Scott PF & Erskine WD 1994. Geomorphic effects of a large flood on fluvial fans. *Earth Surface Processes and Landforms* 19, 95–108.

Simanton RJ, Herbert BO & Renard KG 1978. Hydrologic effects of rangeland renovation. In *Proceedings of the First International Rangeland Congress*, ed DN Hyder, Denver Colorado USA August 14–18, 1978, Society for Range Management, Denver, Colorado, 331–334.

Simanton JR, Weltz MA & Larson HD 1991. Rangeland experiments to parameterize the water erosion prediction project model: Vegetation canopy cover effects. *Journal of Range Management* 44 (3), 276–282.

Smith TR & Bretherton FP 1972. Stability and the conservation of mass in drainage basin evolution. *Water Resources Research* 8 (6), 1506–1529.

Stein Jr OR 1983. Erodibility and related soil properties of three reclaimed surface mined soils, MSc thesis, Purdue University, Indiana.

Stocking MA 1994. Assessing vegetative cover and management effects. In *Soil erosion research methods*, 2nd edn, ed R Lal, Soil and Water Conservation Society, Ankeny IA, 211–232.

Thomas MF 1994. *Geomorphology in the tropics: A study of weathering and denudation in low latitudes.* John Wiley & Sons, Chichester.

Toy TJ & Hadley RF 1987. *Geomorphology and reclamation of disturbed land*. Academic Press, Sydney.

Tucker G 1996. Modelling the large scale interaction of climate, tectonics and topography. PhD thesis, Pennsylvania State University, Pennsylvania, USA.

Unger C, Armstrong A, McQuade C, Sinclair G, Bywater J & Koperski G 1989. Planning for rehabilitation of the tailings dam at the Ranger uranium mines. In *Proceedings of the North Australian Rehabilitation Workshop* No 11, NT Department of Mines and Energy, Darwin, 153–165.

Unger CJ & Milnes AR 1992. Rehabilitation at Ranger uranium mines. In *Conservation and development issues in north Australia*, eds I Moffat & A Webb, North Australia Research Unit, ANU, Darwin, 221–231.

Waggitt PW & Riley SJ 1992. Stabilisation objectives for the rehabilitation of the Ranger uranium mine. In *Proceeding of the international symposium, Land reclamation: Advances in research & technology*, eds T Younos, P Diplas & S Mostaghimi, American Society of Agricultural Engineers, Michigan, 204–212.

Ward TA, Flanagan JC & Hubery RW 1983. Rehabilitation of the Mary Kathleen uranium mine site after closure. In *Proceedings of the International Specialist Conference on Water regime in relation to milling, mining and waste treatment including rehabilitation with the emphasis on uranium mining*, 4–9 September, Darwin, NT, Australian Water and Wastewater Association, Sydney.

Watson DA & Laflen JM 1986. Soil strength, slope, and rainfall intensity effects on interril erosion. *Transactions of the American Society of Agricultural Engineers* 29, 98–102.

White B, Jeffreys JT, Aspinall TO, Brett J, Johnson M & Stevens C 1993. Mine planning. In *Australasian coal mining practice*. Monograph Series No 12, eds AJ Hargraves & CH Martin, The Australasian Institute of Mining and Metallurgy, Melbourne, 188–202.

Willgoose GR 1992. *User manual for SIBERIA (Version 7.05)*. Research Report No. 076.04.1992. Department of Civil, Surveying and Environmental Engineering, The University of Newcastle, NSW.

Willgoose G 1995. A preliminary assessment of the effect of vegetation on the long-term erosional stability of the proposed above-grade rehabilitation strategy at Ranger uranium mine. Open file record 119, Supervising Scientist for the Alligator Rivers Region, Canberra. Unpublished paper.

Willgoose GR & Kuczera G 1995. Estimation of subgrid scale kinematic wave parameters for hillslopes. *Hydrological Processes* 9, 469–482.

Willgoose GR & Loch RJ 1996. An assessment of the Nabarlek rehabilitation, Tin Camp Creek and other mine sites in the Alligator Rivers Region as test sites for examining long term erosion processes and the validation of the SIBERIA model. Internal report 229, Supervising Scientist, Canberra. Unpublished paper.

Willgoose G & Riley S 1993. Application of a catchment evolution model to the prediction of long term erosion on the spoil heap at Ranger uranium mine: Stage 1 report. Open file record 107, Supervising Scientist for the Alligator Rivers Region, Canberra. Unpublished paper.

Willgoose GR, Bras RL & Rodriguez-Iturbe I 1989. Modelling of the erosional impacts of land use change: A new approach using a physically based catchment evolution model. In *Hydrology and Water Resources Symposium 1989*, Christchurch NZ, National Conference publication no 89/19, The Institute of Engineers Australia, Melbourne, 325–329.

Willgoose GR, Bras RL & Rodriguez-Iturbe I 1991a. Results from a new model of river basin evolution. *Earth Surface Processes and Landforms* 16, 237–254.

Willgoose GR, Bras RL & Rodriguez-Iturbe I 1991b. A coupled channel network growth and hillslope evolution model 1. Theory. *Water Resources Research* 7, 1671–1684.

Willgoose GR, Bras RL & Rodriguez-Iturbe I 1991c. A coupled channel network growth and hillslope evolution model 2. Nondimensionalization and applications. *Water Resources Research* 7, 1685–1696.

Willgoose GR, Bras RL & Rodriguez-Iturbe I 1992. The relationship between catchment and hillslope properties: implications of a catchment evolution model. *Geomorphology* 5, 21–37.

Willgoose GR, Kuczera GA & Williams BJ 1995. *DISTFW-NLFIT: Rainfall-runoff and erosion model calibration and model uncertainty assessment suite user manual*. Research Report No. 108.03.1995. Department of Civil, Surveying and Environmental Engineering, The University of Newcastle, New South Wales, Australia.

Wischmeier WH & Smith DD 1978. *Predicting rainfall erosion losses: A guide to conservation planning*. Agriculture Handbook No 537.2, US Department of Agriculture, Science and Education Administration, Washington.

Wockner GW & Freebairn DM 1991. Water balance and erosion study on the eastern Darling Downs: An update. *Australian Journal of Soil and Water Conservation* 4, 41–47.